

**FIRE PATTERNS WITHIN A SUCCESSIONAL GRADIENT OF A SAGEBRUSH
STEPPE/JUNIPER WOODLAND**

A Thesis

Presented in Partial Fulfillment of the Requirements for the

Degree of Master of Science

with a

Major in Rangeland Ecology and Management

in the

College of Graduate Studies

University of Idaho

by

Aaron Roth

April 2004

Major Professor: Dr. Stephen C. Bunting, Ph.D.

AUTHORZZTION TO SUBMIT

THESIS

This thesis of Aaron D. Roth, submitted for the degree of Master of Science with a major in Rangeland Ecology and Management and titled “Fire patterns within a successional gradient of a sagebrush steppe/juniper woodland” has been reviewed in final form. Permission, as indicated by the signatures and dates given below, is now granted to submit final copies to the College of Graduate Studies for approval.

Major Professor _____ Date _____

Stephen C. Bunting

Committee
Members _____ Date _____

James L. Kingery

_____ Date _____

Paul Gessler

Department
Administrator _____ Date _____

Karen L. Launchbaugh

Discipline’s
College Dean _____ Date _____

Steven B. Daley Laursen

Final Approval and Acceptance by the College of Graduate Studies

_____ Date _____

Katherine G. Aiken

ABSTRACT

Western juniper (*Juniperus occidentalis* spp. *occidentalis*) encroachment across broad expanses of the northern Great Basin has become a great concern to land managers and ecologists. The detrimental and exponential expansion of western juniper has left many wondering the exact extent of the problem. By using remote sensing and GIS technologies mapping vegetation communities is possible across broad, large-scale areas in sagebrush steppe juniper woodland landscapes. Three advanced classification procedures were compared to map western juniper encroachment based on Potential Vegetation Types and Structural Stage attributes using a Landsat 7 Enhanced Thematic Mapper Plus (ETM+) satellite image. The supervised classification methods utilized procedures based on both parametric and nonparametric statistics. The nonparametric procedure out-performed the other parametric methods and achieved an overall map accuracy of 69% based on 32 classes. Mapping western juniper encroachment along a successional gradient is possible and can be beneficial in prioritizing areas for prescribed burning and other management practices. In addition custom fuel models were created to cover the same extent as the classification map and allowed for fire-landscape pattern relationships to be addressed. Using two fire simulation methods, fire frequency data were produced which allowed for a statistical comparison between the spatial pattern, or the arrangement of different vegetation types along a successional gradient, and fire frequency. Results suggest that vegetation arrangement of early successional stages has little or no influence on fire frequency. But as western juniper encroaches and site characteristics become dominated by later successional stages, the spatial arrangement of the landscape becomes an important factor in determining fire frequency.

ACKNOWLEDGEMENTS

As with most successful ventures in life this project was a combination of efforts by many, not the work of one. Without the help of many I would still be working in front of a computer down stairs in the GIS/Remote Sensing Lab. I would like to thank Dr. Bunting, Dr. Kingery, Dr. Gessler, and the soon to be Dr. Strand. Thank you Dr. Bunting for giving me the opportunity, direction, and insight to work on and successfully completed this project. You have provided me with everything that I have expected and so much more. Thank you Dr. Kingery and Dr. Gessler for serving on my committee. Thank you Eva for somehow always finding the time and a way to answer and solve all of my questions with such a busy schedule. I can't thank you enough and will always carry with me the knowledge you have provided. Many thanks go out to Curt Yanish for all of his outstanding assistance, advice, and willingness to help in any way. Other people that I need to recognize include Mark Finney who found the time to look at our fuel models and create a fire frequency grid, which was instrumental in looking at landscape-fire pattern relationships. A special thanks goes out to Jeremey Kleinsmith and Ramona Flatz who not only helped collect data but endured the trials of a remote field season. Lastly I would like to recognize and thank the Lower Snake River District BLM for providing the funding for this project and I hope the map is equal to the experience and education that I have received.

I would like to dedicate this thesis to all the people along the way who have believed in me and given me the opportunity to achieve to the best of my potential. I would especially like to dedicate this work to my family who has been more than supportive and have gone above and beyond the call of duty in helping me realize my dreams. Without their foundation and guidance I do not know where I would be.

TABLE OF CONTENTS

Title Page.....	i
Authorization to Submit Thesis.....	ii
Abstract.....	iii
Acknowledgements and Dedication.....	iv
Table of Contents.....	v
List of Tables.....	vii
List of Figures.....	viii
Introduction.....	1
Objectives.....	3
Literature Review.....	4
Methods.....	21
Results.....	38
Discussion.....	44
Conclusions.....	59
Literature Cited.....	61
Tables.....	68
Figures.....	74
Appendix A.....	89
Appendix B.....	94
Appendix C.....	110
Appendix D.....	110
Appendix E.....	110

Appendix F.....	111
Appendix G.....	112
Appendix H.....	113
Appendix I.....	113
Appendix J.....	114
Appendix K.....	114
Appendix L.....	114

LIST OF TABLES

Table

1.	Potential Vegetation Type and Structural Stage attributes based on cover types (Bunting et al. 2002b).....	68
2.	Vegetation indices used in the classification and how each was derived.....	69
3.	Summary of the number of training sites, validation sites, and the total number of pixel used for each class.....	69
4.	Forty-four classes used in first classification attempt.....	70
5.	Classes combined to create final thirty-two classes.....	70
6.	Thirty-four classes used in secondary classification attempts.....	70
7.	Thirty-two classes used in the final classification.....	70
8.	Eighteen custom fuel model names, numbers, and descriptions (Yanish 2002) including the three new models.....	71
9.	Positive and negative trends and significance of each landscape metric for Artrv W1 using method A and B within each of the three watersheds.....	72
10.	Positive and negative trends and significance of each landscape metric for Artrv W2 using method A and B within each of the three watersheds.....	72
11.	Positive and negative trends and significance of each landscape metric for Artrv W4 using method A and B within each of the three watersheds.....	73
12.	Positive and negative trends and significance of each landscape metric for Artrv W5 using method A and B within each of the three watersheds.....	73

LIST OF FIGURES

Figures

1.	Mountain big sagebrush PVT-SS classes successional diagram with fire as the disturbance.....	74
2.	Owyhee Plateau study area and locations of the Silver City Range, South Mountain, and Juniper Mountain.....	75
3.	Fuel measurement plot design diagram Yanish (2002).....	76
4.	The three HUC 6 th order watershed used in objective 3 including Current Creek, Smith Creek, and Red Canyon.....	76
5.	Overall accuracy and kappa statistic for each of the three classification methods.....	77
6.	Low sagebrush Potential Vegetation Type User's vs. Producer's accuracy comparison for each classification method.....	77
7.	Big sagebrush Potential Vegetation Type User's vs. Producer's accuracy comparison for each classification method.....	78
8.	Bitterbrush Potential Vegetation Type User's vs. Producer's accuracy comparison for each classification method.....	78
9.	Forest Potential Vegetation Types User's vs. Producer's accuracy comparison for each classification method.....	79
10.	Curl-leaf mountain mahogany Potential Vegetation Type, annuals, rock, and wet meadow classes User's vs. Producer's accuracy comparison for each classification method.....	79
11.	Water and mine classes User's vs. Producer's accuracy comparison for each classification method.....	80
12.	Final Nonparametric classification map.....	81
13.	Vegetation maps of the three watersheds used to compare landscape arrangement to fire frequency in objective 3.....	82
14.	Fire frequency maps of the three watersheds used in objective 3 created by method A using 100 fires.....	83

15.	Fire frequency maps of the three watersheds used in objective 3 created by method B using 25,000 fires.....	84
16.	Artrv W4 significant trend for the landscape metric Patch Density across each watershed using both fire frequency methods.....	85
17.	Artrv W5 significant trend for the landscape metric Landscape Shape Index across each watershed using both fire frequency methods.....	86
18.	Artrv W5 significant trend for the landscape metric Patch Density across each watershed using both fire frequency methods.....	87
19.	Artrv W5 significant trend for the landscape metric Simpson's Diversity across each watershed using both fire frequency methods.....	88

INTRODUCTION

Western juniper (*Juniperus occidentalis* spp. *occidentalis*) encroachment across the landscape has become a major concern to land managers due to the effect it is having on changing landscape patterns and process (Wall et al. 2001). Introduction of domestic livestock, fire suppression, climate change, and human disturbance have all been proposed for causing exponential expansion in the past 120 years (Burkhardt and Tisdale 1976, Shinn 1980). Important research has focused on the western juniper successional gradient, and the effects fire plays on controlling and manipulating the vegetation (Miller et al. 2000). Prescribed burning can be successfully used to reverse western juniper encroachment up to a threshold or successional boundary where fires become difficult to start and carry across the landscape, many times resulting in ineffective applications (Miller et al. 2000, Yanish 2002).

Creating maps based on vegetation seral stages and inventories of fine fuels over large remote areas would have been virtually impossible 30 years ago. Modern technology, including remote sensing, GIS, and computer processing software allow users to create land classification maps based on desirable outputs. Fairly successful results have been reported for discriminating different shrub species or different classes of tree species (Jackubauskas et al. 1998, Wolter et al. 1995). With so many potential uses, a large amount of attention has been focused on research and the development of methods to most accurately produce vegetation maps (Bobbe et al. 2001). Numerous vegetation indices, classification procedures, and accuracy measurements have been developed (Skidmore and Turner 1988, Kent et al. 1988). With the increased potential in vegetation classification, the overall demand and broad scale utilization should continue to increase.

Modern technology has also been the driving force behind our understanding of wildfires and landscape patterns at different scales (Albright and Meisner 1999). From simple models not so many years ago, the development of fire predictability models has greatly increased (Albright and Meisner 1999). Current models not only predict fire rates of spread and intensity, but also can include observed variables such as weather conditions, slope, aspect, elevation, and fuel moisture (Andrews and Queen 1999, Finney and Andrews 1999). GIS-layers and custom fuel models not only increase the ability to accurately predict fire behavior, but also create endless opportunities to study fire patterns across the landscape (Finney and Andrews 1999). Numerous landscape level metrics have been developed to measure landscape fragmentation, patch density, or the human effects on landscape pattern (Ritters et al. 1995). Important information can be derived from landscape metrics that may be helpful to explain important processes vital to a particular landscape.

Although landscape metrics have been used to better understand many ecologically important issues including applications in fire, little work has been done to better understand how the spatial arrangement of vegetation across a landscape can be linked to fire behavior and the overall fire frequency. Work that suggests a relationship exists include Miller and Urban (1999) who stated forest pattern influences aspects of the fire regime by controlling fuel interaction and connectivity. Hargrove et al. (2000) found that under moderate fire conditions simulated fires were constrained by the spatial arrangement of the most flammable fuels and concluded under these conditions fire patterns were the result of the interaction between landscape pattern and fire dynamics. Turner and Romme (1994) believe crown fire behavior is a function of time and landscape structure and when fuel moistures and wind are moderate and not extreme, landscape pattern constrained crown fire behavior. When

conditions are extreme, landscape patterns have little influence. With the development of GIS, fire prediction models such as FARSITE, and programs like FRAGSTATS, the ability to compare landscape metrics to fire frequency may lead to better understanding of how landscape patterns influence fire behavior and frequency.

The purpose of this study is to look at relationships between the spatial arrangement of the vegetation and resulting influence on fire frequency in southwestern Idaho. A combination of field data and computer-generated models were used to better understand fire-landscape pattern relationships.

The specific objectives for this study include:

- 1) Classify a large remote area using fine-scale classes based on Potential Vegetation Type (PVT) and Structural Stage (SS).
- 2) Develop a representative fuel description for important classes determined by the supervised classification.
- 3) Quantify the relationships between vegetation arrangement and the resulting effects on fire frequency.

LITERATURE REVIEW

SAGEBRUSH STEPPE/JUNIPER WOODLANDS

Western juniper, a common component in the northern Great Basin woodland community type has become an increasing concern to land managers, local residents, and ecologists alike (Bates et al. 2000, Miller et al. 2000, Miller and Rose 1995, Burkhardt and Tisdale 1969). Prolific expansions across broad elevational boundaries, soil types, understory vegetation communities, and previously juniper free areas, have left many people wondering why this is occurring (Wall et al. 2001, Burkhardt and Tisdale 1969). Such attention probably would not be given to western juniper except for the fact that there are many detrimental effects on previously diverse sagebrush steppe and aspen community types, and properly functioning riparian areas (Miller and Wigand 1994, Miller and Rose 1995). Western juniper is affecting watersheds as a whole (Miller and Rose 1995, Wall et al. 2001, Miller and Wigand 1994, Buckhouse and Mattison 1980). A number of hypotheses have been created to try to determine the reasons western juniper has becoming so prevalent. The main supported ideas include climate change, change in fire regime, introduction of domestic livestock, and changes made by human influences such as landscape fragmentation by development of roads and manmade structures (Shinn 1980, Soule` and Knapp 1999, Miller and Rose 1999, Burkhardt and Tisdale 1976, Miller and Wigand 1994). Although varying levels of scientific research have supported these ideas, a combination of events seems most likely.

Climate variability can have a large impact on a plants distribution and productivity. Since the arrival of western juniper into the northern Great Basin, the distribution and

numbers have varied greatly (Miller and Wigand 1994). These large fluctuations can be attributed mostly to changes in temperature and precipitation patterns (Miller et al. 1999b). Historically western juniper was found on rock outcrops, scabland, fractured rock, and other rocky fire protected areas (Burkhardt and Tisdale 1969, Miller et al. 1999b, Burkhardt and Tisdale 1976). Western juniper now occupies 3.2 million ha in varying stages across the northern Great Basin (Miller and Wigand 1994), and at least 162,000 ha can be found in Idaho alone (Burkhardt and Tisdale 1969). The majority of the expansion has occurred in the past 120 years (Miller and Wigand 1994). On Juniper Hill in California, 84% of existing western juniper on big sagebrush (*Artemisia tridentata* spp. *wyomingensis*) sites became established between 1890 and 1920 (Young and Evans 1981). In central Oregon, Miller and Rose (1999) estimated juniper expansion rates in both low sagebrush (*Artemisia arbuscula*) and mountain big sagebrush (*Artemisia tridentata* spp. *vaseyana*) communities began in 1875 to 1885 and peaked between 1905 and 1915. On the Owyhee Plateau Burkhardt and Tisdale (1969) reported juniper expansion began in the 1860's, continued slowly until 1900 and increased the greatest in the 1930's and 1940's. Favorable climate conditions occurring during this time period included mild wet winters and cool moist springs (Miller and Rose 1999). In comparing tree ring widths in central Oregon between 1700 and 1996, 70% of the years between 1875 and 1915 exceeded the long term average for growth (Miller and Rose 1999). Increased precipitation coincided with maximum juniper establishment for this time period and location (Miller and Rose 1999). Historically restricted in distribution western juniper encroachment and expansion across vast regions has been unprecedented and can partially be explained by changing climate conditions.

Fire frequency plays a major role in controlling and suppressing western juniper encroachment (Miller and Rose 1999, Miller and Wigand 1994, Miller et al. 1999a). Fire is also important in creating variable seral structure and diversity across the landscape, which can be vital to many wildlife species (Miller et al. 1999a, Miller and Wigand 1994). Historically fire frequencies that kept juniper at low levels in sagebrush steppe have been estimated at 12-15 years for mountain big sagebrush sites in central Oregon (Miller and Rose 1999), and 30 to 40 years in similar community types in southwestern Idaho (Burkhardt and Tisdale 1976). Longer fire frequencies on the order of 100 years have been estimated for low sagebrush sites (Miller and Rose 1999) due mostly to the lack of fine fuel accumulations and site potential (Bunting et al. 1999). Western juniper has the ability to alter fire behavior by the effects the successional structure has on the surrounding vegetation composition. Juniper less than 50 years of age has the highest probability of mortality when a stand is burned (Burkhardt and Tisdale 1976, Miller and Rose 1999). The greatest mortality occurs in the seedling and sapling state (Burkhardt and Tisdale 1976) where thin bark and short stature make it susceptible to any fire (Miller and Rose 1999). Western juniper also requires many years to reach maturity. Areas with juniper that have not yet matured can be burned successfully without concerns of reestablishment from juniper seed reserves in the soil. Miller and Rose (1995) found that trees less than 50 years of age produced few cones, while 75% of trees over the age of 50 produced heavy cone crops. As juniper stands progress along a successional gradient, the understory vegetation composition begins to change (Bunting et al. 1999). With this encroachment of juniper, once productive sagebrush stands can be reduced to sagebrush skeletons, surrounded by an increasing amount of bare ground (Miller et al. 2000, Miller and Wigand 1994). With loss of sagebrush and graminoid fuels

and greater distance between continuous fuels, the ability to carry fire in later successional stages of western juniper is greatly reduced (Yanish 2002).

Human manipulation and policy have also had an immeasurable effect across the landscape. Native cultures historically used broadcast burning across sections of the landscape for hunting, vegetation manipulation, and war, as observed by early explorers (Shinn 1980). Introduction of domestic livestock reduced fine fuels across landscapes that had not been exposed to large herds of herbivores in the past (Shinn 1980). Public perception of fire being undesirable and the main cause of forest and rangeland damage quickly lead to a national policy of fire suppression (Burkhardt and Tisdale 1976, Shinn 1980). Roads and man made structures restrict rates of spread when wildfires occur (Burkhardt and Tisdale 1976).

In a diverse fire-maintained system fine fuel reduction reduces the number of fires (Burkhardt and Tisdale 1976) and fire size on the landscape (Yanish 2002). The major cause of fine fuel reduction in the northern Great Basin during the 1860's to 1880's was the introduction of livestock (Burkhardt and Tisdale 1969, Miller and Wigand 1994). High stocking rates of both cattle and sheep quickly reduced the amount of fine fuels or grasses needed for fire spread (Burkhardt and Tisdale 1969). Indirectly, domestic livestock have altered the fire regime by reducing fine fuels. Livestock have directly caused juniper encroachment by seed dissemination; reducing or removing preferred forage species, and increasing safe sites for juniper establishment by increasing the shrub density (Burkhardt and Tisdale 1969). Western juniper can more readily establish under a shrub or tree canopy compared to being out in open interspaces (Miller and Rose 1995, Burkhardt and Tisdale 1976). Less than 20% of juvenile juniper plants across 22 sagebrush-dominated sites were

found in the interspaces. Juniper seedlings found beneath a sagebrush canopy grew faster than saplings growing in the interspaces (Miller and Rose 1995). Burkhardt and Tisdale (1976) believe this occurs because shrubs create a microclimate which moderate environmental conditions like soil moisture, creating more favorable conditions. Caldwell and Richards (1989) believe increased surface moisture can be related to hydraulic lift, or deep root water extracted during the night that is brought to the surface and released into the surface soil horizons to be used by the shallow root system during the day. Evidence suggests that not only mountain big sagebrush benefit but desert wheatgrass (*Agropyron desertorum*) can take advantage of increased surface soil moisture. With increasing numbers of safe sites, western juniper has the potential to colonize sites more rapidly over a much larger area.

All of the above factors have left a fire dependant landscape altered for more than a century. Western juniper, an aggressive competitor, has taken advantage of these changes and has become more dominant on the landscape. Land managers are faced with increased problems and shrinking windows of opportunity in which to apply prescribed fires to reverse the trend. As juniper approach 50% of maximum potential canopy cover in mountain big sagebrush sites, the mountain sagebrush declines to 20% of the maximum canopy cover (Miller et al. 2000). Projected times for western juniper to reach closed canopy and successional influence in mountain big sagebrush (*Artemisia tridentata* spp. *vaseyana*) / Idaho fescue (*Festuca idahoensis*) community types ranges from 25-70 years, and 80 years in aspen stands (Miller and Rose 1999, Young and Evans 1981).

Solutions to the problem are possible and depend on the social and economic values of an ever-changing society. Ecological guidelines have been developed by Eddleman

(1999) to better understand and question the short-term, long-term, and landscape-level consequences of restoration efforts. Methods that have successfully removed juniper include mechanical treatments, prescribed fire, herbicide applications, and harvest for products such as fence post (Burkhardt and Tisdale 1969). Each method has economic and ecological negatives and positives that must be considered. But without human manipulation vast landscapes may become more homogeneous as late-seral closed canopy juniper woodlands become more dominant.

Prescribed burning is a useful tool for juniper removal and reduction, and a beneficial way to reintroduce fire to the landscape (Wall et al. 2001, Bunting 1987). The ability to properly choose sites is vitally important in successfully meeting vegetation manipulation objectives (Bunting 1987). The ability to carry fire and remove juniper readily occurs during early phases of woodland initiation (Bunting 1987, Miller et al. 2000, Yanish 2002). But as juniper begins to dominate the site, a threshold is crossed making a reversal to shrublands less likely (Miller et al. 2000). Lack of fuels and inability to kill large dominant trees make successful application of prescribed fire difficult (Bunting 1987). Yanish (2002) found mountain big sagebrush sites were more successfully burned during early- and early mid-successional stages (Fig. 1). Low sagebrush sites would most successfully burn during early- and mid- successional stages. The length of time that mountain big sagebrush is within these limits is very short where as the length of time for low sagebrush is much longer.

Clearly the encroachment of western juniper has many ecological consequences. The understanding of the current juniper encroachment as well as the effects has been well documented (Wall et al. 2001, Miller et al. 2000). Methods for removal have been met with mixed results and lessons learned suggest the need to know the location and the extent of the

area affected which then can be prioritized to maximize successful removal. Encroachment of western juniper is a great concern in the northern Great Basin and possible solutions need to be addressed.

REMOTE SENSING

Modern technology and the invention of the computer have given a new perspective of how we manage our natural resources. Remotely sensed data and improved software interpretation packages allow managers to characterize landscape at different scales. Land classification maps are among the most useful and desired products for predicting current and future vegetation patterns or community types found across a given area (Knick et al. 1997, Clark et al. 2001). The ability to accurately and efficiently predict plant community classes over extensive areas is the desire and challenge for most users (Clark et al. 2001).

While spatial resolution (Jackubauskas et al. 1998), and map accuracies (Skidmore and Turner 1988) have both been past concerns, progress in methodology (Wolter et al. 1995), finer spatial resolution (Jackubauskas et al. 1998), and better accuracy assessment guidelines (Bobbe et al. 2001) has led to acceptance of remote sensing to map vegetation classes.

The majority of the early work was used to map agricultural field differences by crops or growth stages, or in forestry applications to discriminate between key overstory species (Wolter et al. 1995), cover type, and to inventory timber (Franklin et al. 1986). The two main methods to create a land classification map are supervised and unsupervised classifications. An unsupervised classification allows the computer to determine unique classes within the image, and requires no prior knowledge of the study site. While supervised classification uses prior knowledge to define unique classes and uses the computer to classify the image (Jensen 1996). For this study supervised classification techniques were

used due to the availability of ground training sites and evidence of higher overall accuracies (Heide 2002). Heide (2002) concluded that utilizing ground collected training sites to create a classification map utilizing a supervised classification procedure results in an accuracy of 77% compared to an unsupervised method that achieved an overall accuracy of 50%.

Along with different classification methods, additional information can be gained by incorporating additional data layers, which can be composed of vegetation indices, textural information, band combinations, or ancillary data such as soils, slope and aspect, or Digital Elevation Models (DEM) (Kent et al. 1988, Cohen and Spies 1992, Jensen et al. 2001). Some of the common vegetation indices include the Normalized Difference Vegetation Index (NDVI) (Deering et al. 1975), the Moisture Stress Index (MSI) (Rock et al. 1986), and the Tassel Cap transformation, which can produce three useful layers including the Brightness Index, the Greenness Index, and the Wetness Index (Crist 1985, Cohen and Spies 1992, Huang et al. 2002). Cohen and Spies (1992) found that the Wetness Index was the best in estimating structural attributes of Douglas-fir (*Pseudotsuga menziesii*) /Western Hemlock (*Tsuga heterophylla*) forest stands using Landsat data. The wetness value corresponds to the degree of maturity in the forest due to the insensitivity of topographically induced illumination angle, which can be a great concern in complex mountainous regions (Cohen and Spies 1992). Fiorella and Ripple (1993) found similar results for wetness in determining structural attributes for mixed conifer species in western Oregon. The Wetness Index performed better than single bands and most band combinations.

When considering complex or simple vegetation patterns across the landscape the physiological or phenological activity at different times of the year can be used to distinguish among similar vegetation types (Jackubauskas et al. 1998, Clark et al. 2001). By acquiring

imagery during different phenological stages, different plants can be distinguished from the surrounding vegetation due to a unique signature at a particular growth form. In separating four distinct sagebrush communities, Jackubauskas et al. (1998) used NDVI values and compared June and August data (summer) with October images (fall). It was determined that the greatest spectral difference occurred in August, after peak greenness in June, but before senescence of vegetation in October (Jackubauskas et al. 1998). Clark et al. (2001) also had the greatest map accuracies when comparing and creating classification images for early August compared to early June. Overall accuracy was 70.5% in August compared to 54.4% in early June when classifying intermountain plant communities in southwestern Idaho (Clark et al. 2001).

Methods have been developed to classify unknown pixels for different types of data based on their statistical distribution. Parametric and nonparametric classification procedures have both been successfully developed for use in remote sensing image classification. The most common method employs parametric algorithms such as: minimum distance to mean, Euclidean distance, and parallel piped (Jensen 1996). Clark et al. (2001) used a maximum likelihood classification procedure for nine vegetation classes and had overall accuracy of maps generated by Landsat at 60% and SPOT at 65.5% for the same area. Jackubauskas et al. (1998) used a Euclidean distance algorithm to classify 4 sagebrush communities resulting in a 65% overall accuracy. Kent et al. (1988) also used a maximum likelihood classification on classes ranging from old growth conifer, clear-cuts, regeneration, deciduous forest, rock outcrops and others, and found Landsat TM map accuracies in the range of 60 to 70%. Jensen et al. (2001) used a jackknife discriminant analysis classification procedure to classify 4 grassland, 5 shrubland, and 6 woodlands classes based on PVT, and achieved accuracies

ranging from 54 to 77% for grassland classes, 62 to 100% for shrubland classes, and 70 to 100% for woodlands. A complete accuracy assessment was not completed due to sample size (Jensen et al. 2001).

Nonparametric classification methods such as a nonparametric classifier developed by Skidmore and Turner (1988) and a nonparametric discriminant function developed by Knick et al. (1997) are used and sometimes result in higher accuracies using the same data set compared to some of the common parametric algorithms (Skidmore and Turner 1988, Heide 2002, Bunting et al. 2002b). For example Skidmore and Turner (1988) classified an image into eight classes of different forest age based on structure and including a water and urban class to create a continuous map. Using the nonparametric method the overall accuracy was 70% (Skidmore and Turner 1988). Comparing this with an overall accuracy of 56%, and 50% for a maximum likelihood and Euclidean distance procedures, respectively (Skidmore and Turner 1988). Bunting et al. (2002b) found nonparametric statistical methods to be 5 to 10% more accurate compared to linear discriminant analysis and had an 87% overall accuracy for PVT and a 72% overall accuracy for the successional stages of western juniper within each PVT. Heide (2002) also compared parametric and nonparametric methods to differentiate the amount of conifer encroachment into aspen stands with a total of 12 classes being defined. The parametric supervised classification based on Fisher's Discriminant Analysis resulted in an overall accuracy of 63%. A nonparametric supervised classification based on the same training data had an overall accuracy of 77% (Heide 2002). Compared to traditional parametric classification techniques, nonparametric techniques provide an increase in overall accuracy especially when dealing with projects focused on precise class separation.

Along with understanding the important differences between parametric and nonparametric classification techniques a balance between accuracy and precision must be reached and understood. Even though the overall accuracy of a map may be high the precision or number of ecologically significant classes may be low. On the other extreme a map may have many ecologically significant classes but have a low overall accuracy. Understanding the difference between these two definitions will make evaluation of maps and future efforts more useful in mapping the question being asked. Remote sensing technologies offer a solution in mapping large study areas to address concerns of western juniper encroachment. The ability to balance accuracy and precision will be made by the analyst and mapping objectives. Increasing accuracies can be achieved by utilizing additional ancillary layers and by selecting the appropriate spatial resolution and classification techniques. A map with good accuracy and precision can have many applications.

FUEL AND FIRE MODELING

For many years land managers have tried to understand and predict the behavior and pattern of wildland fire (Burgan and Rothermel 1984, Campbell et al. 1996). Fuel models and fire modeling have increased in complexity over the years (Finney and Andrews 1999, Albright and Meisner 1999). Computer programs have increased the potential to look at variable landscapes with different fuel conditions and increase the ability to predict rates of spread and intensity (Rothermel 1983), along with many other fire characteristics. BEHAVE (BEHAVE fire behavior prediction and fuel modeling system) allows the user to develop individual site-specific models (Burgan and Rothermel 1984), or the ability to use broadly defined default models developed by Anderson (1982). Although BEHAVE is very useful in

predicting many important fire characteristics, the non-spatial output makes looking at fire pattern across different fuel models, landscape patterns, weather conditions, and topographic variability, inefficient and impractical (Campbell et al. 1996). Progress in the development of remote sensing, GIS, and computer power potential have lead to the development of complex computer programs that can capture fire behavior over time and space across complex landscapes (Albright and Meisner 1999). FARSITE™ (Fire Area Simulator) is a fire behavior model that addressed many complex questions. FARSITE utilizes GIS created layers to monitor fire effects across variable landscapes under changing environmental conditions (Andrews and Queen 2001, Finney and Andrews 1999, Finney 1998).

Most fire spread models are based on mathematical models (Rothermel 1972), and require numerical inputs to produce results. Fuel parameters needed include: heat content, moisture of extinction, particle density, loading by size class for live and dead fuels, surface to volume ratio, and mean depth to fuels (Andrews and Queen 2001). Methods for collecting fuel data, that are most commonly used, were developed by Brown (1974) and Brown et al. (1982). Inventory of large woody debris can be based on weight, volume, and depth of downed woody material. Dead twigs, branches, stems, and trunks of trees that have fallen, or are located on the ground, are considered downed woody material. Diameter classes categorize woody materials. Materials from 0-0.6 cm are called 1-hour fuel, 0.6-2.5 cm are called 10-hour fuel, and 2.5-7.6 cm are considered 100-hour fuel. Detailed information on weights and volumes per area by fuel class can be calculated (Brown 1974). Additional methods for inventory of fuels including duff, litter, herbaceous vegetation, shrubs, and small trees have been developed (Brown et al. 1982).

By collecting fuel data, custom fuel models can be created. Yanish (2002) created custom fuel models along a western juniper successional gradient, in southwestern Idaho because the 13 models developed by Anderson (1982) used as standards in BEHAVE, did a poor job of accurately predicting fire behavior in a sagebrush steppe/juniper woodland system. Using the NEWMDL in BEHAVE, fuel models can be created using field collected measurements (Burgen and Rothermel 1984). Although BEHAVE has spatial limitations, newly created or the standard fuel models are still the basis for predicting rate or spread and intensity in more complex spatial and temporal models such as FARSITE (Albright and Meisner 1999, Finney and Andrews 1999). Along with incorporating BEHAVE into FARSITE, a GIS-data layer based on fuels and vegetation is also required (Finney and Andrews 1999). Campbell et al. (1996) used a GIS fuels layer created by an unsupervised/supervised procedure to create a GIS-based fire behavior prediction model. FARSITE applications are numerous and include three main types: re-creation of past fires, modeling active fires, and the simulation of fire across a known landscape under certain assumed conditions (Finney and Andrews 1999). Yanish (2002) not only addressed fuel characteristics affects of fire along a successional gradient, but also looked at the role of herbivory in removing fine fuels and the consequences on fire behavior. Other applications of FARSITE include tactical support on active fires, and prioritizing and locating fuel treatment areas (Finney and Andrews 1999). FARSITE also produces maps of fire growth or perimeter positions and fire behavior patterns that are suitable for Arc View applications (Finney and Andrews 1999).

The development of custom fuel modeling procedures and methods has lead to the rapid expansion of fire behavior models. These complex spatial and temporal models have

opened new doors to better understanding landscape level fire issues. Caution must be taken in understanding the limitations and assumptions of these models before research is conducted and results are applied to management questions. Utilizing custom fuel models and addition GIS layers FARSITE has the potential to accurately predict fire behavior from a landscape perspective.

LANDSCAPE PRESPECTIVE

With an increase in the successful implementation of remote sensing and GIS integration, the ability to manage and study large remote areas has increased the number of areas studied at the landscape level (O'Neill et al. 1997, Turner 1990). With an ever-widening view, scientists have begun to try to link ecological function and process (Gustafson 1998) to spatial and temporal landscape patterns. A landscape is a mosaic of patches of different spatial arrangement giving each landscape a unique pattern (Urban et al. 1987). Landscape pattern can be influenced by many variables including historical site evolution, disturbance regimes, human interaction, and current land use. By understanding the complexity and variability of the landscape a greater understanding of the driving forces behind the system can be achieved and result in more effective management.

Many landscape indices have been developed that try to capture important aspects of landscape pattern (O'Neill et al. 1988) at different scales. Important and vital information can be extracted from a landscape perspective by properly defining the grain and extent (Turner et al. 1993). Grain is considered the finest level of spatial or temporal resolution within a data set (Turner et al. 1993, McGarigal and Marks 1995). For example a 30x30-m pixel for a Landsat image would be the finest possible grain for that image. Extent defines the size of the study area or the temporal time frame under review (Turner et al. 1993

McGarigal and Marks 1995). Examples include 6th order catchments or the entire Owyhee Plateau physiographic region.

Along with understanding grain and extent there are three levels of metrics at which a landscape can be measured (McGarigal and Marks 1995). Levels of metrics include patches, classes, and landscapes. Since the purpose of this project was focused on comparing different landscapes, landscape-level metrics were utilized. Landscape-level metrics include all patch types or classes over the entire extent of the landscape and can be beneficial in understanding properties of the patch mosaic (McGarigal 2002). Currently many metrics exist and the ecological importances of some have not been shown. However, many studies (Urban et al. 1987, O'Neill et al. 1997, Turner 1990) use a number of different metrics to measure change, pattern, and structure from a landscape perspective. Many metrics measuring similar landscapes compute the same characteristics or produce redundant information making the number of current metrics and their ecological important difficult to understand. Ritter et al. (1995) tested 55 different metrics and found that six univariate metrics could explain 87% of the variability of the landscape. Eighty-five different maps from across the United States with a few broad rangeland and shrubland classes were used in the analysis. Turner (1990) suggests using simple indices and measures can capture aspects of landscape pattern.

Numerous examples exist where different metrics have been tested on different types of landscapes resulting in a better understanding of the driving forces of that system (O'Neill et al. 1988, Keane et al. 1999, Turner et al. 1993). Keane et al. (1999) utilized a fire succession model for a real landscape using fire modeling and forest successional modeling to test different metrics over variable time with different management strategies and climate

conditions. With simulated maps composed of dominant tree species, above ground standing crop, leaf area index and net primary production (NPP) the following metrics were tested: patch density, edge density, evenness, contagion, and interspersion. By comparing the metrics across all simulated maps, some general results could be found. Changes in landscape pattern over time are more influenced by fire than climate alone in the simulations (Keane et al. 1999). Future landscapes may be more diverse and patchy if fires are allowed to burn, resulting in uneven aged stands becoming unevenly distributed, resulting in a high edge to density number and lower contagion (Keane et al. 1999). Chuvieco (1999) used Landsat remote sensing technologies and landscape principles to compare landscape indices on pre- and post-fire conditions. Metrics tested include compactness, fractal dimension, number of patches, average patch size, shape, and diversity. Results conclude that the mean patch size was nearly twice the mean pre-fire size. Compactness was reduced resulting in more complexity in patch shape. Diversity values were reduced after the fire and fractal dimension increased after the fire resulting from increased shape diversity. Chuvieco (1999) concluded that compactness and fractal dimension provided an estimate of shape and heterogeneity as a result of fire.

As mentioned previously, humans have altered the fire frequency and fire regime across much of the landscape. Not only has this lead to fewer fires, but it has also lead to the change in spatial and temporal extent to which fires will burn in the future (Urban et al. 1987). Fire suppression and fuel accumulation may now burn larger areas under increasing intensity (Urban et al. 1987). Contagion and fractal dimension metrics may be important in understanding human influences across the landscape (Gustafson 1998, Krummel et al. 1987). Contagion is a measure of clumpiness or the tendency of patch types to be spatially

aggregated (McGarigal 2002, Gustafson 1998). For example this could be important in locating probable continuous seed source areas of a particular species after a fire. Fractal dimension has been correlated to the degree of human manipulation of the landscape (O'Neill et al. 1988). O'Neill et al. (1988) found that landscapes dominated by agriculture had simple polygons and low fractal dimensions and landscapes dominated by forests had complex shapes and high fractal dimension (O'Neill et al. 1988). A landscape highly manipulated by man could be separated from a natural undisturbed landscape.

Landscapes demonstrate important ecological patterns. Many methods have been developed to measure patterns and link the results to ecological processes. Many landscape metrics have been developed to test different aspects of landscape pattern. By utilizing computer generated maps, fire prediction models, and landscape statistics the main goal of this research was to better understand the influence of the spatial arrangement of numerous successional classes to fire behavior characteristics such as fire frequency.

METHODS

Study Site Description

The Owyhee Plateau is located in southwestern Idaho in Owyhee County. The study area is defined by the Idaho boundary on the western edge, and an elevational boundary of 1250 m on the north and eastern edge, and by the Owyhee River on the southern edge. The Owyhee Plateau can be characterized by three small mountain ranges, the Silver City Range being furthest north, Juniper Mountain being furthest south and South Mountain in the middle (Fig. 2). Steep canyons and complex terrain are interwoven with broad flat tables. Elevation for the study site ranges from 1250 to 2600 m.

Average annual precipitation ranges from 250 to 560 mm (WRCC 2003) and falls primarily as late fall rain and winter snow, which can persist in the higher elevation until mid-summer. Average temperatures range from -6.6 °C in December and 26.7 °C in July (WRCC 2003), with large variability due to elevational changes across the study site.

Soils and geology over the study site vary considerably in both age and complexity. The underlying pre-Tertiary granite basement rock exposed in the Owyhee Mountains is composed of quartz-diorite, quartz-monzonite, granodiorite, and is considered a part of the Idaho batholith (Harkness 1998). Common soil series include the Enko series (Camborthids), Graylock series (Cryorthents), and Nazaton series (Cryoborolls), Poisoncreek series (Agrixerolls), and Takeuchi series (Haploxerolls), which are common to the Silver City Range. The Paleozoic metamorphic rock of South Mountain is the oldest parent material of the area and can be described by a thick dark surface layer with weakly developed subsoil (Harkness 1998). Common soil series include the Ola series (Haploxerolls) and the Povey series (Cryoborolls). Juniper Mountain is a result of a basaltic eruption and is

described by a large area of ash-flow tuff and ignimbrite (Harkness 1998). Soils series found on Juniper Mountain include the Avtable series (Haploxeralfs), Douglas series (Haplargids), Dranyon series (Cryoborolls), Gaib series (Argixerolls) and Nipandtuck series (Torriorthents), which were formed from silicic flow rock (Harkness 1998).

Common tree species found on the Owyhee Plateau include western juniper, curl-leaf mountain mahogany (*Cercocarpus ledifolius*), Douglas-fir, quaking aspen (*Populus tremuloides*), and a small component of subalpine fir (*Abies lasiocarpa*). Common shrub species include mountain big sagebrush, low sagebrush, shiny-leaf ceanothus (*Ceanothus velutinus*), antelope bitterbrush (*Purshia tridentata*), green rabbitbrush (*Chrysothamnus viscidiflorus*), mountain snowberry (*Symphoricarpos oreophilus*), bittercherry (*Prunus emarginata*), and chokecherry (*Prunus virginiana*). Common grass and grass-like species include, bluebunch wheatgrass (*Pseudoroegneria spicata*), Idaho fescue, mountain brome (*Bromus marignatus*), Sandberg bluegrass (*Poa secunda*), Kentucky bluegrass (*Poa pratensis*), squirreltail (*Elymus elymoides*), Great Basin wildrye (*Leymus cinereus*), and elk sedge (*Carex garberi*). Common forb species include western yarrow (*Achillea millifolium*), arrowleaf balsamroot (*Balsamorhiza sagittata*), sticky geranium (*Geranium viscosissimum*), mule's ear (*Wyethia amplexicaulis*), buckwheat (*Eriogonum* spp.), paintbrush (*Castilleja* spp.), and lupine (*Lupinus* spp.).

OBJECTIVE 1

Objective one was to develop a supervised classification for the Owyhee upland study area utilizing a Landsat 7 ETM + image to map western juniper encroachment. The first step in this process was collecting field measurements called training sites. Training sites were based on Potential Vegetation Type (PVT) or vegetation taxa based on groupings of habitat

types that have similar overstory composition, structure and environmental requirements and Structural Stage (SS) which are successional stages defined along a gradient ranging from: herbland, open and closed shrublands, initiation woodland, young woodland, young multi-story, and old multi-story woodland (Bunting et al. 2002b). Training sites were used to identify locations of known vegetation later in the process. Some training sites were set aside as validation sites and used to assess overall map accuracy. The next step was to reference the satellite image of the study area. Geo-referencing is required to most accurately place the training sites on the image. Next the numbers of bands and band combinations or vegetation indices were chosen. Different bands correspond to different physical or on the ground measurements, while vegetation indices are useful in reducing topographic effects. After all the layers have been combined, defining and marking known areas of each of the vegetation types was completed. With the help of black and white aerial photographs, boundaries between different classes were defined. When each vegetation class's spectral signature was defined, classification was completed. Different methods of classification have been developed over the years with each method having advantages and disadvantages based on the underlying principles of that method and the statistics of the data set. The final and most important step in creating the classification map was a quantitative accuracy assessment. The accuracy assessment was computed using the validation pixels with a cross validation procedure (Foody 2002). An error matrix was completed for each of the classification techniques. Once the classification was complete and a map was created decision rules were used to increase the overall quality of the map by restricting the distribution of certain classes based on aspect and elevational boundaries.

Preliminary Landscape Classification

Classification of common plant communities found on the Owyhee Plateau was based on PVT and SS (Table 1). Community classes were modified from the ICBEMP mid-scale classification analysis described by Quigley et al. (1996) and Hessburg et al. (1999), which take into account overstory composition, structure, and environmental requirements for large broad habitat types of the Columbia Basin (Bunting et al. 2002b). Bunting et al. (2002a) described the 17 PVT's used at the broad scale across the Columbia Basin. These PVT's were modified to a much finer scale using soil information and known presence or absence of western juniper on specific sites for the study area (Bunting et al. 2002b). PVT's were also used for the tree species Douglas-fir, subalpine fir, and aspen. Aspen communities were considered as a PVT for the mapping purposes only with the understanding that these sites can and will eventually be replaced by a conifer species which would represent the sites actual PVT.

The main interest of this study was focused on PVT's with the potential to develop into juniper woodlands. PVT's of focus include mountain big sagebrush, low sagebrush, bitterbrush, and curl-leaf mountain mahogany. Three cover types based on the previously mentioned PVT's were used to account for areas supporting western juniper. Cover types developed include herbaceous vegetation, shrubland, and woodlands (Bunting et al. 2002b). A structural stage classification was also developed based on modifications from Hessburg et al. (1999) and used by Bunting et al (2002b). Structural stages include; herbland, open and closed shrubland, initiation woodland, young multi-story woodland, and old multi-story woodlands, which were further modified for this study do to results presented by Bunting et al. (2002b). A structural stage outline was also used for the forest PVT's. Structural stages

include sapling forest, pole forest, young multi-story forest, and old multi-story forest. Smaller components of the landscape also defined by PVT's include mountain shrub, wet meadow, annuals, and rock. Disturbance by mining and water classes were used to create a continuous map. PVT and SS detailed descriptions can be seen in Appendix A.

Training Sites

Training sites greater than 100x100 m were placed in the center of relatively large homogeneous areas with respect to PVT and SS, and were located using a Magellan GPS unit. For each class determined from the PVT and SS classification at least 8-10 training sites were collected, providing enough plots for the training and validation data sets. Vegetation canopy by percent was estimated ocularly, and broken down into specific groups including: juniper, tall shrub, Douglas-fir, aspen, medium shrub, perennial and annual grasses, and perennial and annual forbs. The six most abundant species based on percent canopy cover was also estimated. At each site elevation, aspect, and slope was recorded. At each site within a forest PVT the percent of trees above 2-m in height or below this height was ocularly measured. During the 2002 summer field season 308 training plots were sampled and during the 2003 season 258 training sites were recorded. Over 425 training plots were also available for the area and were collected between 1999-2001 and used by Bunting et al. (2002b). All GPS point which had an accuracy of less than 3 m when the Wide Area Augmentation System (WAAS) was functional were down loaded to Microsoft© Excel 2000 and imported into Arc View (Version) 3.3© to create shape files.

Satellite Image Processing

The Landsat 7 ETM + satellite image was purchased from USGS Earth Resource Observation System Data Center or (EROS). The image was referenced to Path 42 Row 30

in the Worldwide Reference System (WRS), and was acquired during the first week of August 2002. The image was geo-referenced to the UTM coordinate system, Zone 11 North, Spheroid Clark 1866, North American Datum 27 (NAD 27) and is represented by 30x30-m pixels. Six of the eight bands were used in the classification procedure including bands one through five, and seven, which represents the visible, near infrared, and mid-infrared wavelength regions of the electromagnetic spectrum. Band 6, the thermal band and the panchromatic band were not used due to the difference in spatial resolution. The Data Preparation Module in ERDAS IMAGINE™ (Version) 8.6 was used to subset the image based on a 1250 m elevational boundary for the northern and eastern boundary. The Owyhee River on the southern extent, and the Oregon-Idaho state line for the western boundary. The Modeler Module in ERDAS IMAGINE was used to convert each pixel value to radiance values and then to exo-atmospheric reflectance values, which most accurately allows the data to be quantified.

Additional data layers were created in ERDAS IMAGINE Modeler Module which includes an NDVI layer, a MSI layer, and three Tassel Cap layers using coefficients for Landsat 7 ETM + developed by Huang et al. (2002) which were not normalized. See Table 2 for vegetation indices used and equation used to create them. The ERDAS IMAGINE Interpreter Module was used to stack all layers into one image containing 11 layers used in the classification procedure.

Supervised Classification

Supervised classifications are created using on ground knowledge to create unique signature measurements for each class of interest from the image and then are cross-validated using validation pixels in an error matrix. For each class represented, at least 3 training sites

were used for classes with small importance (Putr R1, R3A, Water, and Abla) and 8 training sites for important classes (Artr, Arar, and Cele PVT's) within the study area. In total, the number of pixels per class varied from 10 to 199 depending on the number of training sites and size of the areas used to define each class. As suggested by Congalton (1991) 50 pixels were used if possible to validate each class characterized by high variability. Validation sites were created by randomly selecting 20% of the training sites within each PVT and SS and placed in an individual file apart from the training sites used in the classification. See Table 3 for a detailed breakdown of number of training and validation sites per class and the total number of pixels used in each class.

The remaining 80% of the training sites were used to refine the spectral signature for each class. Groups of training sites based on PVT's were projected on the Landsat image. Digital orthophoto quarter quadrangles or (DOQQ's) were opened in a separate viewer and represent higher spatial resolution black and white aerial photographs. DOQQ's were used to cover the majority of the study area and saved in separate files based on one of the three mountain ranges. Training sites were also projected on the DOQQ's and were geometrically linked by ERDAS IMAGINE to more accurately define boundaries of each training site. The region-growing tool in ERDAS IMAGINE was used to expand and define the training site boundaries based on similarities to adjacent pixels. The boundaries in some instances were manually manipulated to change the size and shape of the region insuring that each training site represented only one class. Each area of interest or (AOI) was saved as a separate file and was added to the signature editor in ERDAS IMAGINE. For each class all training sites were compared for their spectral uniqueness. Histograms and statistical analysis helped remove outlier-training sites and helped create unique class signatures. The remaining

training site AOI's for each class were reopened and saved as one AOI file. Individual class AOI's were also created for the validation sites and saved in a separate file. All files were then exported into ASCII format for use in Excel and the SAS (Version) 8.02 statistical package.

Nonparametric Discriminant Analysis

The DISCRIM procedure in SAS was used to perform k nearest neighbor nonparametric discriminant analysis. The training set and validation set were imported into SAS and run as a cross validation procedure to determine the accuracy. An adjustment to the number of classes was done at this time if separation appeared to be impossible or sample size was inadequate. The number of pixels within the class of interest as well as what classes were being mixed was considered. If classes were mixed between SS within the same PVT than the classes were combined. If mixed pixels occurred across multiple PVT's than the classes were not changed. The procedure was carried out again for the new number of classes. Next the entire image was classified based on the training sites. Mahalanobis distance in multi-dimensional space was used to assign the pixel values for every pixel in the study site based on the training data. Seven nearest neighbors were used due to the lowest error rate in cross validation described by Heide (2002). Seventh nearest neighbor was used to define the radius of a circle of a particular class based on a set point to that points seventh nearest neighbor to determine density within the circle (SAS 1999). Utilizing a specific squared distance formula the values of r and k determine the irregularity in the density function with low r and k values producing jagged density estimates while large r and k values produce smooth density estimates (SAS 1999). The output file contained values for

every pixel in the study area and was opened as a table in Arc View and used to create a continuous map.

Parametric Discriminant Analysis

The DISCRIM procedure in SAS was used to develop two parametric classification techniques. The first technique involved creating linear equations with coefficients for each class based on pooled covariance matrix statistics, which yields a linear function with the equations (SAS 1999). A classification rule was developed to classify all unknown pixels within a class. The second method used involved a classification criteria based on individual within group covariance matrix, which involved no pooling and yields a quadratic function (SAS 1999). The validation set in both procedures was cross validated against the training data, which produced an error matrix and a corresponding accuracy assessment.

Accuracy Assessment

Validation data was used to assess the accuracy of the three classification methods described above. An error matrix expresses the number of sample pixels assigned to a particular class relative to the actual on-ground verified class (Congalton 1991), and was created for each classification. Overall accuracy, producer's accuracy or error of omission, and user's accuracy or error of commission were calculated for each matrix (Jensen 1996, Story and Congalton 1986). The overall accuracy measures how well the accuracy is for the entire map. This is measured by adding all of the correctly classified pixels together and dividing by the total number of training pixels used in the classification (Congalton 2001). Producer's accuracy is a measure of how well a certain area can be classified from the analyst's perspective. This is calculated by taking the number of correctly defined pixels in a class and dividing by the total number of pixels from that column (Congalton 2001). User's

accuracy measures how accurate the map in the field would be. User's accuracy is calculated by taking the number of correct pixels for a given class and dividing by the total number in that category or row (Story and Congalton 1986). The error matrix was created in Microsoft Excel. In addition a kappa statistic was produced for each classification. The kappa statistic tests to determine whether the results produced in the error matrix are significantly better than random chance (Congalton 1991).

Classification Refinement

Numerous classification attempts were made to find the most desirable number of classes, training sites, and number of pixels used based on the criteria of most accurately mapping young juniper woodland classes. Employing results by Heide (2002) and Bunting et al. (2002b), the nonparametric classification technique appeared to yield the highest overall accuracy and therefore was used in the initial classification setup. The first attempt used 44 classes and 11,564 pixels and achieved an overall accuracy of 40% (Table 4). From looking at the error matrix it quickly became apparent that a number of classes were being confused with very similar classes within the same PVT. At this stage these classes were combined to improve the overall accuracies while maintaining a focus to most accurately map young juniper woodland classes across the mountain big sagebrush, low sagebrush, and bitterbrush PVT's (Table 5). The nonparametric classification was repeated for 34 classes using 11,689 pixels and achieved an overall accuracy of 55% (Table 6). Next the size of AOI's used for the mountain big sagebrush and low sagebrush PVT's were reduced to determine if mixing of pixels was occurring because the size of the AOI boundary was too large. As a result of this process the classes remained the same at 34 but the number of pixels was reduced to 5,674, which resulted in an overall accuracy of 69%. The process of

refining the AOI's for the other PVT-structural stage classes was repeated and the number of pixels was further reduced to 3,110 with 34 classes and achieved an overall accuracy of 76%.

Although the accuracy was high at this point, it was determined that the high accuracy came at the expense of removing too many training sites. If too many training sites are removed the classification will be based on only a few samples that may not cover the variability within a particular class. To create a more accurate map with more training sites, the overall accuracy was reduced with more total pixels being utilized. A better ratio was achieved between the total number of training pixels and the total number of validation pixels for each class falling close to 100 training pixels and 50 validation pixels suggested by Congalton (1991). Two classes were also combined and reduced the final number of classes to 32 (Table 7).

Decision Rules

Decision rules were used to restrict the distribution of particular classes based on known elevational boundaries and aspect characteristics. Information acquired from the training sites about elevation and aspect as well as in the field knowledge and experience was combined to create decision rules. Classes that were involved in the process include Abla, Psme F2, Psme F3, Psme F4, Brte, and Taas. Additional decision rules were used to reclassify areas of known agriculturally active areas that include active crops or hay meadows. Riparian area buffers were also used to create a riparian /broadleaf class where appropriate. Using ARC grid and an AML file this process was possible. A detailed instruction guide providing step-by-step instructions for the entire supervised classification including decision rule procedures can be found in Appendix B.

OBJECTIVE 2

The goal of objective two was to develop a representative fuel description for classes that correspond to the map created by the supervised classification. This involved collecting fuel data plots at the same location as the training sites used to create the classification map. Collecting as many fuel plots within each class as possible, custom fuel models were created using the field collected data in BEHAVE (Version) 4.4. The 15 custom fuel models created by Yanish (2002) were used as a building block to create a continuous fuels map of the study area. Three new custom fuel models were created along with adding additional plots to some of the models created by Yanish (2002) (Table 8). With the completion of the new fuel models a file of all the custom fuel models was created for use in FARSITE (Version 4.04). The map created in objective one was also imported into FARSITE and serves as the landscape vegetation map.

Fuel Data Collection

Fuel data measurements were based on methods developed by Brown et al. (1982). Modifications to the sample plot design were developed by Yanish (2002) and were followed during collection. A double sampling technique using four 50x50-cm quadrats was used to measure the herbaceous biomass and litter component. Each quadrat was examined and the one with the highest biomass was used as the standard to compare the other three quadrats against. The remaining three quadrats were compared as a percentage value of the standard quadrat. A 50x25-cm quadrat measuring litter was also taken from the quadrat with the highest biomass total. The quadrat with the highest herbaceous biomass and largest litter component was clipped or collected, dried, and weighed. Dead woody debris was estimated using a line transect using a planar intercept technique (Brown et al. 1982). Shrub biomass

was measured using two 1-m radius plots and stem counts based on diameter classes to estimate biomass. Tree densities were also estimated based on a 4-m plot or a 10-m plot if no trees were found within the original 4-m plot (Fig. 3). Samples were collected across the study site based on cover type locations from the preliminary supervised classification and knowledge in the field. All sites where grazing during the present year was apparent were not used.

Fuel Data Analysis

Methods for fuel data analysis were developed by Yanish (2002) and were used here to allow utilization of the 15 custom fuel models created. Sampling data was entered into Excel and used in SAS and BEHAVE. Canonical discriminant analysis statistical methods were used because the components of the fuel model were weighted against each other and compared among cover types. Components that were compared include herbaceous average, dead average, cover average, litter average, shrub weight, crown canopy, and down dead woody as described by Yanish (2002). He used BEHAVE to predict flame length and rate of spread using the collected field data. A variety of environmental and topographic conditions were compared to create the representative fuel models. Low, medium, and high fuel moisture content were tested with a slope default of 30%, and wind speed ranging from 0-40 kph at 8 kph intervals. The custom fuel models created in BEHAVE were used as fuels input layer for FARSITE.

OBJECTIVE 3

Objective three was to determine the relationship between the vegetation spatial pattern and resulting fire frequency. This was achieved by creating a fire frequency grid using two different methods with different advantages and disadvantages, and running

FRAGSTATS developed by McGarigal et al. (2002) to produce landscape metrics. The outputs of these processes were analyzed using linear regression statistics.

The models created in BEHAVE were incorporated into FARSITE. An ASCII grid with 30-m resolution was produced for FARSITE using the supervised classification map. The grids used in FARSITE include elevation, slope, aspect, cover type, and crown cover. In Method A FARSITE was used to create fire frequency grids in three watersheds by randomly generating 100 fires within each watershed boundary. A flat landscape was used and weather conditions were set to mimic moderate fire conditions because extreme wildfire conditions will burn across all fuel types regardless of fuel distribution and natural fuel breaks (Turner and Romme 1994), and may cover up relevant fire patterns by burning equally across all fuel types. In method B a minimum travel time method (Finney 2002) was used to create a fire frequency grid across an area that encompassed the three watersheds. Slope, aspect, and elevational layers were utilized to create a realistic landscape and weather conditions were set to mimic wildfire conditions to test fire behavior under wildfire conditions.

Landscape Metric Selection

Nine landscape metrics were selected to compare the vegetation spatial arrangement with fire frequency. Five basic groups of metrics were selected to measure a variety of landscape patterns. Within each of these groups a metric or multiple metrics were selected to best represent the group as a whole. Because little work has been completed to analyze the spatial arrangement of juniper and fire frequency, a variety of metrics were selected to determine which group type and individual metrics produced the best relationships. Groups include: Area/Density/Edge, Shape, Isolation/Proximity, Contagion/Interspersion, and Diversity. Group one consists of the metrics Patch Density, Edge Density, and Mean Area.

Group two used the metric Landscape Shape Index (LSI). Group three is represented by the landscape metric of Euclidean Nearest Neighbor Distance. Group four metrics include Contagion and the Interspersion and Juxtaposition Index (IJI). Group five metrics include Simpson's Diversity Index and Simpson's Evenness Index. Metrics were selected to cover a variety of groups with commonly used metrics selected from each group. The ability to convey important information along with a past record of being ecologically relevant was also a determining factor in metric selection.

Landscape Pattern Analysis

Method A

Three HUC sixth order watersheds were used to evaluate the effects of landscape pattern on fire occurrence. These watersheds include: Red Canyon, Smith Creek, and Current Creek (Fig. 4). Due to the complex nature of fire behavior prediction and computational time in FARSITE, the slope, aspect, and elevational data layers were not used and in its place a flat landscape was developed. Within each watershed four woodland PVT-SS classes were compared, Artrv W1, Artrv W2, Artrv W4, and Artrv W5. In each watershed 100 random points were generated and served as independent fire start locations. Fire parameters remained the same for each time step across all trial runs by using the same temperature, humidity, elevation, and wind speed. Wind direction was the only exception as a random direction was selected for each FARSITE run. Wind direction was randomly selected to insure that the leeward side behind a stationary fire direction would be burned instead of producing an edge effect where the leeward side would not burn at all. Without changing wind direction a large proportion of certain sections of the watersheds would be burned with high frequency while other areas would not be burned at all. By changing wind

direction some of this problem was resolved. All fires simulated moderate fire conditions and burned for six hours during the month of August. Fuel moistures were set to mimicked moderate burning parameters making the assumption that burning under wildfire conditions would result in uniform fire behavior across all fuel types. All fire outputs were saved as shape files then converted to grids to create the fire frequency layer for each watershed.

With the frequency grid of how many times each pixel burned, hypothetical relationships between fire occurrence and the vegetation patterns were tested. Vegetation pattern was characterized by using ecologically significant landscape metrics. Artrv W1, Artrv W2, Artrv W4, and Artrv W5, were used in the analysis to determine in which successional stage results would be significant and most strongly correlated. Grids were created for each class by masking out all other classes and then were converted to shape files. The shape file was then assigned x and y coordinated to each pixel value which was then used to randomly select points. Within each class and in each watershed 25 to 30 pixels were randomly selected making sure that the pixels were not located next to each other. In Current Creek Artrv R3B and Artrv W1 classes were combined to provide enough random locations. Using the 25 to 30 pixels per class, a reference square of 15x15 pixels was centered over each random pixel. Each of the reference areas were then clipped out of the vegetation layer by Arc View, saved as a grid, and run independently through FRAGSTATS to produce the landscape metrics. Metrics that were analyzed include; Patch Density, Mean Area, Edge Density, Landscape Shape Index, Euclidean Nearest Neighbor Distance Distribution, Simpson's Diversity Index, and Simpson's Evenness Index, Contagion, and the Interspersion and Juxtaposition Index (McGarigal et al. 2002). Each of these metrics was then compared to the fire frequency values from the center of each corresponding pixel and analyzed

statistically for each watershed. Statistical analysis involved using SAS to produce linear regression equations to determine the relationship of landscape metrics and fire frequency.

Method B

In method B to develop a fire frequency grid, wildfire conditions were created across the simulated natural environment. The fuel model layer, slope layer, aspect layer, elevation layer, along with weather and wind conditions were used to create a fire frequency grid using the fire growth minimum travel time method developed by Finney (2002) which is computationally more efficient than FARSITE. The most important difference between the two methods was using this method the fire environment was kept constant. Although the methods to measure fire spread are different, the results between the minimum travel time method and FARSITE are very similar (Finney 2002). Random start locations totaling 25,000 fires were used and produced a pixel-by-pixel probability of the number of times each pixel burned divided by the total number of fires across the landscape, which was then multiplied by 100 to create the fire frequency information. The entire landscape developed by Yanish (2002) was used to keep edge effects outside the watershed boundaries of interest, as wind direction was held constant throughout the process. Comparisons between the four successional stages utilized the same random points and same FRAGSTATS outputs used in method A. The only difference in analysis came from using the fire frequency values from the minimum travel time grid. Instead of having fire frequency values ranging from zero to 17, pixel values for the minimum travel time method divided the number of times each pixel burned by 25,000, which was then multiplied by 100 to produce values ranging from 0 to 5.7.

RESULTS

Accuracy of the Nonparametric Discriminant Classification

An accuracy of 69% was achieved with 32 classes and 3,546 training pixels (Fig. 5). Although this cannot be said for all classes, the most prevalent PVT's had higher numbers of training sites, validation sites, and pixels compared to some classes that represent only a small fraction of the study area. The kappa statistic computed for the nonparametric classification was 68% (Fig. 5). Of the 32 classes used in the nonparametric technique, 17 classes had higher user's accuracy and 18 classes had higher producer's accuracy compared to the quadratic parametric technique. Classes that achieved the highest overall accuracies include Water, Taas, and Mines. Important vegetation classes that achieved high accuracies using the nonparametric approach include: Arar R1, Putr R3A, Artr W4, Potr F4, and Psme F4. Classes that the nonparametric method had the most trouble classifying correctly include: Artr W1, Artr W2, Arar W1, Arar W4, Arar W4, and Arar W5. See Fig. 6-11 for a detailed comparison between each of the methods user's vs. producer's accuracies based on PVT-structural stage classes. Since this technique produced the highest overall accuracy and the majority of the higher user's accuracy this technique was used to create the final vegetation map (Fig. 12).

Accuracy of the Linear Parametric Discriminant Classification

An accuracy of 52% was achieved using 32 classes and 3,546 training pixels (Fig. 5). The kappa statistic computed for the linear parametric classification was 50% (Fig. 5). One of the 32 classes had higher producer's accuracies compared to the nonparametric method and two classes had higher user's accuracies than the nonparametric method. Two classes had the same results for producer's accuracy and one class for user's accuracy. Classes with

the highest accuracies using the linear parametric technique include: Water, Mines, Taas, and Brte. Important vegetation classes with high accuracy include: Putr R1, Putr R3A, Artr W4, Psme F2, and Psme F4. Classes with user's and producer's accuracy below 40% using this method include: Artr R3B, Arar W1, Artr W2, Cele*4, and Mountain Shrub. See Fig. 6-11 for a detailed comparison between each of the methods user's and producer's accuracies based on PVT-structural stage classes.

Accuracy of the Quadratic Parametric Discriminant Classification

An accuracy of 64% was achieved using 32 classes and 3,546 training pixels (Fig. 5). The kappa statistic computed for the quadratic parametric classification was 62% (Fig. 5). Eleven of the 32 classes had higher producer's accuracies compared to nonparametric results. Of the 32 classes of user's accuracies again eleven classes were higher than the nonparametric technique. Four classes achieve the same user's accuracy regardless of technique, while three classes had the same producer's accuracy regardless of the classification method. Classes with the highest accuracies using the quadratic parametric technique include: Water, Taas, and Mines. Important vegetation classes that achieved high accuracies using this method include: Putr R1, Putr R3A, Putr W2*7, Artr*2, and Artr W4. Classes with low accuracies using this technique include: Arar W1, Artr W1, Arar W2, and Arar W4. See Fig. 6-11 for a detailed comparison between each of the methods user's and producer's accuracies based on PVT-structural stage classes.

Decision Rules

Congalton (2001) suggest visual inspection is one of five ways of assessing map accuracy. With this in mind and due to the complex nature of the study area, additional refinement of the map was developed. By understanding some of the plant communities'

tendencies including strengths and weaknesses in relationship to establishment patterns, decisions rules based on elevation, aspect, and in the field experience were used to create a better final product. Brte was removed from Juniper Mountain due to observational experience and the severe mixing that occurred to known areas of Arar R1. It was felt that this would create a more accurate map for this area. Also, all of the Putr PVT-SS classes were removed from Juniper Mountain. Again years of experience of exploring this area help make the decision that the Putr classes were mixed with the Artr classes known to be at these locations. Similar mixing also occurred on South Mountain and the Silver City Range. Because the majority of the training sites came from these two areas and far less on the ground experience was present, these classes were not altered. An elevational boundary was considered for Putr PVT's, but would have provided little significant improvement. Elevational boundaries that were utilized included restricting Abl a and Psme F2, F3, and F4 above 1900 m, Brte below 1850 m, and Taas below 1500 m.

A perceived large increase in the overall map quality was achieved by using aspect rules. Both Brte and Taas annual classes were restricted to south facing (140-250°) aspects. The forested classes including Abl a, Psme F2, F3, F4 where limited to northern (250-60°) aspects. This restricted the distribution of many classes, particularly Psme F3, which was over estimated. In addition, classes that were known not to be located on a mountain range were removed automatically. For example Abl a was removed from South Mountain and Juniper Mountain while all the Psme PVT's were removed from Juniper Mountain. Tables of the decision rules can be found in Appendix C and D.

Fuel Model Comparisons

The seven dependent variables including herbaceous average, dead average, cover average, litter average, shrub weight, crown canopy, and down dead woody were significantly different when compared among cover types (p-value <0.0001). Canonical discriminant analysis was performed to test the effects of succession on the dependent variables. The first five canonical correlations layers each had a p-value <0.0001. The three most important variables in three layers with the highest amount of information were crown cover, herbaceous biomass, and shrub biomass. The top three variables explain 90% of the variation in fuel loading due to the successional stages. The first canonical model can distinguish successional stages from one another with ($r^2=0.71$) with a p-value <0.0001. Detailed information about fuel distribution, fire behavior, and management implications along the successional gradient can be found in work done by Yanish (2002).

Fire-Landscape Pattern Relationships

Statistical analysis was compared across the four successional classes (Artrv W1, W2, W4, W5) within the three watersheds using both method A and B. Vegetation distribution as well as fire frequency grids for methods A and B can be seen in Fig. 13-15. A positive (+) or negative (--) trend, along with the p-value for each successional class and landscape metric can be seen in Tables 9-12. Each landscape metric was evaluated for consistent trends and significant trends. A consistent trend occurs when either all signs for a given metric are positive or negative across each watershed and method. Significant trends were considered to be those with a p-value less than 0.1.

Artrv W1

Within the Artrv W1 class there were not any consistent trends or significant trends (Table 9). There were seven significant individual metrics within Current creek including two in method A and five in method B. Significant metrics in method A include Contagion ($r^2 = 0.155$) and Simpson's Evenness ($r^2 = 0.122$). Significant metrics in method B include Edge Density ($r^2 = 0.206$), Landscape Shape Index ($r^2 = 0.197$), Contagion ($r^2 = 0.110$), Simpson's Diversity ($r^2 = 0.152$) and Simpson's Evenness ($r^2 = 0.161$). Red Canyon produced five significant results including two from method A and three from method B. Significant metrics in method A include Mean Area ($r^2 = 0.117$), and Simpson's Diversity ($r^2 = 0.104$). Significant results in method B include Patch Density ($r^2 = 0.178$), Edge Density ($r^2 = 0.104$), and Mean Area ($r^2 = 0.111$). There were no significant results for Artrv W1 within Smith Creek watershed. For the Artrv W1 class method A produced four significant results while method B produced eight.

Artrv W2

Within the Artrv W2 class seven consistent trends became apparent although none of the trends were significant (Table 10). Positive trends include Patch Density, Edge Density, the Landscape Shape Index, and the Interspersion and Juxtaposition Index. Negative trends include Mean Area, Nearest Neighbor, and Contagion. Method A produced eight significant single results while method B produced seventeen. Method A produced four of the eight significant results from Smith Creek. Method B produced eight significant results from Current Creek and nine significant results from Red Canyon, with none coming from Smith Creek.

Artrv W4

Within the Artrv W4 class eight trends were found with four being significant trends (Table 11). The four consistent trends include two positive trends (Simpson's Diversity, Simpson's Evenness) and two negative trends (Nearest Neighbor, Contagion). Significant positive trends include Patch Density (Fig. 18), Edge Density, and the Landscape Shape Index (Fig. 19). The single negative significant trend was the metric Mean Area. Method A and B both produced twenty-two individual significant results. Current Creek method A produced five significant results while method B produced seven. Red Canyon method A produced nine significant results while method B produced eight. Smith Creek method A produced eight significant results while method B produced seven.

Artrv W5

Three outliers were removed from method A due to the fire frequency being much greater than any of the other fire frequency values, which drastically altered the results. Within the Artrv W5 class again eight trends were found with four being significant, although the trends were not located on the same metrics as in the Artrv W4 class (Table 12). The four consistent trends include three positive trends (Edge Density, the Landscape Shape Index, and the Interspersion and Juxtaposition Index) and one negative trend (Contagion). Positive significant trends include Patch Density (Fig. 18), Simpson's Diversity (Fig. 19), and Simpson's Evenness. The sole negative significant trend was Mean Area. Method A produced nineteen individual significant results while method B produced twenty-one. Current Creek method A produced four significant results while method B produced six. Both methods in Red Canyon produced eight significant results and both methods in Smith Creek produced seven significant results.

DISCUSSION

The nonparametric method was deemed superior due not only to having the best overall accuracy but also producing the most consistent results. Classes that produced the highest accuracies had a number of traits in common. These included sites dominated by a single species, such as the Brte, Taas, and the Potr F4 and Psme F4 classes, which were dominated by an overstory forest structure. Trouble correctly identifying Abla suggests that like conifer species may be hard to differentiate when having the same or similar site characteristics. Another common trait found in the Arar and Putr PVT when using the nonparametric method was a trend of higher accuracies in the early successional stages with decreased accuracies as succession advances. The Artr PVT also follows this trend in early successional stages but differs when succession advances to the Artr W4 class. This suggests that following disturbance, classes are more distinct and become more similar to other classes as succession advances and the amount of juniper increases. These complex interactions are further complicated by the encroachment of juniper. Although juniper encroaches many sites, nutrient and water availability differ, resulting in different establishment patterns and succession rates across different sites. As succession advances to the Artr W4 class juniper encroachment has become so great that not only has the majority of the sagebrush been killed, but the majority of the site is dominated by a single species. At this stage the spectral signature has drastically changed and appears more similar to sites with a forest overstory. A drop in Artr W5 accuracies occur primarily due to the amount of juniper decreases and the amount of soil site variability greatly increases.

Another reason why the nonparametric method is superior to the other methods is the ability to separate different shrub types whose spectral signature are similar. Because the

nonparametric method has few restrictive rules about statistical distribution and underlying characteristics, greater flexibility and accuracies were achieved when dealing with difficult classes when compared to the parametric methods, which have many ridged data assumptions. One would expect to be able to distinguish between Arar and Artr due to the difference in structure, size, and proportion, but it is more difficult to separate shrub communities with similar characteristics. Artr PVT's and Putr PVT's are similar in many regards to structure and proportion. Also many training sites had both species present and, depending on the amount of each, went into one class or the other. The nonparametric method did the best in separating these three shrub species even though this was a large source of the misclassified pixels. The nonparametric method was also the best in classifying the most difficult classes, CeleR5*3 and Cele*4. Cele classes were very difficult to classify due to large site variability, large understory diversity, within-class variability, and similar spectral characteristics to many other classes. These particular classes were very difficult to locate on the Landsat image when either juniper or Douglas-fir was present. Another possible explanation would be that during the time of the year that the image was taken is the time period when Cele looks most similar to other classes. By determining a time when Cele is physiologically distinct from other species another image acquired during that time could be used in class separation. In the end the Cele PVT was reduced to only two classes, CeleR5*3 which has no conifer component, and Cele*4 which has conifers as a large component. Although the nonparametric was not superior in all classes, this method produced the best accuracies in classes of most abundance and interest.

Parametric vs. Nonparametric Comparisons

Even though the difference between the quadratic parametric technique (64%) and the nonparametric technique (69%) was only about 5% in the overall accuracy, a large difference can be seen when comparing user's vs. producer's accuracies. The nonparametric method produced fairly constant or similar results for both user's and producer's accuracies. In contrast, the linear parametric method resulted in a user's accuracy of about 20% for the forest PVT's and for the Artr R3B and Cele*4 classes. The producer's accuracy using the linear parametric method was at least 20% higher and close to 100% for the Abla class. The reason why this trend occurred maybe related to the classification technique used and the underlying statistical assumptions. Knick et al. (1997) suggests that using nonparametric statistics are more appropriate because they provide a qualitative class separation rather than quantitative relationships, and by using nonparametric techniques incorrect assumptions about distribution of data will not influence variables for class separation. Another concern with both of the parametric technique is that the user's accuracies are so low. This means that on the ground classification is very low and would not be beneficial to land managers for field applications.

The results suggest that nonparametric discriminant analysis produce higher accuracies than linear parametric methods are similar to findings by Bunting et al. (2002b) and Heide (2002). The 5% difference between the two methods falls within findings by Bunting et al. (2002b) that nonparametric methods produced 5-10% higher accuracies in structural stage separation. Results of higher overall accuracies using advanced classification procedures compared to tradition techniques have been reported by Cortijo and Perez De La Blanca (1999), Maselli et al. (1992), Skidmore and Turner (1998) and Cortijo and De La

Blanca (1997). Cortijo and Perez De La Blanca (1999) found that nonparametric approaches produced better results when dealing with complex images with training sites that have highly variable characteristics that commonly overlapped between classes. With such fine scale classes a great deal of overlap occurred when classifying the Owyhee Uplands. Maselli et al. (1992) showed a nonparametric method produced higher kappa values compared to maximum likelihood techniques although overall accuracies were not computed.

Nonparametric Advantages and Disadvantages

Advantages associated with nonparametric classifications include no prior knowledge about the statistical distribution of the data is required (Serpico et al. 1996). No additional information is required to increase the overall map accuracies (Skidmore and Turner 1988), which was supported by our results. Large spectral variations, with highly overlapping characteristics and images with high complexity have been more accurately classified using nonparametric classifications methods (Knick et al. 1997, Cortijo and Perez De La Blanca 1999, Bunting et al. 2002b). Disadvantages of using nonparametric classifiers include susceptibility to erroneous distributions of data not statistically representing the entire population because so few statistical assumptions are considered (Maselli et al. 1992). Other drawbacks include, outliers can negatively influence results, and computational effort can be very complex (Cortijo and Perez De La Blanca 1997). Results also have suggested that large numbers of training sites are required to accurately represent each class (Maselli et al. 1992), which is often costly and time consuming. Lowell (1989) suggests that the nonparametric technique developed by Skidmore and Turner (1988) may in accurately estimate the amount of land in each cover type resulting in a need for improvement to the classification equation. Since nonparametric procedures have been less commonly used, far less research has been

conducted to determine the limitations of these techniques. But at the same time if overall accuracies can be increased and enough training sites are utilized, nonparametric techniques have more advantages than disadvantages.

Layers of Significance

Landsat bands as well as vegetation indices were included in the classification due to the importance and proven value to other remote sensing projects (Bunting et al. 2002b, Heide 2002, Cohen and Spies 1992, Wolter et al. 1995). To determine the importance of each layer statistically a stepwise discriminant analysis using backwards selection was completed in SAS. This showed that the three Tassel Cap layers added little significant value to the classification and therefore were left out. This suggests the values for these three layers may have been similar to the NDVI and MSI layers and therefore were producing redundant information. Since the image was acquired during the late part of the summer in a semi-arid environment, ability to measure moisture and stress may have been more difficult when using the coefficients derived by Huang et al. (2002). The Tassel Cap coefficients created by Huang et al. (2002) consist of five paired Landsat ETM + images from across the United States. In each scene 2000 points were randomly selected and a principle component analysis was completed. When the orthogonality of all six axes was preserved, the transformation was created (Huang et al. 2002). Instead of using coefficients created from other images the NDVI and MSI were ratios of values from the actual Landsat scene. Another possible reason why the Tassel Cap values were found to be of little importance could be the range of values were much different than any of the other layers. Possible a normalization equation such as the one used by Heide (2002) would have been beneficial. This option was not considered before the classification began.

Sources of Error

There are many sources of errors that must be considered when using satellite imagery to create a vegetation classification which include, soil characteristics, phenological stages, terrain complexity, GPS units, and different people collecting field data. During the 2002 field season, while the image appears to be clear, the quality of the image may have been affected by smoke blown in from the large wildfires located in Oregon over much of the summer of 2002. The spatial resolution of the image also presented a problem when trying to define so many classes at a fine scale. Often many of the training sites were not used because a clear boundary between vegetation types was possible on the DOQQ's but was not possible on the Landsat image. Sampling training sites also presented a substantial challenge. The landscape was complex and often did not present large continuous areas of a single class in which to locate training sites. Often training sites were located on areas that on the ground appeared to be large enough but in reality due to many factors were far too small. Small-sized aspen patches were found throughout much of the landscape and increased difficulty in locating large enough training sites for this class. Identifying the structural stage a particular site belonged to based on juniper cover was often difficult. Another challenge occurred when dealing with Putr PVT's. Typically these sites consist of a mixture of both sagebrush and bitterbrush and determining which PVT the site belonged to was difficult. Other difficult class distinctions occurred among young juniper woodland classes where the difference among classes could be the presence or absence of a few trees.

Another underlying problem when working on such a large study area was the difference between parent material and soil characteristics. Silver City is very granitic with light colored soils where as Juniper Mountain is mostly composed of dark volcanic material.

Spectral signature differences could be easily seen when comparing the same class at different site locations. Sites located on Juniper Mountain and parts of South Mountain were very similar but when compared to sites located on the Silver City Range large differences could be seen. This was very evident in both Arar and Artr sagebrush classes as well as with classes that had high amounts of juniper and large amounts of bare ground. Another challenge occurred when the same class was present over all the elevational ranges. Artr R3B located at the top of mountains looked significantly different than did sites found down at lower elevations. Much of these differences can be attributed to two things. First the species composition shifted as elevation increased. Although sagebrush cover remained similar, the amount of snowberry greatly increased. Second the amount of annual precipitation differed greatly. Clearly the higher elevation sites were wetter when the image was taken compared to the low elevation sites, which resulted in the same class having different sites with different phenological stages.

The ability of the GPS unit to accurately depict the exact location was also a source of error. Many GPS points did not fall directly where the locations were taken and presented some problems when dealing with small aspen training sites and areas where topographic variability was complex. Different field workers collected data and a difference in how each observer classified training sites could be seen. This was particularly evident in the R3B, W1, and W2 structural stage classes. What one observer considered a W1 the other observer could classify as R3B or W2 and vice versa. This presented a challenge when looking at training sites on the maps and making sure the AOI's went into the correct class. If this could not be determined they were not used.

Landscape Scale

Issues related to scale will always need to be considered when using satellite imagery to classify a particular site. In this case all products produced have a spatial resolution of 30x30-m pixels. Although this may seem more than adequate when dealing with an entire landscape 30-m pixel resolution has many limitations when looking at questions from a much finer scale. For example, the landscape is far more fragmented and complex than 30-m pixels can display. The heterogeneity of this landscape can be very complex and only partially predictable. By focusing on the landscape at 30-m resolution some of this heterogeneity will be lost. In many cases areas could be classified at 5x5-m pixels or less and still not be very accurate. This also translated in how the fuel models must be used. The fuel models may be very accurate in predicting fire behavior and fire characteristic across the entire landscape or a single watershed but are not very accurate when looking at fine scale fire pattern issues. Fire-landscape pattern relationships were also confined to this scale. The loss of some of the heterogeneity due to mixed pixels or incorrectly classified pixels can and probably did have an influence on the fire-landscape pattern results.

Fire-Landscape Patterns

Although the significance and the predictive power of the fire-landscape pattern results are not very robust, simple trends and relationships become more strongly developed as juniper becomes more dominate across the landscape. Even though sagebrush steppe with small amounts of juniper have the majority of the fuels and fire potential the overall spatial arrangement of the vegetation across the landscape does not heavily influence fire frequency until the landscape is characterized by closed canopy or old growth juniper woodlands. This suggests that the spatial arrangement of communities dominated by sagebrush steppe has

little or no influence on fire frequency regardless of high fuel loads and the potential for large fires. As juniper begin to dominate the landscape the relationship of fuel loading, continuity, and fire becomes greater, which reduces fire potential, making the spatial arrangement of the vegetation more important. The ability to demonstrate general trends in fire-landscape pattern relationships is directly correlated with the encroachment of juniper woodlands and the resulting successional development over time.

Since Artrv W1 is still dominated by sagebrush vegetation and the presence of juniper has only a small influence on altering landscape fire characteristics, the abundance of this class has little affect on fire-landscape pattern relationships. Even though none of the trends within the Artrv W2 class are significant the trends clearly indicate the positive and negative trends that become significant in later successional stages. This suggests that the abundance and distribution of this class is important and demonstrates that with a knowledge of the successional advancement of this class, that in time, results will be similar to those found in the Artrv W4 and W5 classes. Another interesting note is that the majority of the significant results for the Artrv W2 class come from method B. This suggests two things. Method B may be a superior method in testing fire-landscape pattern relationships, which can be seen across each of the successional stages. Second, the total amount and distribution of Artrv W4 and Artrv W5 may influence the patterns across the landscape when looking at classes with small amounts of juniper. Both Current Creek and Red Canyon have large percentages of the watershed dominated by late succesional stages of juniper (W4 and W5). Smith Creek on the other hand had roughly half of watershed dominated by early successional classes and the other half dominated by later successional classes. This difference may help explain why

the results in method B for Current Creek and Red Canyon were more conclusive than in Smith Creek.

Shifting from sagebrush-dominated classes to classes dominated by juniper increased the number of consistent and significant trends. Patch Density showed a positive significant trend in both Artrv W4 and Artrv W5. This demonstrates that fire occurrence increases as Patch Density increases on the landscape. Since fires rarely burn through large areas of old growth juniper due to lack of fuels, fire size would remain small allowing for increased patch numbers at the start of each successive burn. As juniper encroachment continues and moves to later successional stages a cycle begins to emerge among fire frequencies, fire size or patch density, and the amount of juniper present on the landscape. Even as fire frequency increases, the spatial arrangement of the Artrv W4 and Artrv W5 classes restricts fire size. As fire size is reduced and remains small, the natural and most successful controller of western juniper, fire, will become a non-factor across the landscape resulting in the increase in area and extend of juniper across the landscape. Edge Density increases with Patch Density and also has a positive relationship under these conditions. After a consistent trend in Artrv W2 significant trends were found in both Artrv W4 and Artrv W5 for Edge Density. When fire size is limited by landscapes dominated by juniper then more patches result in high edge densities.

Again the Landscape Shape Index metric followed this positive trend in the Artrv W2 and Artrv W5 classes and becomes significant in the Artrv W4 class. Using the same logic, more fire, more patches, more edge, the landscape shape or disaggregating of patches across the landscape should increase. Over time a homogenous landscape dominated by juniper

with high fire frequency would result in the landscape becoming more heterogonous and complex thus increasing the Landscape Shape Index metric value. Along these same lines of thought, the negative trend of Mean Area, which was present in the Artrv W2 and significant in the Artrv W4 and Artrv W5 class, would be expected. As the homogeneous landscape becomes more frequently burned, thus increasing Patch Density and Edge Density, the landscape would become increasingly fragmented with different successional stages over time. Fire size would remain small resulting in more patches with smaller area or total mean area.

Simpson's Diversity and Simpson's Evenness both produced a positive trend in the Artrv W4 class and a positive significant trend in the Artrv W5 class. Simpson's Diversity measures the probability that any two patches selected would be different, thus having higher diversity (McGarigal and Marks 1995). This metric did not become significant until the landscape arrangement limited the size of all fires regardless of fire frequency. With an increased in the number of fires being very small in extent, small patches would be created, which over time, would follow multiple successional pathways resulting in many patch types with a high amount of diversity. Taking this trend a step further the overall evenness of the landscape should also increase as fire frequency increases which can be measured by the Simpson's Evenness metric. Simpson's Evenness suggests that when fire frequency increases within areas dominated by old growth juniper the resulting distribution of patch types are close to equal, which implies greater landscape evenness.

Although the next set of metrics address similar questions, results never became significant trends. The Contagion metric produced a consistent trend across Artrv W2, W4, and W5. The Interspersion and Juxtaposition Index on the other hand showed a consistent

trend in the Artrv W2 and W5 classes but not in the Artrv W4 class. Although neither had many significant results the trend directions agree with the predicted outcome. Contagion, a measure of aggregation or clumpiness shows a negative trend. This would be expected, as fire frequency increases patches would become more disconnected and fragmented, resulting in a lower Contagion value. On the other hand the Interspersion and Juxtaposition Index metric measures the extent to which types are interspersed with higher valued being more interspersed and lower values representing areas where patch types are poorly interspersed (McGarigal and Marks 1999). Thus random fires across a landscape would produce many patches and as fire frequency increased, over time interspersion of different patch types would increase, as is the case for the positive trend for the Interspersion and Juxtaposition Index within the Artrv W5 class. Nearest Neighbor is the final metric to discuss which produced a negative consistent trend within the Artrv W2, Artrv W4, and almost Artrv W1 class. The negative trend suggests that increasing fire frequency decreases the distance of one type to its nearest neighbor.

Comparisons Between Method A and B

Although the results between method A and B may seem similar, in actuality they are not, due to a number of differences. Problems with method A include changing fuel moistures which start out constant but due to how FARSITE was developed, change over time, and wind direction which had to be randomly selected to create the fire frequency grid. Method B produced more relevant results across all classes and in most watersheds. Although results from Method A may have been higher in some cases the significance of the results must be viewed with caution. Method B results are more realistic and relevant due to

how the fire frequency grids were created in each method. Method B used slope, aspect, and elevation layers to create the frequency grid were as method A was based on a flat landscape. Although the p-values and r^2 values are very similar between the two methods the results from method B are much more realist when compared to an actual landscape. Another difference between the two methods was the fire conditions used to create the fire frequency grids. Along with the proportion of older successional stages located within the Current Creek and Red Canyon watersheds, the wildfire weather conditions used in method B may explain the large increase in significant results. Because of the high amount of older classes, the limited number of fires, and moderate fire conditions used in method A, apparent patterns did not become present until higher number of fires and wildfire conditions were used.

Sources of Concern

When modeling fire behavior the results are only as good as the layer inputs and the numerous other variables involved. The input layers created by Yanish (2002) allowed greater understanding far beyond any standard fuel models for juniper woodland systems. Yet at the same time the complex requirements of FARSITE provide a challenge when looking at fire-landscape pattern relationships. First and foremost FARSITE continuously computes values based on environmental changes. The goal of the fire-landscape pattern process was to create as close to the same fire conditions as possible. Areas where this was not possible within FARSITE include changes in fuel moisture, shading, aspect, elevation, and slope. By manipulating the DEM ASCII file and creating a flat landscape the slope, aspect, and elevational variables were kept constant throughout all runs. Another challenge occurred when dealing with wind directions. By having all fires started within a particular watershed wind directions could not be held constant. Constant wind conditions resulted in a

portion of the watershed practically being unaffected by fire which causes severe edge effects. Another problem that became apparent was the spatial arrangement of the different fuel models across the landscape. Within the Red Canyon watershed the majority of the upper area was dominated by Artrv W5 fuel type, which has low flammability and is very difficult to burn. On the other hand the lower section of the watershed is dominated by Artrv R3B or Artrv W1, which is highly flammable and burns easily under most conditions. In initial testing each half of the watershed was burned with 50 fires. The lower half had fire frequencies from zero to fifteen and produced a nice coverage across the area. The upper half was dominated by old growth juniper. In this section the fire frequency ranged from zero to four and only covered a small percentage of the area. Because the fuel characteristics were distinctively different, fire frequency was highly variable across different sections of the landscape. This was also a concern in the Smith Creek and Current Creek watersheds and more than likely influence the results.

Another problem that hindered analysis was selecting the appropriate fire conditions and number of fires burned per watershed. Initially known wildfire conditions were used. After many failed attempts fire conditions were reduced to moderate levels by changing the fuel moistures, and resulting patterns became apparent in the Red Canyon watershed. Hopes were high that similar results could be reproduced in the other two watersheds but were not nearly as successful. This in part can be attributed to the fire frequency grids, which was dependant on the number of fires per watershed. What may have been the optimal number of fires in Red Canyon watershed may not have been for the other two study areas. Within the Smith Creek watershed, the larger fire size and resulting distribution resulted in a higher fire frequency across a larger proportion of the watershed. The Current Creek watershed posed

different challenges. Instead of burning a large portion of the watershed, a large amount of the study area burned very little. This can be related to the fact that old growth juniper fuel types or very rocky areas where fire spread is limited dominate a high percentage of the watershed. This may have had an influence on the results for these watersheds.

Final Thoughts

Although some consistent trends and significant trends were found within the Artrv W2, W4, and W5 classes the overall strength of the relationships were expected to be greater. Clearly method B produced a better fire frequency grid, which was created to mimic wildfire conditions. Due to time constraints method B was not tested under moderate fire conditions, which may have influenced the strength of the results. It also has become apparent that the percentage of each class and location and proximity to similar classes can have a great influence on the results when method A was used. By burning 25,000 fires in method B this problem was reduced. Another consideration on why relationships within the sagebrush classes were not present may stem from the size of the square used to run the landscape metrics on. Because the size of fires started within the sagebrush communities tend to be significantly larger than those started in the old growth the scale at which the fire-landscape patterns may be present could easily be different. Possibly if a square size of 25x25 or 50x50 pixels was used in the analysis the Artrv W1 and W2 perceived fire-landscape pattern relationships would be more apparent. Another possible idea to reduce the possibility of selecting one random pixel surrounded by classes on the opposite fire behavior extreme, and thus altering the results, would be to stratify the watershed based on a certain class and then select random points within these stratified area.

CONCLUSIONS

Although western juniper encroachment has gone unnoticed by many for a long time, the environmental changes and consequences are becoming increasingly apparent. Considerable recent research has focused on age structure and life history (Miller and Rose 1995, 1999), and development of methods of juniper reduction (Bunting 1987, Eddleman 1999). In order to manage juniper encroachment understanding the distribution of western juniper successional stages within a landscape is required. With such a large species range, covering multiple states, accurately mapping juniper encroachment would not be possible without the use of remote sensing technologies. Although there are many valid concerns and problems with using remote sensing data, this is the most efficient solution when mapping a problem that is located across such a large landscape.

In attempts to achieve the highest overall map accuracy three different classification procedures were tested. The method that produced the best overall accuracy (69%) and most consistent results was the nonparametric discriminant approach. Second was the parametric quadratic discriminant method with an overall accuracy of 64%, followed by the parametric linear discriminant method with an overall accuracy of 52%. Although early successional classes and classes dominated by a single species achieved the highest overall accuracies, we were able to successfully map juniper encroachment along a successional gradient. Overall accuracies are lower than findings by Bunting et al. (2002b) due mostly to the addition of more PVT's and PVT-structural stage classes, increased study area size, and greater soil and site differences within the study area.

NDVI and MSI improved the overall accuracy. The three Tassel Cap layers; brightness, greenness, and wetness did not improve the classification results. These ancillary

layers probably provided the same information as NDVI and MSI, or a problem could have resulted when the value range was different than the other layers, which may have been resolved by normalizing the data in some fashion. Aspect and elevational boundary rules were very important in increasing the overall quality of the map. By using field-collected data as well as on the ground knowledge and experience, the overall product was improved. With a quality map land managers will have the opportunity to prioritize locations where controlled fire will be most effective both from an ecological and economical perspective.

Although the results from the fire-landscape pattern analysis were not strongly predictive, important trends and relationships between landscape configuration and fire do exist. Method B clearly produced more consistent results across all successional classes compared to method A. Wildfire conditions used in method B compared to moderate fire conditions used in method A can partially explain this. Differences in how the fire frequency grids were created in method A and B suggest utilizing slope, aspect, and elevation in method B are important factors in fire occurrence and results from method B may have greater interpretive value than results from method A which used a flat landscape.

Variability across the watersheds in regards to the amount of late successional classes and the distribution across each watershed also affected the results. This suggests that the spatial arrangement of late successional classes such as Artrv W4, and Artrv W5 influence the fire frequency potential across both moderate and wildfire fire conditions. Last and most importantly, the spatial arrangement and amount of western juniper does influence fire behavior suggesting that along with other commonly studied fire variables such as fuel moisture and weather conditions, arrangement of the different patch types is an important component when predicting fire potential in sagebrush steppe/ juniper woodland systems.

LITERATURE CITED

- Albright, D. and B.N. Meisner. 1999.** Classification of fire simulation systems. Fire Management Notes. 59:5-11.
- Anderson, H.A. 1982.** Aids to determining fuel models for estimating fire behavior. USDA Forest Service. General Technical Report. INT-122. 22p.
- Andrews, P.L. and L.P. Queen. 2001.** Fire modeling and information system technology. International Journal of Wildland Fire. 10:343-352.
- ArcGIS 8.3. 2002.** Environmental Systems Research Institute, Inc. Headquarters: Redlands, CA.
- ArcView GIS 3.3. 2002.** Environmental Systems Research Institute, Inc. Headquarters: Redlands, CA.
- Bates, J.D., R.F. Miller, and T.J. Svejcar. 2000.** Understory dynamics in cut and uncut western juniper woodlands. Journal of Range Management. 53:119-126.
- BEHAVE. Release 4.4. 1997.** USDA Forest Service. Fire Sciences Lab. Missoula, MT.
- Bobbe, T., H. Lachowski, P. Maus, J. Greer, and C. Dull. 2001.** A primer on mapping vegetation using remote sensing. International Journal of Wildland Fire. 10:277-287.
- Brown, J.K. 1974.** Handbook for inventorying downed woody material. USDA Forest Service. General Technical Report. INT-16. 48p.
- Brown, J.K., R.D. Oberheu, and C.M. Johnston. 1982.** Handbook for inventorying surface fuels and biomass in the interior west. National Wildfire Coordinating Group NFES-2125. U.S. Department of Agriculture, U.S. Department of Interior, and National Association of State Foresters, 48p.
- Buckhouse, J.C. and J.L. Mattison. 1980.** Potential soil erosion of selected habitat types in the high desert region of Central Oregon. Journal of Range Management. 33:282-285.
- Bunting, S.C. 1987.** Use of prescribed burning in juniper and pinyon-juniper woodlands. Pp. 141-144. *In*. Proceeding--Pinyon-Juniper Conference. USDA Forest Service. General Technical Report. INT-215.
- Bunting, S.C., J.L. Kingery, and E. Strand. 1999.** Effects of succession on species richness of the western juniper woodland/sagebrush steppe mosaic. Pp. 76-81. *In*. Proceedings: Ecology and Management of Pinyon-Juniper Communities Within the Interior West. USDA Forest Service. RMRS-P-9.

- Bunting, S.C., J.L. Kingery, M.A. Hemstrom, M.A. Schroeder, R.A. Gravenmier, and W.J. Hann. 2002a.** Altered rangeland ecosystems in the interior Columbia Basin. USDA Forest Service. General Technical Report. PNW-GTR 553. 71p. (Quigley, Thomas M., ed; Interior Columbia Basin Ecosystem Management Project: scientific assessment).
- Bunting, S.C., E.K. Strand, and J.L. Kingery. 2002b.** Landscape dynamics of the western juniper woodland/sagebrush steppe mosaic. Final Report. Department of Rangeland Ecology and Management and College of Natural Resources Remote Sensing and Geographic Information Systems Laboratory. University of Idaho, Moscow. 19p.
- Burgan, R.E. and R.C. Rothermel. 1984.** BEHAVE: Fire behavior prediction and fuel modeling system--. USDA Forest Service. General Technical Report. INT-167. 126p.
- Burkhardt, J.W. and E.W. Tisdale. 1969.** Nature and successional status of western juniper vegetation in Idaho. *Journal of Range Management*. 22:264-270.
- Burkhardt, J.W. and E.W. Tisdale. 1976.** Cause of juniper invasion in Southwestern Idaho. *Ecology*. 57:472-484.
- Caldwell, M.M. and J.H. Richards. 1989.** Hydraulic lift: water efflux from upper roots improves effectiveness of water uptake by deep roots. *Oecologia*. 79:1-5.
- Campbell, J., D. Weinstein, and M. Finney. 1996.** Intergrading GIS and BEHAVE for forest fire behavior modeling. Pp. 363-275. In. J.D. Greer, (ed.). *Remote sensing: People in partnership with technology*. American Society of Photogrammetry and Remote Sensing, Bethesda, MD.
- Chuvieco, E. 1999.** Measuring changes in landscape pattern from satellite images: short-term effects of fire on spatial diversity. *International Journal of Remote Sensing*. 20: 2331-2346
- Clark, P.E., M.S. Seyfried, and B. Harris. 2001.** Intermountain plant community classification using Landsat TM and SPOT HRV data. *Journal of Range Management*. 54:152-160.
- Cohen, W.B. and T.A. Spies. 1992.** Estimating structural attributes of Douglas-Fir/Western Hemlock forest stands from Landsat and SPOT imagery. *Remote Sensing of Environment*. 41:1-17.
- Congalton, R.G. 2001.** Accuracy assessment and validation of remotely sensed and other spatial information. *International Journal of Wildland Fire*. 10:321-328.

- Congalton, R.G. 1991.** A review of assessing the accuracy of classifications of remotely sensed data. *Remote Sensing of Environment*. 37:35-46.
- Cortijo, F.J., and N. Perez De La Blanca. 1999.** The performance of regularized discriminant analysis versus non-parametric classifiers applied to high-dimensional image classification. *International Journal of Remote Sensing*. 20: 3345-3365.
- Cortijo, F.J., and N. Perez De La Blanca. 1997.** A comparative study of some non-parametric spectral classifiers. Applications to problems with high-overlapping training sites. *International Journal of Remote Sensing*. 18:1259-1275.
- Crist, E.P. 1985.** A thematic mapper tassell cap equivalent for reflectance factor data. *Remote Sensing of Environment*. 17:301-306.
- Deering, D.W., J.W. Rouse, R.H. Haas, and J.A. Schell. 1975.** Measuring forage production of grazing units from Landsat MSS data. *Proceedings*. Tenth International Symposium of Remote Sensing of Environment. Ann Arbor: ERIM. 2:1169-1178.
- Eddleman, L.E. 1999.** Ecological guidelines for management and restoration of pinyon and juniper woodlands. Pp. 366-370. *In*. Proceedings: Ecology and Management of Pinyon-Juniper Communities Within the Interior West. USDA Forest Service. RMRS-P-9.
- ERDAS IMAGINE. Release 8.6. November 2002.** Leica Geosystems. St. Gallen, Switzerland.
- FARSITE. Release 4.04. 2003.** USDA Forest Service. Fire Sciences Lab. Missoula, MT. <http://farsite.org/>
- Fiorella, M. and W.J. Ripple. 1993.** Determining successional stage of temperate coniferous forests with Landsat satellite data. *Photogrammetric Engineering & Remote Sensing*. 59:239-246.
- Finney, M.A. 2002.** Fire growth using minimum travel time methods. *Canadian Journal of Forest Resources*. 32:1420-1424.
- Finney, M.A. 1998.** FARSITE: Fire area simulator-model. USDA Forest. Service Research Paper. RMPS-RP-4
- Finney, M and P.L. Andrews. 1999.** FARSITE—A program for fire growth simulation. *Fire Management Notes*. 59:13-15.
- Foody, G.M. 2002.** Status of land cover classification accuracy assessment. *Remote sensing of Environment*. 80:185-201.

- Franklin, J., T.L. Logan, C.E. Woodcock, and A.H. Strahler. 1986.** Coniferous forest classification and inventory using Landsat and digital terrain data. *IEEE Transactions on Geoscience and Remote Sensing*. GE-24:139-149.
- Gustafson, E.J. 1998.** Quantifying landscape spatial pattern: What is the state of the art? *Ecosystems*. 1:143-156.
- Hargrove, W.W., R.H. Gardner, M.G. Turner, W.H. Romme, and D.G. Despain. 2000.** Simulating fire patterns in heterogeneous landscapes. *Ecological Modelling*. 135: 243-263.
- Harkness, A.L. 1998.** Soil survey of Owyhee county area, Idaho. U.S. Department of Agriculture, Natural Resource Conservation Service. 809p.
- Heide, S.C. 2002.** Comparison of methods to detect conifer encroachment into aspen stands using Landsat 7 ETM + satellite imagery. M.S. Thesis. University of Idaho, Moscow. 75p.
- Hessburg, P.F, B.G. Smith, S.D. Kreiter, C.A. Miller, R.B. Salter, C.H McNicoll, and W.J. Hann. 1999.** Historical and current forest and range landscapes in the interior Columbia River basin and portions of the Klamath and Great Basins. USDA Forest Service. General Technical Report. PNW-GRT-458. 357p.
- Huang, C., B. Wylie, L. Yang, C. Homer, and G. Zylstra. 2002.** Derivation of a tasseled cap transformation based on Landsat 7 at-satellite reflectance. *International Journal of Remote Sensing*. 23:1741-1748.
- Irish, R.R. 2000.** Landsat 7 science data user's handbook. Report 430-15-01-003-0. National Aeronautics and Space Administration.
http://ltpwww.gsfc.nasa.gov/IAS/handbook/handbook_toc.html
- Jackubauskas, M., K. Kindscher, and D. Debinski. 1998.** Multitemporal characterization and mapping of montane sagebrush communities using Indian IRS LISS-II imagery. *Geocarto International*. 13:65-74.
- Jensen, J.R. 1996.** Introductory digital image processing. Prentice Hall. Upper Saddle River, New Jersey. 318p.
- Jensen, M.E., J.P. Dibenedetto, J.A. Barber, C. Montagne, and P.S. Bourgeron. 2001.** Spatial modeling of rangeland potential vegetation environments. *Journal of Range Management*. 54:528-536.
- Keane, R.E., P. Morgan, and J.D. White. 1999.** Temporal patterns of ecosystem processes on simulated landscapes in Glacier National Park, Montana, USA. *Landscape Ecology*. 14:311-329.

- Kent, E., M. Sondheim, and B. Yee. 1988.** Methods for improving accuracy of thematic mapper ground cover classifications. *Canadian Journal of Remote Sensing*. 14:17-31.
- Knick, S.T., J.T. Rotenberry, and T.J. Zarriello. 1997.** Supervised classification of Landsat thematic mapper imagery in a semi-arid rangeland by nonparametric discriminant analysis. *Photogrammetric Engineering & Remote Sensing*. 63:79-86.
- Krummel, J.R., R.H. Gardner, G. Sugihara, R.V. O'Neill, and P.R. Coleman. 1987.** Landscape patterns in a disturbed environment. *OIKOS* 48:321-324.
- Lowell, K.E. 1989.** A probabilistic modification of the decision rule in the Skidmore/Turner supervised nonparametric classifier. *Photogrammetric Engineering & Remote Sensing*. 55:897-900.
- Maselli, F., C. Conese, L. Petkov, and R Resti. 1992.** Inclusion of prior probability derived from a nonparametric process into the maximum likelihood classifier. *Photogrammetric Engineering & Remote Sensing*. 58:201-207.
- Miller, C. and D.L. Urban. 1999.** A model of surface fire, climate and forest pattern in the Sierra Nevada, California. *Ecological Modelling*. 114:113-135.
- Miller, R.F. and J.A. Rose. 1995.** Historic expansion of *Juniperus occidentalis* (western juniper) in Southeast Oregon. *Great Basin Naturalist*. 55:37-45.
- Miller, R.F. and J.A. Rose. 1999.** Fire history and western juniper encroachment in sagebrush steppe. *Journal of Range Management*. 52:550-559.
- Miller, R.F. and P.E. Wigand. 1994.** Holocene changes in semiarid pinyon-juniper woodlands. *BioScience*. 44:465-474.
- Miller, R., T. Svejcar, and J. Rose. 1999a.** Conversion of shrub steppe in juniper woodland. Pp. 385-390. *In*. Proceedings: Ecology and Management of Pinyon-Juniper Communities Within the Interior West. USDA Forest Service. RMRS-P-9.
- Miller, R.F., T.J. Svejcar, and J.A. Rose. 2000.** Impact of western juniper on plant community composition and structure. *Journal of Range Management*. 53:574-585.
- Miller, R., R. Tausch, and W. Waichler. 1999b.** Old-growth juniper and pinyon woodlands. Pp. 375-384. *In*. Proceedings: Ecology and Management of Pinyon-Juniper Communities Within the Interior West. USDA Forest Service. RMRS-P-9.

- McGarigal, K. 2002.** Landscape pattern metrics. Pp. 1135-1142. *In.* A. H. El-Shaarawi and W. W. Piegorsch, (eds.) *Encyclopedia of Environmetrics Volume 2:1135-1142.* John Wiley & Sons, Sussex, England.
- McGarigal, K., and B. J. Marks. 1995.** FRAGSTATS: spatial pattern analysis program for quantifying landscape structure. USDA Forest Service. General Technical Report. PNW-351. 122p.
- McGarigal, K., S. A. Cushman, M. C. Neel, and E. Ene. 2002.** FRAGSTATS: Spatial Pattern Analysis Program for Categorical Maps. Computer software program produced by the authors at the University of Massachusetts, Amherst. Available at the following web site: www.umass.edu/landeco/research/fragstats/fragstats.html
- O'Neill, R.V., C.T. Hunsaker, K.B. Jones, K.H. Ritters, J.D. Wickham, P.M. Schwartz, I.A. Goodman, B.L. Jackson, and W.S. Baillargeon. 1997.** Monitoring environmental quality at the landscape scale. *BioScience.* 47:513-519.
- O'Neill, R.V., J.R. Krummel, R.H. Gardner, G. Sugihara, B. Jackson, D.L. DeAngelis, B.T. Milne, M.G. Turner, B. Zygmunt, S.W. Christensen, V.H. Dale, and R.L. Graham. 1988.** Indices of landscape pattern. *Landscape Ecology.* 1:153-162.
- Quigley, T.M., R.W. Haynes, and R.T. Graham tech. eds. 1996.** Integrated scientific assessment for ecosystem management in the interior Columbia basin and portions of the Klamath and Great Basins. USDA Forest Service. General Technical Report. PNW-GTR-382. 303p.
- Ritters, K.H., R.V. O'Neill, C.T. Hunsaker, J.D. Wickham, D.H. Yankee, and S.P. Timmins. 1995.** A factor analysis of landscape pattern and structure metrics. *Landscape Ecology.* 10:23-39.
- Rock, B.N., J.E. Vogelmann, D.L. Williams, A.F. Volgelmann, and T. Hoshizaki. 1986.** Remote detection of forest damage. *BioScience.* 36:439-445.
- Rothermel, R.C. 1972.** A mathematical model for predicting fire spread in wildfire fuels. USDA Forest Service. General Technical Report. INT-115. 40p.
- Rothermel, R.C. 1983.** How to predict the spread and intensity of forest and range fires. USDA Forest Service. General Technical Report. INT-143. 161p.
- SAS Institute Inc. 2001.** Version 8.02 of the SAS systems for Windows NT. SAS Institute Inc. Cary, N.C.
- SAS Institute Inc. 1999.** SAS/ STAT® User's Guide, Version 8. SAS Institute Inc. Cary, NC. 3884p.

- Serpico, S.B., L. Bruzzone, and F. Roli. 1996.** An experimental comparison of neural and statistical non-parametric algorithms for supervised classification of remote-sensing images. *Pattern Recognition Letters*. 17:1331-1341.
- Shinn, D.A. 1980.** Historical perspective on range burning in the inland Pacific Northwest. *Journal of Range Management*. 33:415-423.
- Skidmore, A.K. and B.J. Turner. 1988.** Forest mapping accuracies are improved using a supervised nonparametric classifier with SPOT data. *Photogrammetric Engineering & Remote Sensing*. 54:1415-1421.
- Soule', P.T. and P.A. Knapp. 1999.** Western juniper expansion on adjacent disturbed and near relict sites. *Journal of Range Management*. 52:525-533.
- Story, M. and R.G. Congalton. 1986.** Accuracy assessment: A user's perspective. *Photogrammetric Engineering and Remote Sensing*. 52:397-399.
- Turner, M.G. 1990.** Spatial and temporal analysis of landscape patterns. *Landscape Ecology*. 4:21-30.
- Turner, M.G. and W.H. Romme. 1994.** Landscape dynamics in crown fire ecosystems. *Landscape Ecology*. 9:59-77.
- Turner, M.G., W.H. Romme, R.H. Garder, R.V. O'Neill, and T.K. Kratz. 1993.** A revised concept of landscape equilibrium: Disturbance and stability on scaled landscapes. *Landscape Ecology*. 8:213-227.
- Urban, D.L., R.V. O'Neill, and H.H. Shugart, Jr. 1987.** Landscape ecology. *BioScience*. 37:119-127.
- Wall, T.G., R.F. Miller, and T.J. Svejcar. 2001.** Juniper encroachment into aspen in the northwest Great Basin. *Journal of Range Management*. 54:691-698.
- Western Regional Climate Center. 2003.** Division of Atmospheric Sciences. Desert Research Institute. Reno, NV. <http://www.wrcc.dri.edu/>
- Wolter, P.T., D.J. Mladenoff, G.E. Host, and T.R. Crow. 1995.** Improving forest classification in the northern lake states using multi-temporal Landsat imagery. *Photogrammetric Engineering & Remote Sensing*. 61:1129-1143.
- Yanish, C. 2002.** Western juniper succession: Changing fuels and fire behavior. M.S. Thesis. University of Idaho, Moscow. 76p.
- Young, A.Y. and R.A. Evans. 1981.** Demography and fire history of a western juniper stand. *Journal of Range Management*. 34:501-505.

Table 1. Potential Vegetation Type and Structural Stage attributes based on cover types (Bunting et al. 2002b).

PVT (Potential Vegetation Type)	SS (Structural Stage)
Shrubland	
Arar (Low sagebrush)	R1, R3A, R3B
Artrv (Mountain big sagebrush)	R1, R3A, R3B
Artrw (Basin big sagebrush)	R1, R3A, R3B
Putr (Bitterbrush)	R1, R3A, R3B
Cele (Mountain mahogany)	R5A, R5B, R7
Woodland	
Arar (Low sagebrush)	W1, W2, W4, W5
Artrv (Mountain big sagebrush)	W1, W2, W4, W5
Artrw (Basin big sagebrush)	W1, W2, W4, W5
Putr (Bitterbrush)	W1, W2, W4, W5
Cele (Mountain mahogany)	W1, W2, W4, W5
Forest	
Psme (Douglas-fir)	F2, F3, F4, F5
Potr (Quaking aspen)	F2, F3, F4, F5
Abla (Subalpine fir)	
Other	
Rock	W4, W5
Meadow	R2
Mountain Shrub (Bittercherry, chokecherry, shinny-leaf ceanothus)	R6
Brte (Cheatgrass)	
Taas (Medusahead)	
Mines (Disturbance)	
Water	
R1-Open herbland	F2- Sapling forest
R3A-Open low-med shrubland <10% shrub	F3- Pole forest
R3B- Open low-med shrubland 10-67% shrub	F4- Young multi-story forest
R5A-Open tall shrubland <10% shrub, <5% trees	F5- Old multi-story forest
R5B-Open tall shrubland 10-67% shrub, <5% trees	R2- Closed herbland
R7-Multi-strata tall shrubland <67% shrub, 5-10% trees	R6- Closed tall shrubland
W1-Woodland initiation	
W2-Young woodland	
W4-Mixed-aged woodland	
W5-Mature juniper woodland	

Table 2. Vegetation indices used in the classification and how each was derived.

Vegetation Indices	Equation
NDVI	$\text{Bandtm4} - \text{Bandtm3} \div \text{Bandtm4} + \text{Bandtm3}$
MSI	$\text{Bandtm5} \div \text{Bandtm4}$
Tassel Cap Brightness	$0.3561\text{tm1} + 0.3972\text{tm2} + 0.3904\text{tm3} + 0.6966\text{tm4} + 0.2286\text{tm5} + 0.1596\text{tm7}$
Tassel Cap Greenness	$- 0.3344\text{tm1} - 0.3544\text{tm2} - 0.4556\text{tm3} + 0.6966\text{tm4} - 0.0242\text{tm5} - 0.2630\text{tm7}$
Tassel Cap Wetness	$0.2626\text{tm1} + 0.2141\text{tm2} + 0.0926\text{tm3} + 0.0656\text{tm4} - 0.7629\text{tm5} - 0.5388\text{tm7}$

Table 3. Summary of the number of training sites, validation sites, and the total number of pixel used for each class.

Class name	Training sites	Training pixels	Validation sites	Validation pixels
ABLA	5	10	2	7
ARARR1	5	68	2	50
ARARR3*9	18	200	7	64
ARARW1	10	97	4	58
ARARW2	9	179	7	54
ARARW4	13	131	7	50
ARARW5	15	112	3	109
ARTRR1*1	9	166	4	70
ARTRR3B	15	170	6	139
ARTRT*2	15	105	3	50
ARTRW1	9	148	7	56
ARTRW2	9	94	8	108
ARTRW4	12	182	7	59
ARTRW5	12	154	7	74
BRTE	6	46	2	7
CELE*4	20	105	13	118
CELER5*3	12	41	6	24
MINES	4	88	2	145
MNTSHRUB	8	121	5	61
POTRF4	11	87	7	85
PSMEF2	6	76	2	54
PSMEF3	5	69	2	29
PSMEF4	15	113	5	104
PUTRR1	3	88	3	55
PUTRR3A	3	55	1	14
PUTRR3B*5	15	199	7	106
PUTRW1*6	9	90	4	24
PUTRW2*7	20	112	7	91
ROCKW*8	10	171	4	82
TAAS	8	120	2	56
WATER	4	100	2	100
WETMEADOW	6	49	1	3
TOTAL	321	3546	149	2106

Table 4. Forty-four PVT-structural stage classes used in first classification attempt.

ABLA	ARTRR1	ARTRW5	MINES	PUTR-2W2	ROCKW5
ARARR1	ARTRR3A	BRTE	MNTSHRUB	PUTRR1	TAAS
ARARR3A	ARTRR3B	CELER5A	POTRF4	PUTRR3A	WATER
ARARR3B	ARTRTW1	CELER5B	PSMEF2	PUTRR3B	WETMEADOW
ARARW1	ARTRTW2	CELER7	PSMEF3	PUTRW1	
ARARW2	ARTRW1	CELEW2	PSMEF4	PUTRW2	
ARARW4	ARTRW2	CELEW4	PUTR-2R3B	PUTRW4	
ARARW5	ARTRW4	CELEW5	PUTR-2W1	ROCKW4	

Table 5. PVT-structural stage classes combined to create the final thirty-two classes.

ARTRR1*1	ARTRR1, ARTRR3A
ARTRT*2	ARTRTW1, ARTRTW2
CELER5*3	CELER5A, CELER5B
CELE*4	CELER7, CELEW2, CELEW4, CELEW5
PUTRR3B*5	PUTR-2R3B, PUTRR3B
PUTRW1*6	PUTR-2W1, PUTRW1
PUTRW2*7	PUTR-2W2, PUTRW2, PUTRW4
ROCK*8	ROCKW4, ROCKW5
ARARR3*9	ARARR3A, ARARR3B

Table 6. Thirty-four PVT-structural stage classes used in secondary classification attempts.

ABLA	ARARW4	ARTRW2	MINES	PUTRR1	ROCKW5
ARARR1	ARARW5	ARTRW4	MNTSHRUB	PUTRR3A	TAAS
ARARR3A	ARTRR1*1	ARTRW5	POTRF4	PUTRR3B*5	WATER
ARARR3B	ARTRR3B	BRTE	PSMEF2	PUTRW1*6	WETMEADOW
ARARW1	ARTRT*2	CELE*4	PSMEF3	PUTRW2*7	
ARARW2	ARTRW1	CELER5*3	PSMEF4	ROCKW4	

Table 7. Thirty-two PVT-structural stage classes used in the final classification.

ABLA	ARARW5	ARTRW4	MNTSHRUB	PUTRR3A	WATER
ARARR1	ARTRR1*1	ARTRW5	POTRF4	PUTRR3B*5	WETMEADOW
ARARR3*9	ARTRR3B	BRTE	PSMEF2	PUTRW1*6	
ARARW1	ARTRT*2	CELE*4	PSMEF3	PUTRW2*7	
ARARW2	ARTRW1	CELER5*3	PSMEF4	ROCK*8	
ARARW4	ARTRW2	MINES	PUTRR1	TAAS	

Table 8. Eighteen custom fuel model names, numbers, and descriptions (Yanish 2002) including the three new models.

Plots Collected in 2003	Fuel Model	Model Name	Description
25	*37	ARAR R1	Low sagebrush herbaceous grassland
25	*37	ARTR R1	Mountain big sagebrush herbaceous grassland
-	20	TABLE ARAR	Low sagebrush table top
5	21	ARAR R3	Low sagebrush steppe
4	22	ARTR R3	Mountain sagebrush steppe
-	23	ARAR W1	Low sagebrush steppe with juniper
-	24	ARTR W1	Mountain sagebrush steppe with juniper
5	25	ARAR W2/W4	Open young juniper woodland low sagebrush
-	26	ARTR W2	Open young juniper woodland mountain sagebrush
5	27	ARTR W4	Young multi-story juniper woodland mountain sagebrush
-	28	CELE W4	Juniper woodland / mountain mahogany
5	29	ARAR W5	Old multi-story juniper woodland low sagebrush
5	30	ARTR/CELE W5	Old multi-story juniper woodland / mountain mahogany / mountain sagebrush
-	31	ROCK W5	Old multi-story juniper and rock
24	32	POTR F4	Aspen
-	33	MNT. SHRUB	Chokecherry, bittercherry, shiny leaf ceanothus
1	34	WET MEADOW	Wet meadow
18	*35	PSME F2	Mountain sagebrush steppe with an open young Douglas-fir forest
30	*36	PSME F4	Old multi-story Douglas-fir forest

* Fuel models not included in Yanish (2002).

Table 9. Positive and negative trends and significance of each landscape metric for Artrv W1 using method A and B within each of the three watersheds.

Metric	Current Creek		Red Canyon		Smith Creek	
	Method A	Method B	Method A	Method B	Method A	Method B
Patch Density	-- 0.6508	+ 0.1199	-- 0.2181	+ 0.0253	-- 0.6175	-- 0.6572
Edge Density	+ 0.2702	+ 0.0118	-- 0.2269	+ 0.0942	-- 0.4364	-- 0.8953
LSI	+ 0.2266	+ 0.0141	-- 0.2265	+ 0.1002	-- 0.4565	-- 0.9583
Mean Area	+ 0.4869	-- 0.3493	+ 0.0749	-- 0.0835	+ 0.3895	+ 0.5045
Nearest Neighbor	-- 0.2872	-- 0.4870	-- 0.1576	-- 0.1686	+ 0.5782	-- 0.3336
Contagion	-- 0.0315	-- 0.0733	+ 0.5302	-- 0.3256	-- 0.8691	-- 0.7307
IJI	+ 0.8005	-- 0.7961	-- 0.7191	+ 0.5002	+ 0.6487	+ 0.8350
Simpson's Diversity	+ 0.1905	+ 0.0329	-- 0.0938	+ 0.8390	-- 0.2991	-- 0.4212
Simpson's Evenness	+ 0.0586	+ 0.0278	-- 0.1826	+ 0.8369	-- 0.4800	-- 0.7297

Bold text indicates significant results with a p-value <0.1.

Table 10. Positive and negative trends and significance of each landscape metric for Artrv W2 using method A and B within each of the three watersheds.

Metric	Current Creek		Red Canyon		Smith Creek	
	Method A	Method B	Method A	Method B	Method A	Method B
Patch Density	+ 0.8121	+ 0.0063	+ 0.5202	+ 0.0024	+ 0.1448	+ 0.8560
Edge Density	+ 0.3327	+ 0.0001	+ 0.4693	+ 0.0213	+ 0.2155	+ 0.4423
LSI	+ 0.3557	+ 0.0001	+ 0.4687	+ 0.0219	+ 0.2155	+ 0.4423
Mean Area	-- 0.6441	-- 0.0028	-- 0.5690	-- 0.0058	-- 0.1328	-- 0.7128
Nearest Neighbor	-- 0.2703	-- 0.0577	-- 0.0413	-- 0.0859	-- 0.0433	-- 0.2751
Contagion	-- 0.2362	-- 0.0129	-- 0.2829	-- 0.0294	-- 0.0286	-- 0.5946
IJI	+ 0.7810	+ 0.5927	+ 0.3232	+ 0.0203	+ 0.0122	+ 0.5839
Simpson's Diversity	+ 0.0659	+ 0.0222	+ 0.5005	+ 0.0080	+ 0.0276	-- 0.8642
Simpson's Evenness	+ 0.0916	+ 0.0266	+ 0.4332	+ 0.0119	+ 0.0179	-- 0.9934

Bold text indicates significant results with a p-value <0.1, bold metric indicates the same sign (+or--) across each watershed and method.

Table 11. Positive and negative trends and significance of each landscape metric for Artrv W4 using method A and B within each of the three watersheds.

Metric	Current Creek		Red Canyon		Smith Creek	
	Method A	Method B	Method A	Method B	Method A	Method B
Patch Density	+ 0.0069	+ <0.0001	+ 0.0218	+ 0.0080	+ <0.0001	+ 0.0001
Edge Density	+ 0.0218	+ 0.0002	+ 0.0997	+ 0.0105	+ <0.0001	+ 0.0005
LSI	+ 0.0242	+ 0.0002	+ 0.0997	+ 0.0105	+ <0.0001	+ 0.0006
Mean Area	-- 0.0230	-- 0.0004	-- 0.0664	-- 0.0184	-- <0.0001	-- 0.0007
Nearest Neighbor	-- 0.7660	-- 0.1508	-- 0.0814	-- 0.0387	-- 0.3173	-- 0.0766
Contagion	-- 0.6135	-- 0.0951	-- 0.0512	-- 0.0251	-- 0.0034	-- 0.0099
IJI	-- 0.6818	-- 0.7982	+ 0.0578	+ 0.1136	+ 0.0440	+ 0.0848
Simpson's Diversity	+ 0.0285	+ 0.0036	+ 0.0341	+ 0.0173	+ 0.0090	+ 0.2675
Simpson's Evenness	+ 0.1460	+ 0.0225	+ 0.0548	+ 0.0353	+ 0.0315	+ 0.2351

Bold text indicates significant results with a p-value <0.1, bold metric indicates the same sign (+or--) across each watershed and method.

Table 12. Positive and negative trends and significance of each landscape metric for Artrv W5 using method A and B within each of the three watersheds.

Metric	Current Creek		Red Canyon		Smith Creek	
	Method A	Method B	Method A	Method B	Method A	Method B
Patch Density	+ 0.0415	+ 0.0003	+ 0.0002	+ 0.0057	+ 0.0039	+ 0.0104
Edge Density	+ 0.2991	+ 0.0014	+ 0.0042	+ 0.0472	+ 0.0266	+ 0.0096
LSI	+ 0.3029	+ 0.0018	+ 0.0042	+ 0.0490	+ 0.0227	+ 0.0096
Mean Area	-- 0.0533	-- 0.0016	-- 0.0006	-- 0.0079	-- 0.0237	-- 0.0138
Nearest Neighbor	+ 0.9094	-- 0.8601	+ 0.8590	-- 0.2338	-- 0.7228	-- 0.7164
Contagion	-- 0.2926	-- 0.1051	-- 0.0031	-- 0.0251	-- 0.0652	-- 0.0205
IJI	+ 0.2093	+ 0.5624	+ 0.0082	+ 0.0203	+ 0.2448	+ 0.1570
Simpson's Diversity	+ 0.0087	+ 0.0308	+ 0.0015	+ 0.0169	+ 0.0029	+ 0.0015
Simpson's Evenness	+ 0.0426	+ 0.0873	+ 0.0045	+ 0.0269	+ 0.0081	+ 0.0024

Bold text indicates significant results with a p-value <0.1, bold metric indicates the same sign (+or--) across each watershed and method.

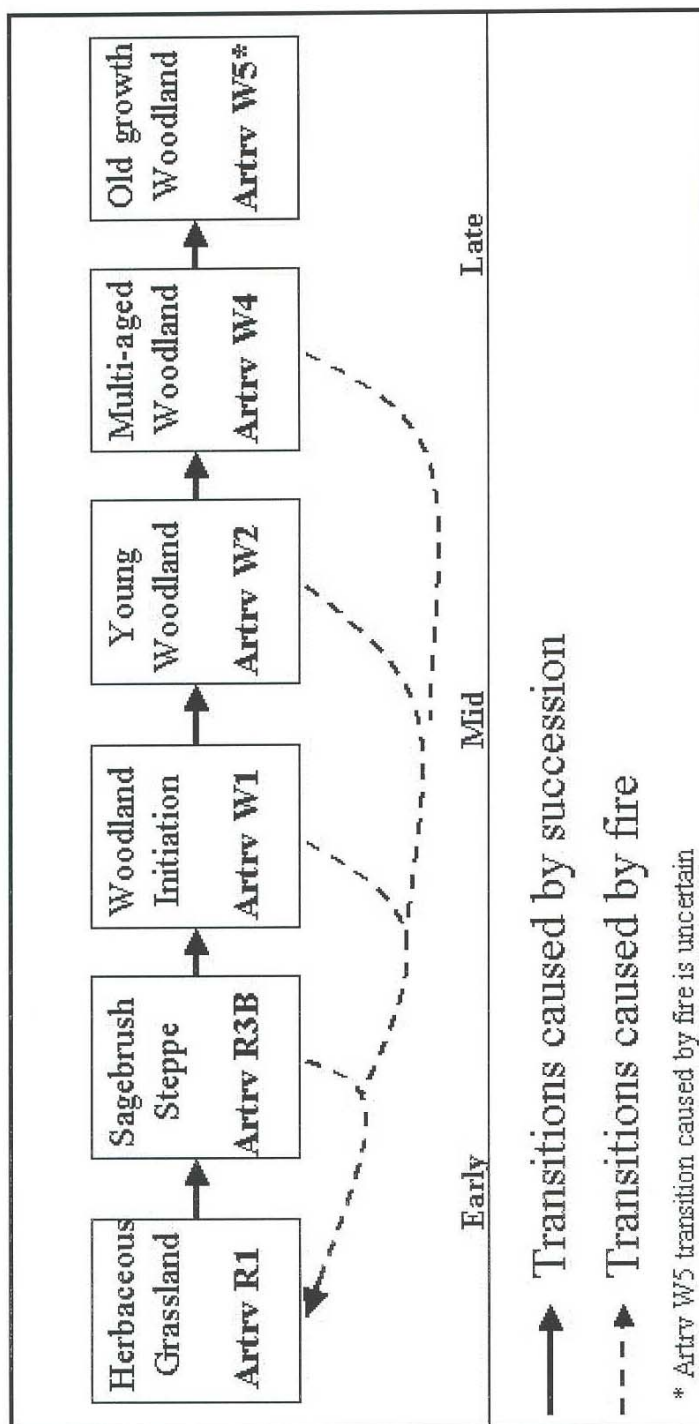


Fig. 1. Mountain Big Sagebrush PVT-SS classes successional diagram with fire as the disturbance.

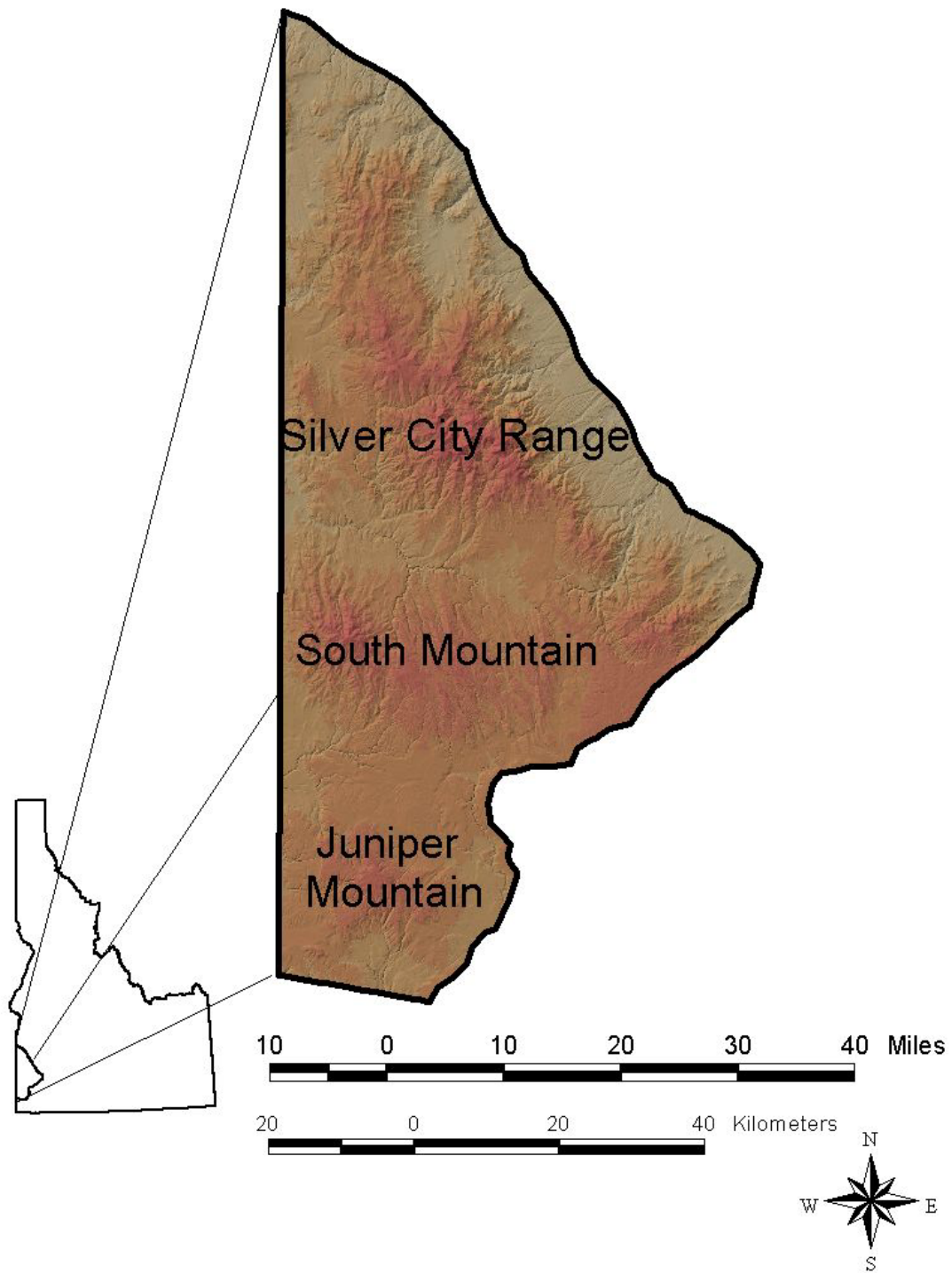


Fig. 2. Owyhee Plateau study area and locations of the Silver City Range, South Mountain, and Juniper Mountain.

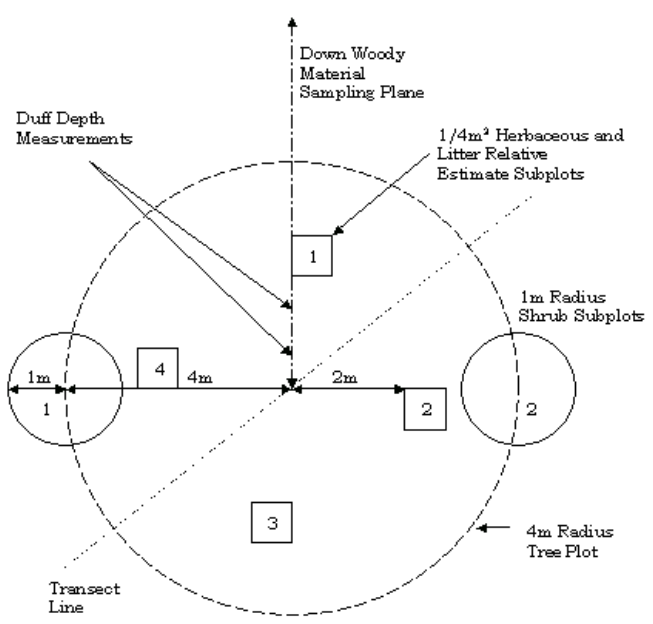


Fig. 3. Fuel measurement plot design diagram Yanish (2002).

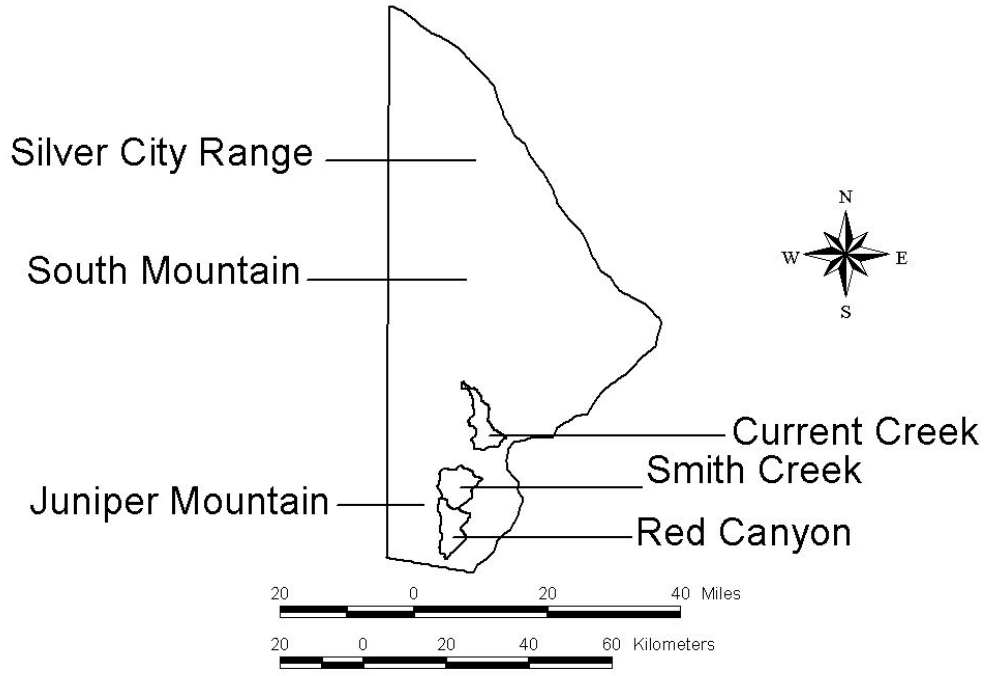


Fig. 4. The three HUC 6th order watersheds used in objective 3 including Current Creek, Smith Creek, and Red Canyon.

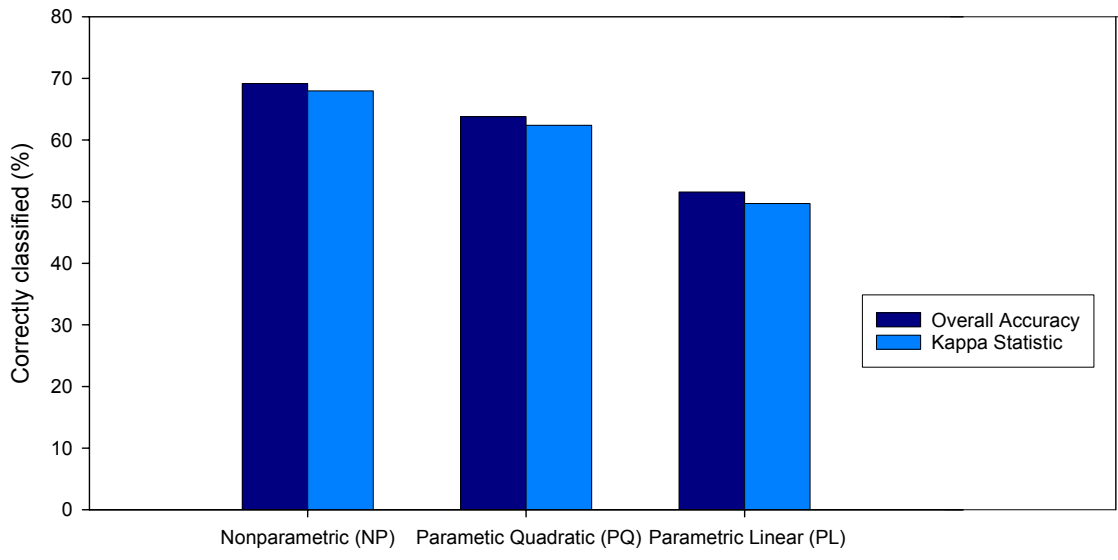


Fig. 5. Overall accuracy and kappa statistic for each of the three classification methods.

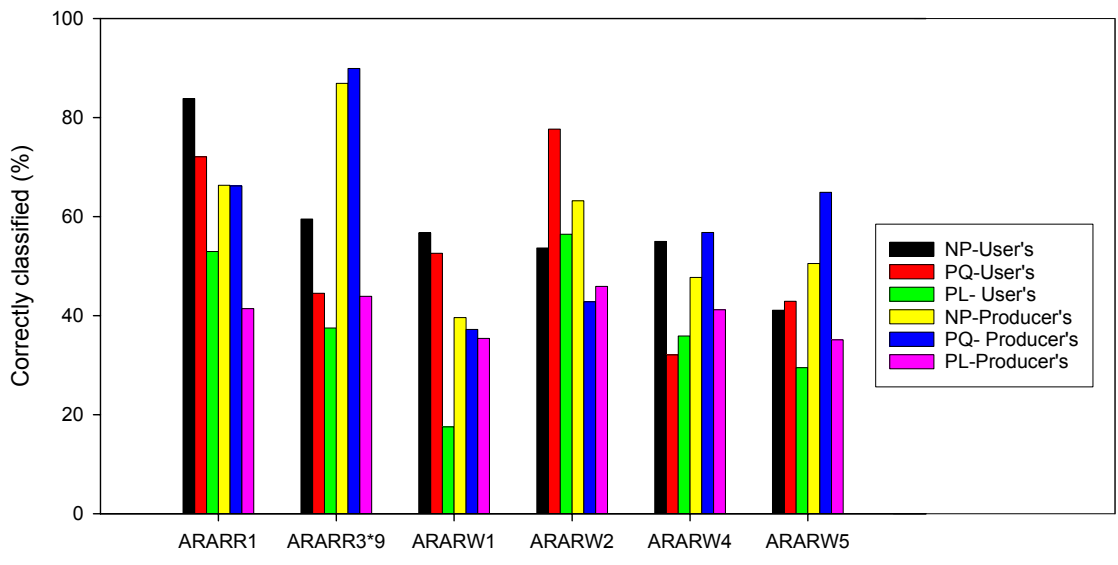


Fig. 6. Low sagebrush Potential Vegetation Type User's vs. Producer's accuracy comparison for each classification method.

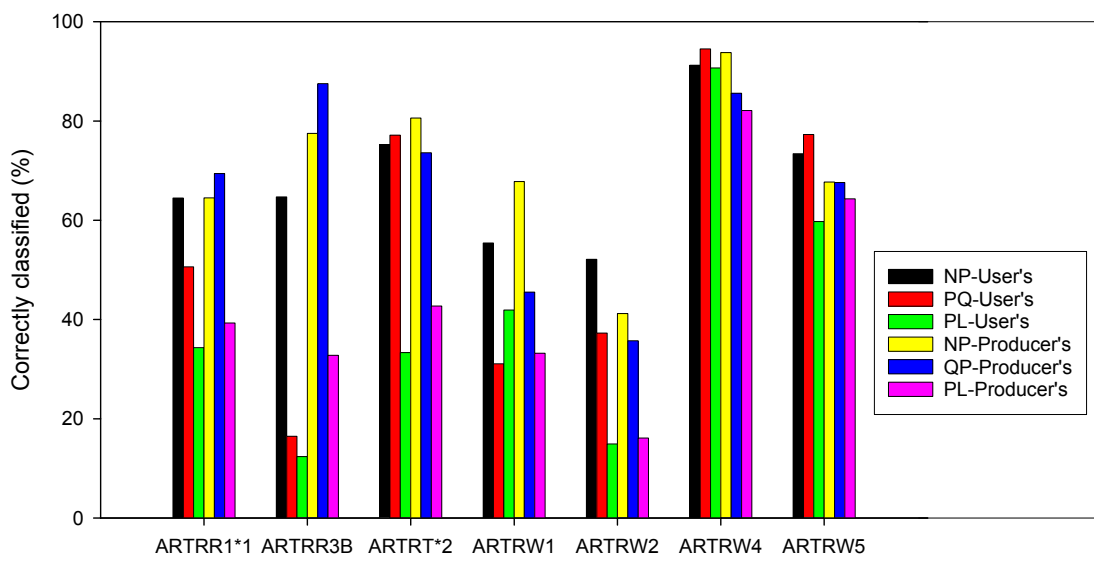


Fig. 7. Big sagebrush Potential Vegetation Type User's vs. Producer's accuracy comparison for each classification method.

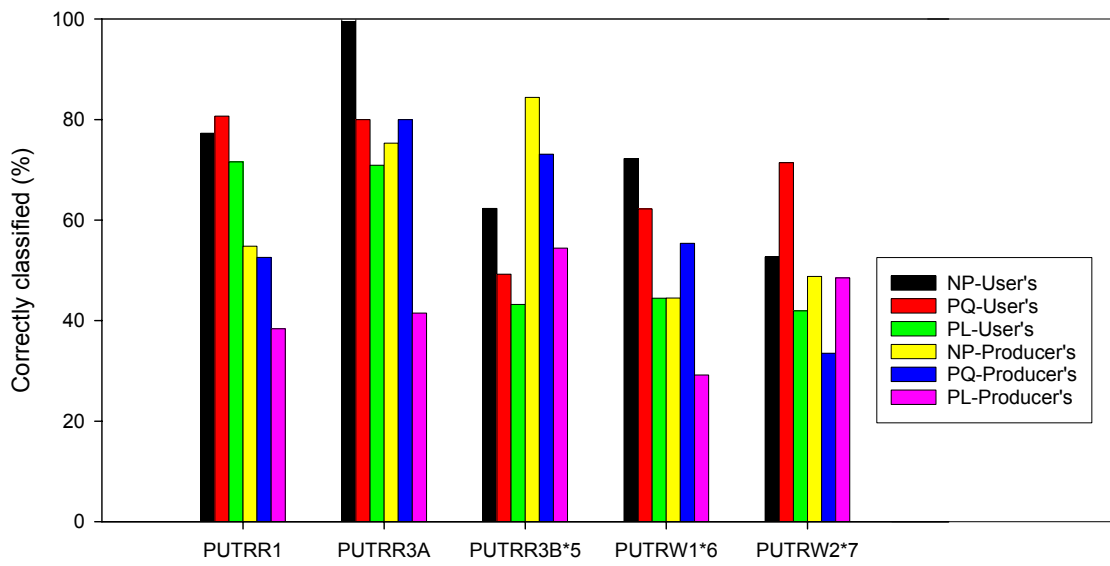


Fig. 8. Bitterbrush Potential Vegetation Type User's vs. Producer's accuracy comparison for each classification method.

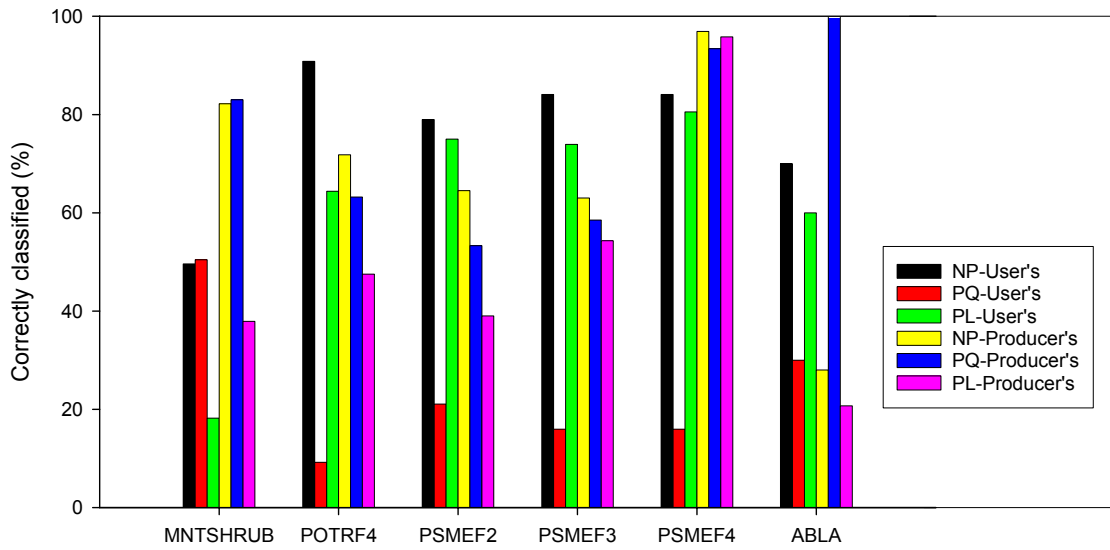


Fig. 9. Forest Potential Vegetation Types User's vs. Producer's accuracy comparison for each classification method.

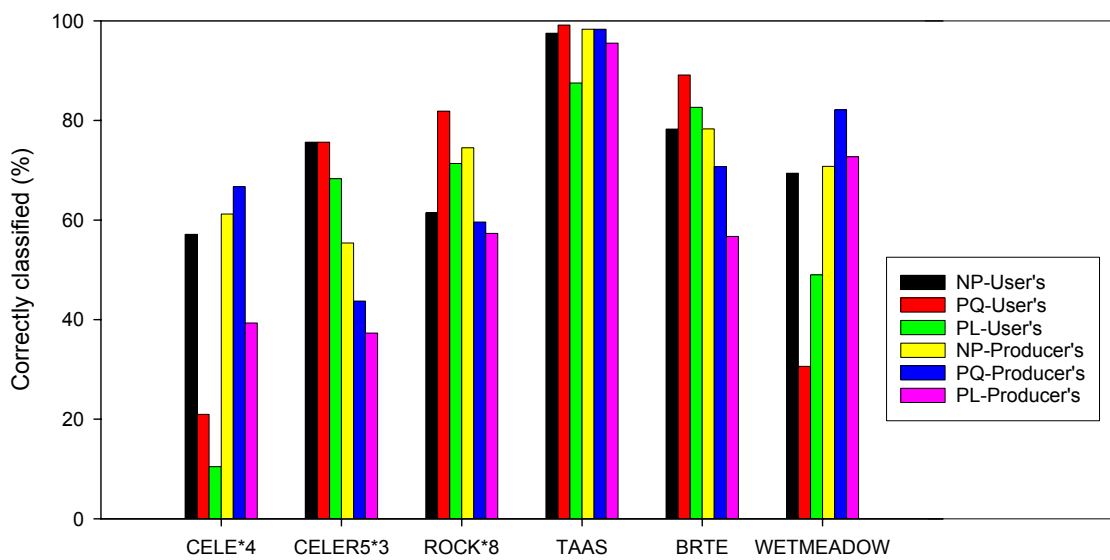


Fig. 10. Curl-leaf mountain mahogany Potential Vegetation Type, annuals, rock, and wet meadow classes User's vs. Producer's accuracy comparison for each classification method.

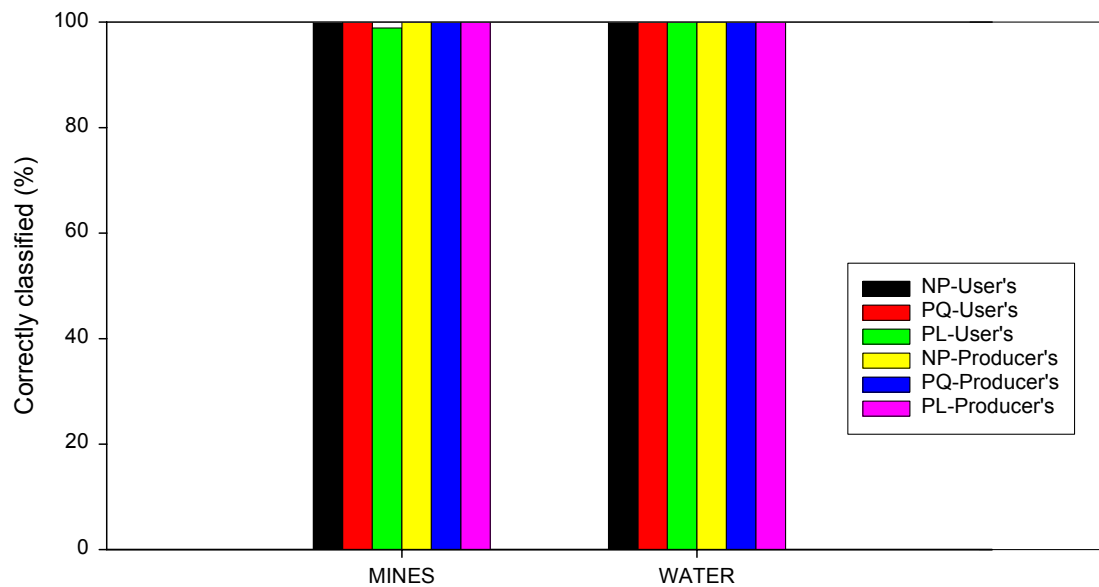


Fig. 11. Water and mine classes User's vs. Producer's accuracy comparison for each classification method.

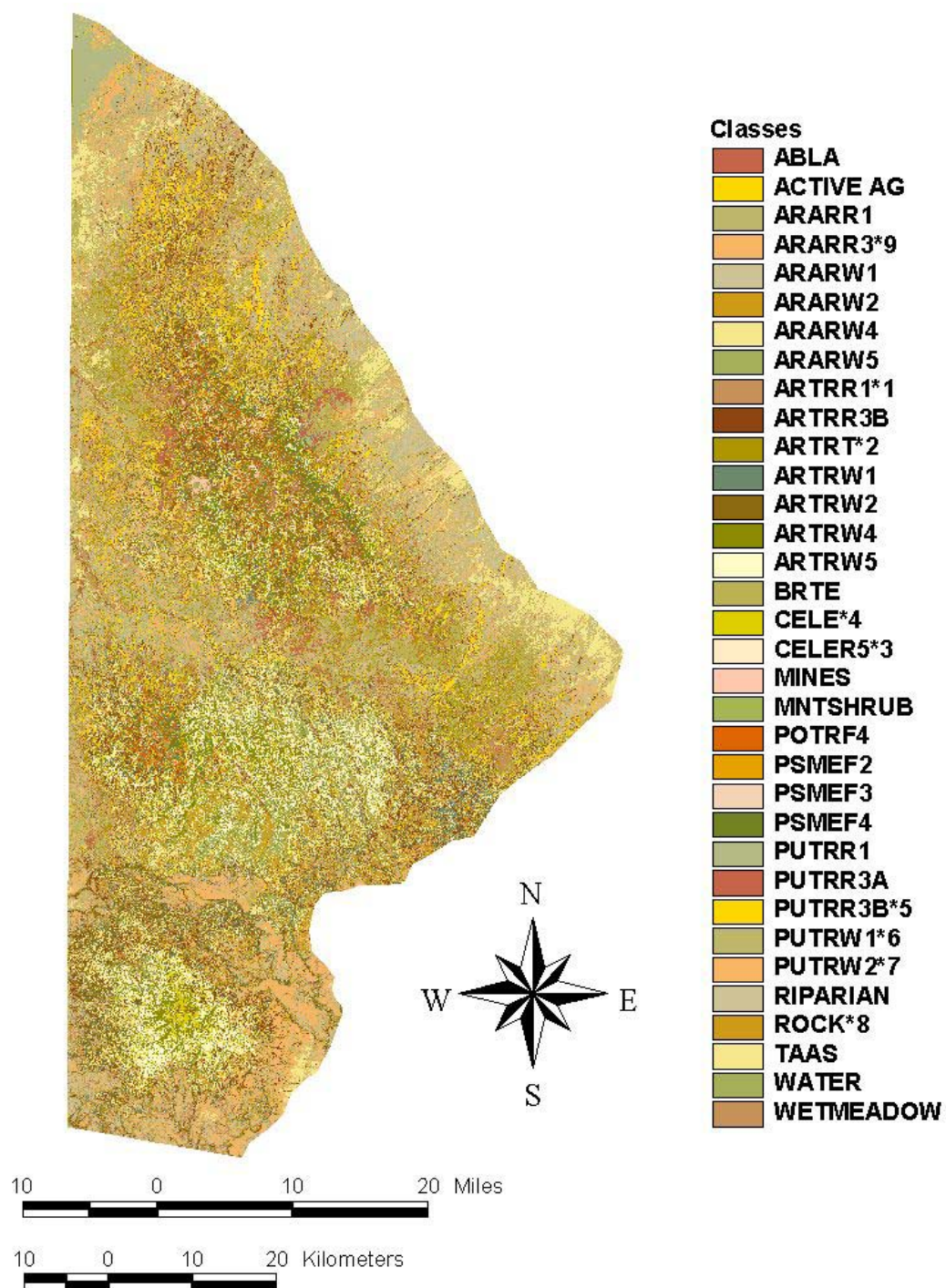


Fig 12. Final Nonparametric classification map.

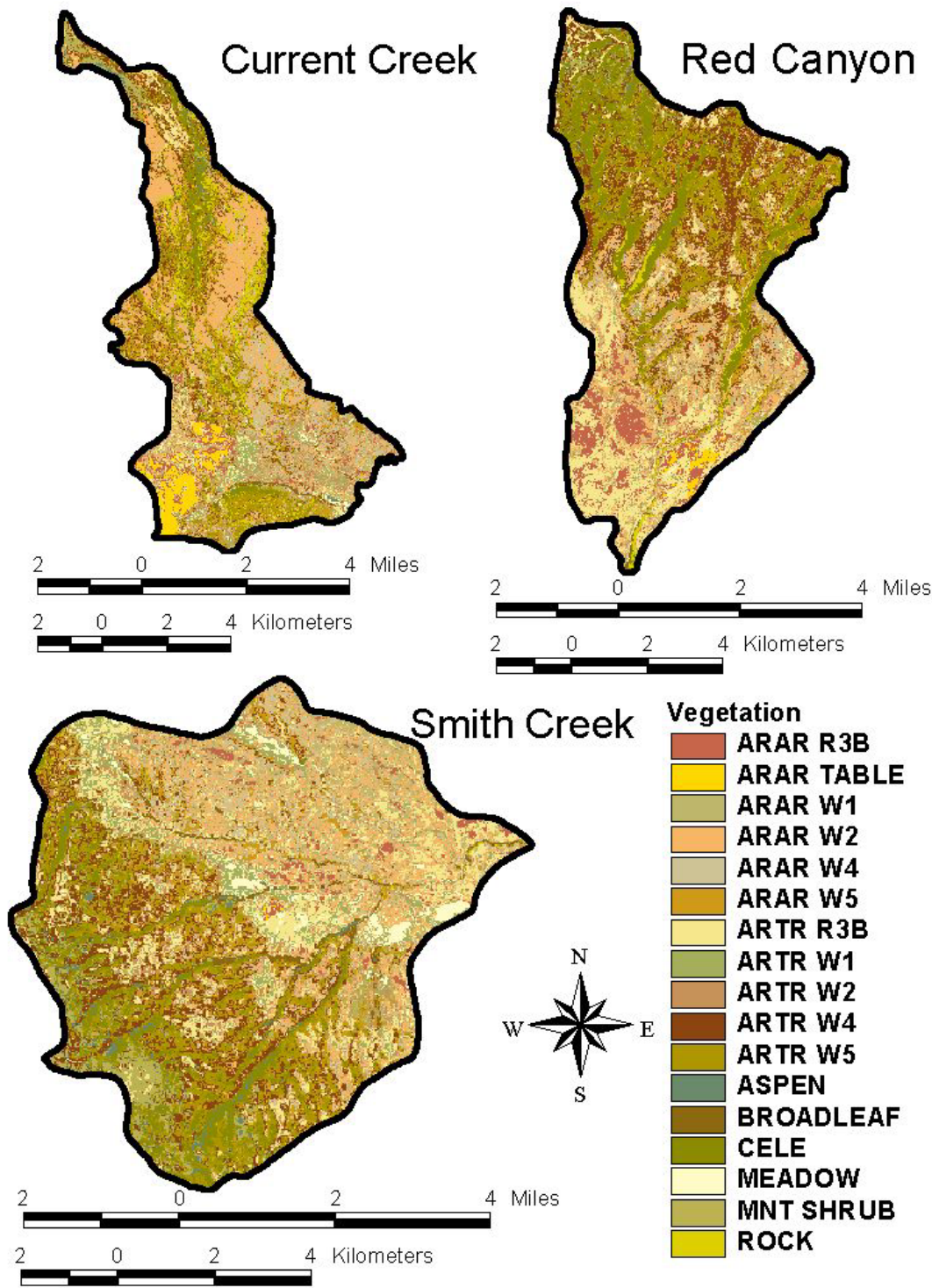


Fig. 13. Vegetation maps of the three watersheds used to compare landscape arrangement to fire frequency in objective 3.

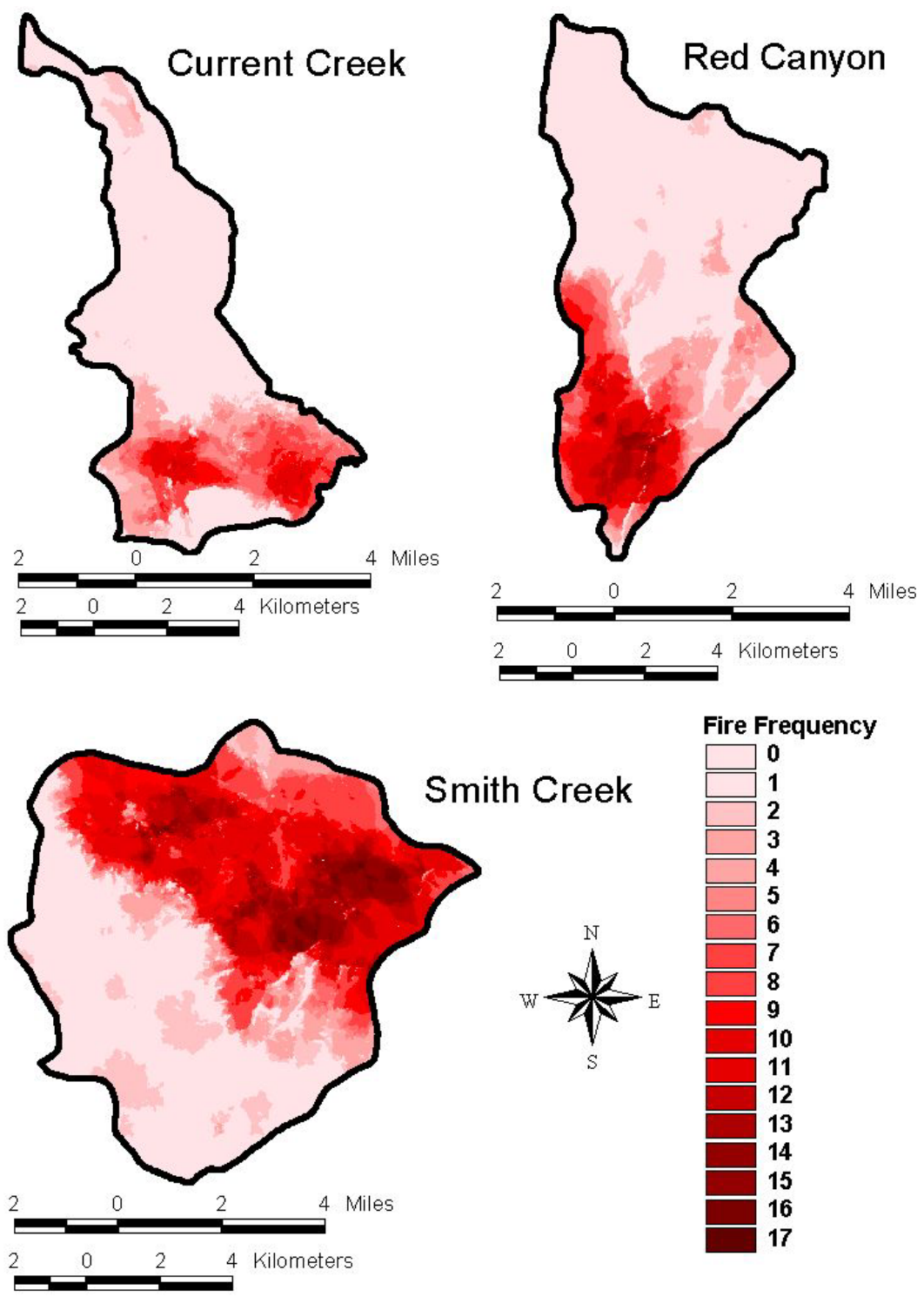


Fig. 14. Fire frequency maps of the three watersheds used in objective 3 created by method A using 100 fires.

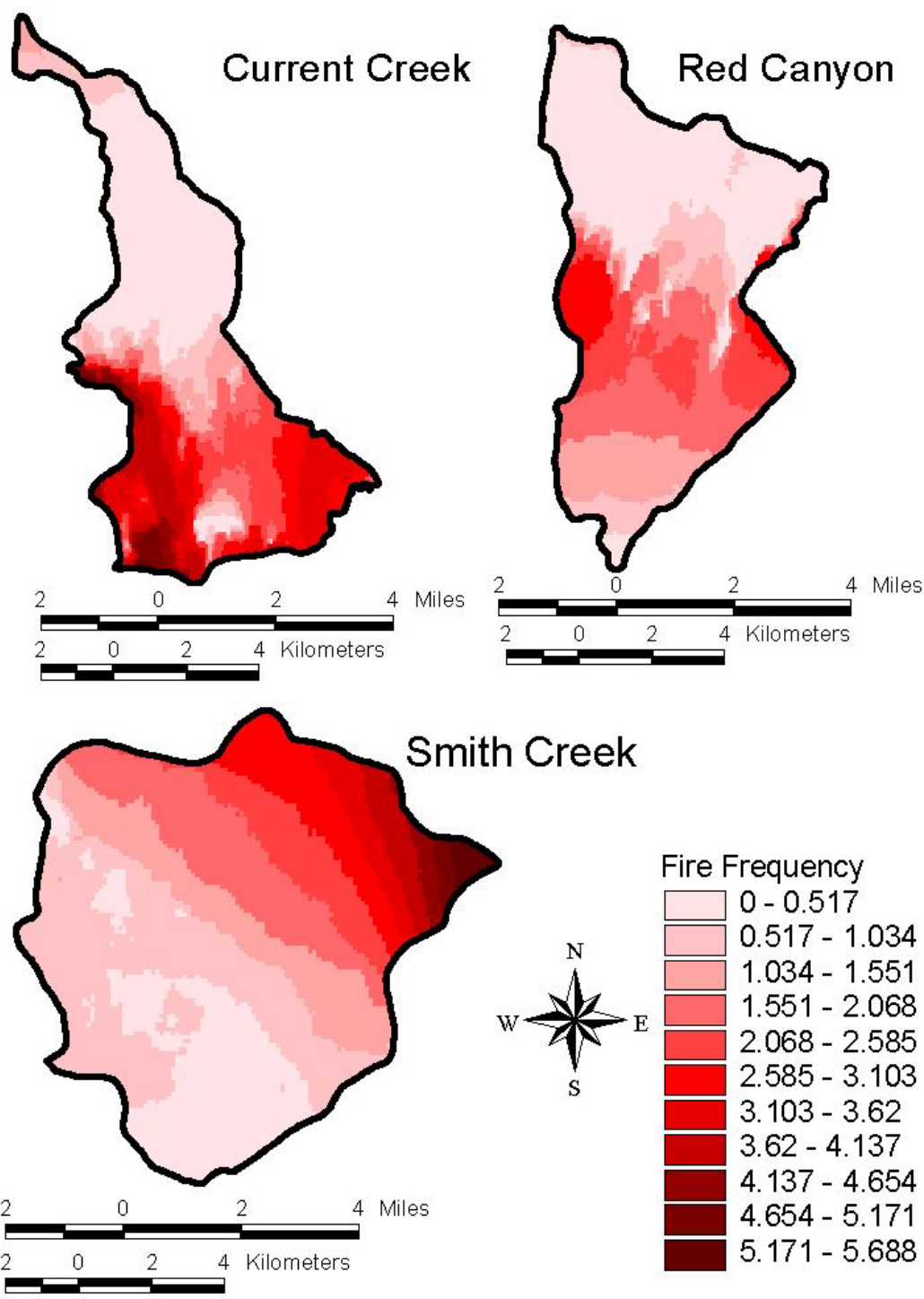


Fig. 15. Fire frequency maps of the three watersheds used in objective 3 created by method B using 25,000 fires.

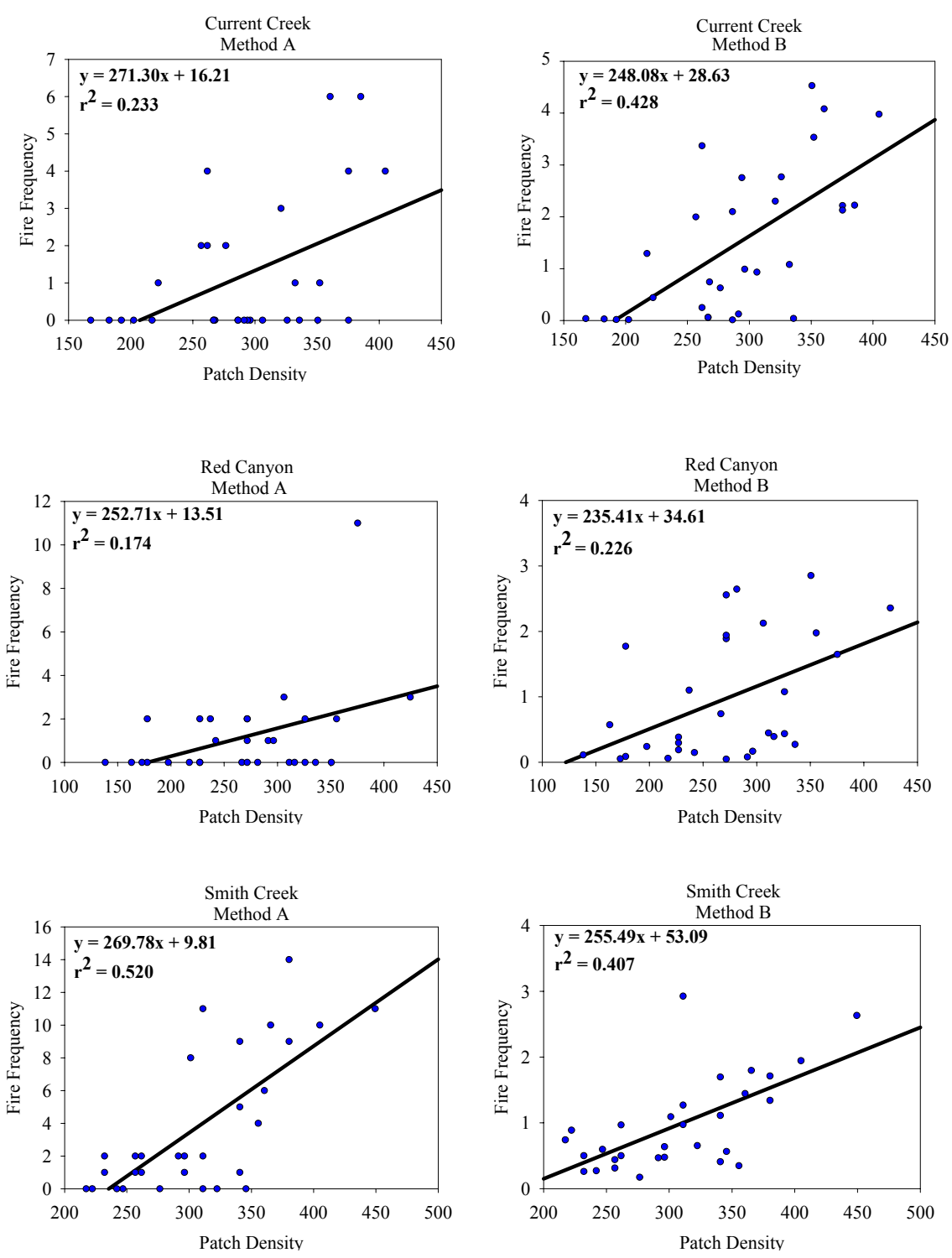


Fig. 16. Artrv W4 significant trend for the landscape metric Patch Density across each watershed using both fire frequency methods.

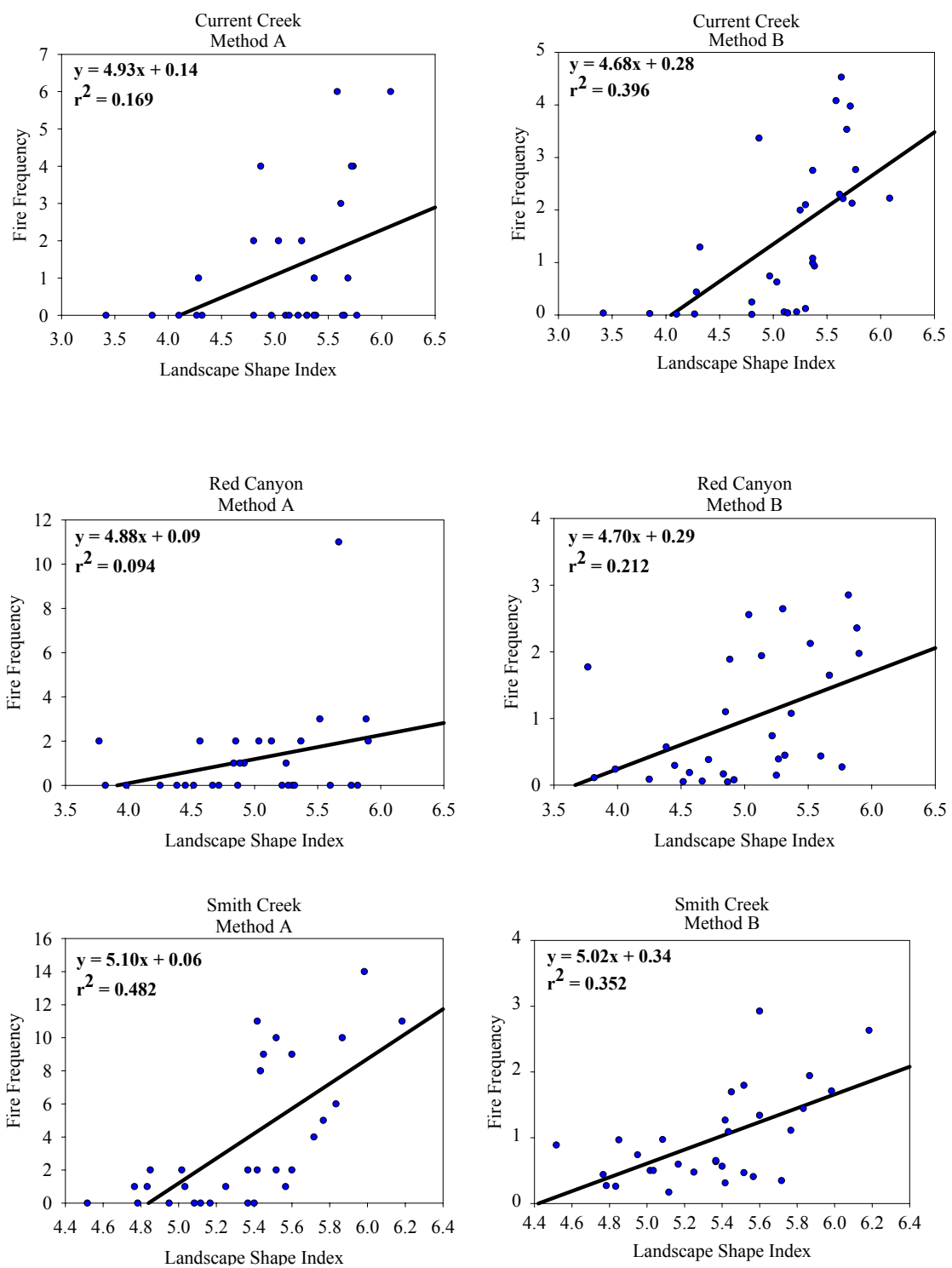


Fig. 17. Artrv W4 significant trend for the landscape metric Landscape Shape Index across each watershed using both fire frequency methods.

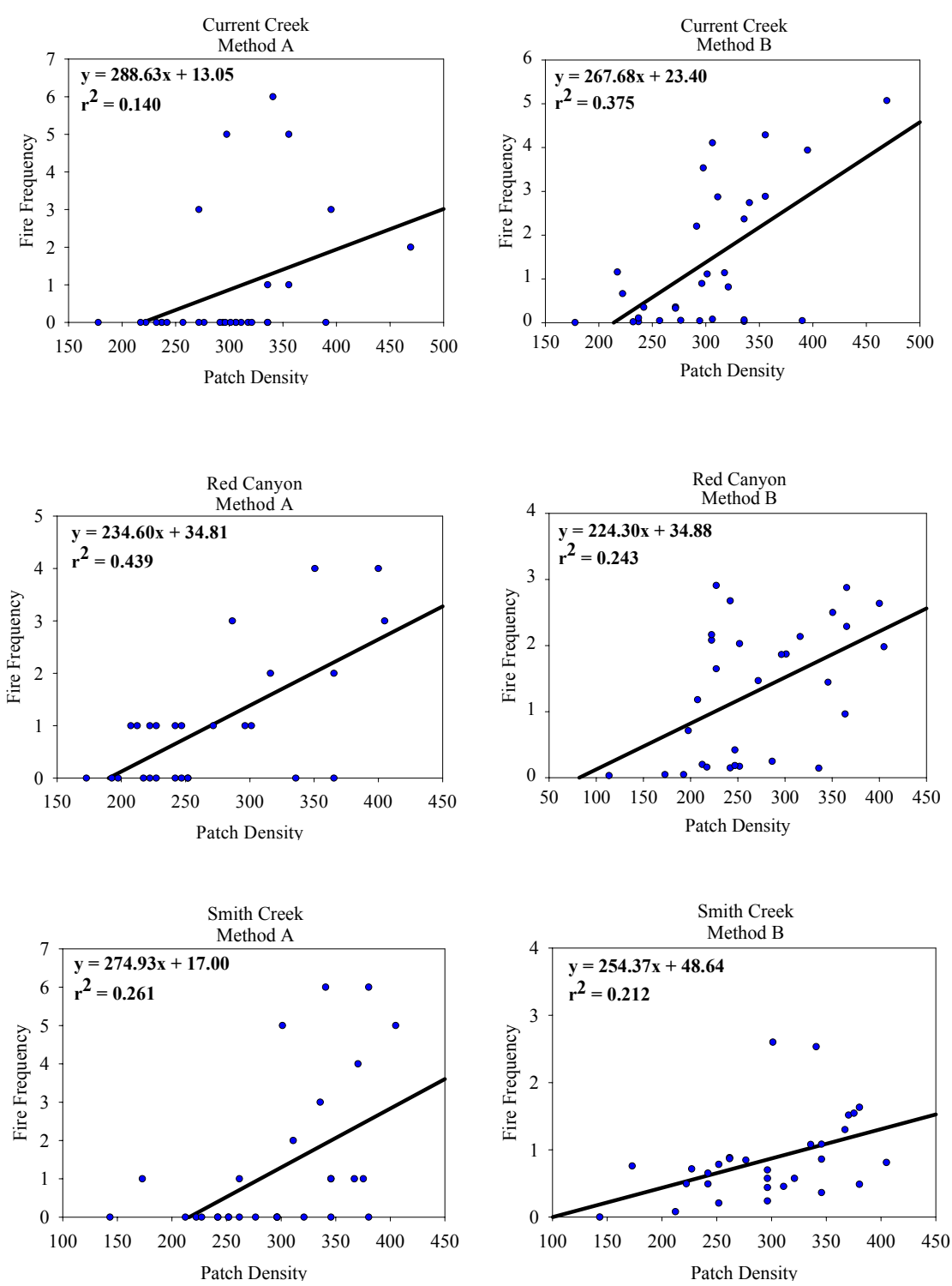


Fig. 18. Artrv W5 significant trend for the landscape metric Patch Density across each watershed using both fire frequency methods.

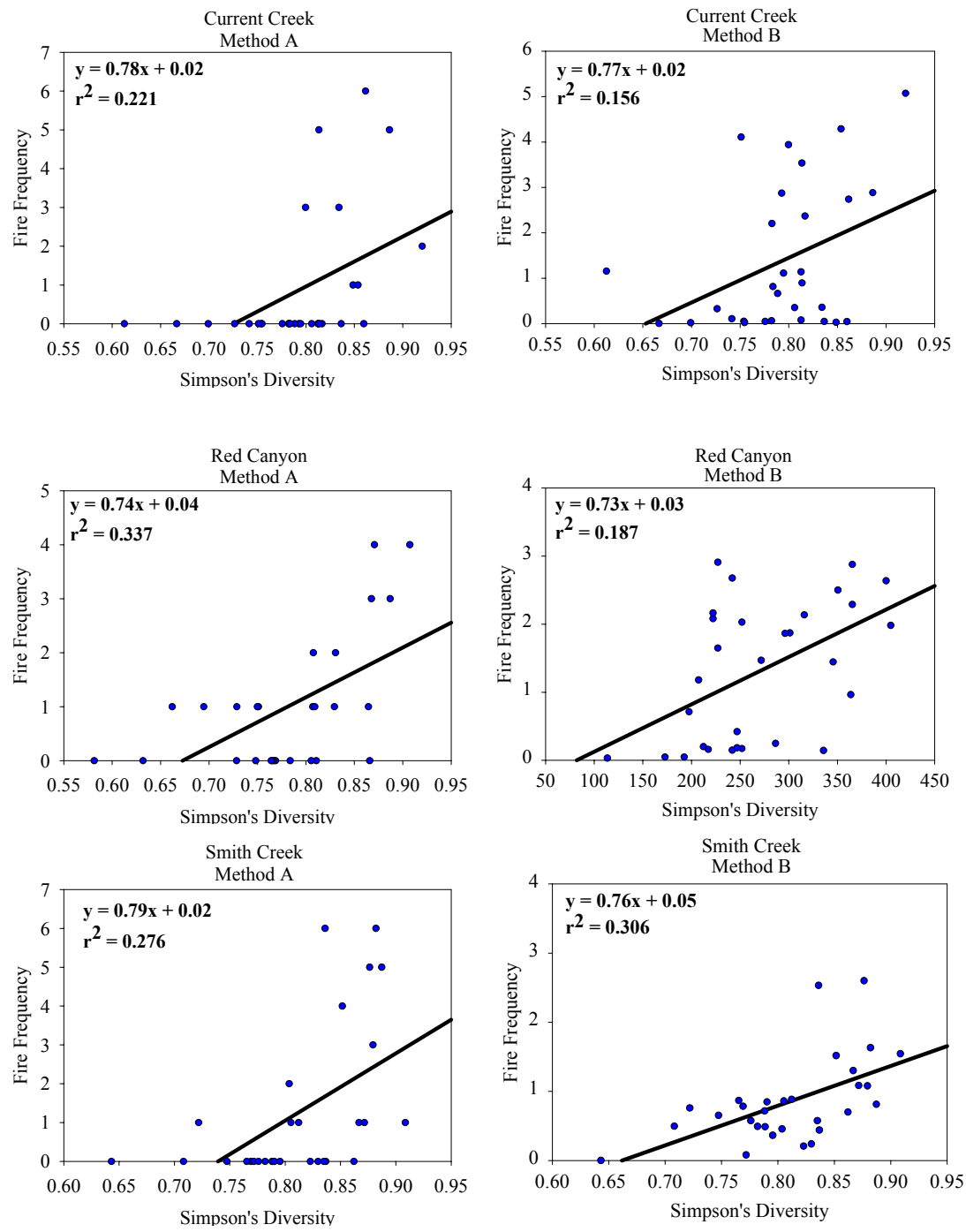


Fig. 19. Artrv W5 significant trend for the landscape metric Simpson's Diversity across each watershed using both fire frequency methods.

Appendix A. Owyhee Plateau cover types/ structural stage descriptions (Adapted from Hessburg et al. 1999, Bunting et al. 2002b).

WOODLAND

Artemisia arbuscula sere (Arar)

- R1 Open herbland:** Shrub cover <5%, herbaceous cover <67%.
- R3 Open low-med shrubland:** Canopy of low (<50cm) shrubs with canopy coverage <67%, tree coverage <2%. Sometimes very open stands of large mature juniper trees are present.
- R3A Open low-med shrubland:** Canopy of low (<50 cm) and/or medium 50-200 cm shrubs with canopy coverage <10%, juniper tree coverage <2%.
- R3B Open low-med shrubland:** Canopy of low (50 cm) and/or medium 50-200 cm shrubs with a canopy coverage 10-67%, juniper tree coverage <2%.
- W1 Woodland initiation:** Juniper canopy (<3%) of usually young, sometimes mid aged junipers present. Juniper is only having minor effects on competition and environment of the site and the sagebrush community is intact directly under juniper trees.
- W2 Young woodland:** Canopy (3-8%) of young and mid aged junipers present. Juniper is beginning to have an effect on the interspaced environment of the site. Sagebrush steppe species are declining and sagebrush skeletons present. However, low sagebrush still remains in interspaces.
- W4 Mixed-aged woodland:** Canopy (>8%) of young and mid aged junipers present. Usually a few mature juniper present. Sagebrush skeletons often present in understory. However, low sagebrush still common in interspaces.
- W5 Mature juniper woodland:** Overstory canopy >8% compose of primarily mature individuals (flat topped trees and *Letharia vulpina* usually present). Trees may not necessarily be large in size. Sagebrush usually present in openings except in the most dense stands of juniper.

Artemisia tridentata vaseyana sere (Artrv)

- R1 Open herbland:** Shrub cover <5%, herbaceous cover <67%.

- R3 Open low-med shrubland:** Canopy of low (<50 cm) and/or medium 50-200 cm shrubs with canopy coverage of <67%, tree coverage <2%.
- R3A Open low-med shrubland:** Canopy of low (<50 cm) and/or medium 50-200 cm shrubs with canopy coverage <10%, juniper tree coverage <2%.
- R3B Open low-med shrubland:** Canopy of low (50 cm) and/or medium 50-200 cm shrubs with a canopy coverage 10-67%, juniper tree coverage <2%.
- W1 Woodland initiation:** Canopy (<5%) of usually young, sometimes mid aged, junipers present. Juniper is having only minor effects on competition and environment of the site and the sagebrush community is intact except directly under juniper trees.
- W2 Young woodland:** Canopy (5-10%) of young and mid aged junipers present. Juniper is beginning to have an effect on the environment of the site. Sagebrush steppe species declining and sagebrush skeletons often present.
- W4 Mixed-aged woodland:** Canopy (>10%) of young and mid aged junipers present. Few or no mature junipers present with sagebrush skeletons often numerous in understory.
- W5 Mature juniper woodland:** Overstory canopy >15% composed of primarily mature individuals (flat topped trees and *Letharia vulpina* usually present). Few sagebrush remain except in larger openings. Some stands are completely dominated by old mature trees. Other stands may have open canopy of mature trees and a co-dominant layer of various aged mid-aged juniper.

***Cercocarpus ledifolius* sere (Cele)**

- R1 Open herbland:** Shrub cover <5%, herbaceous cover <67%.
- R3 Open low-med shrubland:** Canopy of low (<50 cm) and/or medium 50-200 cm shrubs with canopy coverage of <67%, tree coverage <2%. (See *Artemisia tridentata vaseyana* sere).
- R5 Open tall shrubland:** Canopy of tall (>2m) shrubs with <67% coverage. Juniper tree coverage <5%, usually composed of young to mid aged individuals.
- R5A Open tall shrubland:** Canopy of tall (>2m) shrubs with <10% coverage. Trees coverage <5%, usually composed of young to mid aged individuals.
- R5B Open tall shrubland:** Canopy of tall (>2m) shrubs with 10-67% coverage. Tree coverage <5%, usually composed of young to mid aged individuals.

- R7 Multi-strata tall shrubland:** Canopy of tall (>2m) shrubs with <67% coverage. Juniper and Douglas-fir 5-10 % usually composed of young, mid and mature aged individuals.
- W1 Woodland initiation:** Canopy (<5%) of usually young, sometimes mid aged, junipers present. Juniper is having only minor effects on competition and environment of the site and the sagebrush / mountain mahogany community is intact except directly under juniper trees.
- W2 Young woodland:** Canopy (5-10%) of young and mid aged junipers present. Juniper is beginning to have an effect on the environment of the site. Sagebrush / mountain mahogany community species declining and sagebrush skeletons often present.
- W4 Mixed-aged woodland:** Canopy (>10%) of young and mid aged junipers present. Few or no mature junipers present with sagebrush skeletons often numerous in the understory.
- W5 Mature juniper woodland:** Overstory canopy >15% composed of primarily mature individuals (flat topped trees and *Letharia vulpina* usually present). Few sagebrush remain except in large openings.

***Purshia tridentata* sere (Putr)**

- R1 Open herbland:** Shrub cover <5%, herbaceous cover <67%.
- R3 Open low-med shrubland:** Canopy of low (<50 cm) and/or medium 50-200 cm shrubs with canopy coverage of <67%, tree coverage <2%.
- R3A Open low-med shrubland:** Canopy of low (<50 cm) and/or medium 50-200 cm shrubs with canopy coverage <10%, juniper tree coverage <2%.
- R3B Open low-med shrubland:** Canopy of low (50 cm) and/or medium 50-200 cm shrubs with a canopy coverage 10-67%, juniper tree coverage <2%.
- W1 Woodland initiation:** Canopy (<5%) of usually young, sometimes mid aged, junipers present. Juniper is having only minor effects on competition and environment of the site and the sagebrush / bitterbrush community is intact except directly under juniper trees.
- W2 Young woodland:** Canopy (5-10%) of young and mid aged junipers present. Juniper is beginning to have an effect of the environment of the site with sagebrush / bitterbrush steppe species declining and sagebrush skeletons often present.

- W4 Mixed-aged woodland:** Canopy (>10%) of young and mid aged junipers present. Few or no mature junipers present with sagebrush / bitterbrush skeletons often numerous in understory.
- W5 Mature juniper woodland:** Overstory canopy >15% composed of primarily mature individuals (flat topped trees and *Letharia vulpina* usually present). Few sagebrush / bitterbrush plants remain except in larger openings.

FOREST

Populus tremuloides sere (Potr)

- F2 Sapling forest:** Seedlings and saplings $\geq 10\%$ canopy cover with poles, small, and medium trees $\leq 80\%$ canopy cover. Sites characterized by one canopy stratum (may be broken or continuous), minimum shrubs present in the understory, and grass and forbs present.
- F3 Pole forest:** Seedlings and saplings $< 10\%$ canopy cover, poles, and small trees $> 70\%$ canopy cover. Stands are continuously closed canopy of poles and small trees with shrubs, grasses and forbs present.
- F4 Young-multistory forest:** Large trees $< 30\%$ canopy cover, seedlings and saplings present, pole, small and medium trees $\leq 60\%$ canopy cover. Site characterized by a broken overstory canopy with diverse horizontal and vertical distribution of trees and tree sizes.
- F5 Old-multistory forest:** Large trees $\geq 30\%$ canopy cover with seedlings and samplings, poles, small trees, and medium trees $\leq 20\%$ canopy cover. Stands are typically multi-strata stands with diverse horizontal and vertical distribution of trees and tree sizes.

Pseudotsuga menziesii sere (Psme)

- F2 Sapling forest:** Canopy of low (<50 cm) and/or medium 50-200 cm shrubs with a canopy of $< 67\%$, tree coverage 3-8%. Seedling and saplings make up the tree component.
- F3 Pole forest:** Canopy of low (<50 cm) and/or medium 50-200 cm shrubs with a canopy cover of $< 85\%$, tree coverage 8-20%. Seedlings, samplings, and small trees make up the tree component.
- F4 Young-multistory forest:** Large trees $< 30\%$ canopy cover, seedlings and saplings present, pole, small and medium trees $\leq 60\%$ canopy cover. Site characterized by a broken overstory canopy with diverse horizontal and vertical distribution of trees and tree sizes.

- F5 Old-multistory forest:** Large trees $\geq 30\%$ canopy cover with seedlings and samplings, poles, small trees, and medium trees $\leq 20\%$ canopy cover. Stands are typically multi-strata stands with diverse horizontal and vertical distribution of trees and tree sizes.

Abies lasiocarpa sere (Abla)

Mixed-aged forest: Site dominated by subalpine fir.

OTHER COVER TYPES

Rock

- W4 Rock mixed aged woodland:** Canopy ($>15\%$) composed of mostly mid aged juniper with mature individuals also sometimes present. Limited shrub component with sites dominated by a sparse understory consisting of mostly grasses and forbs. Site dominated by bare ground.
- W5 Rock mature woodland:** Canopy ($<15\%$) composed of primarily mature juniper (flat topped trees and *Letharia vulpina* usually present). Limited shrub component with sites dominated by a sparse understory of mostly grasses and forbs. Sites dominated by bare ground.

Wet Meadow (Wet Meadow)

- R2 Closed herbland:** Herbaceous coverage $>67\%$.

Mountain Shrub (Mnt. Shrub)

- R6 Closed tall shrub:** Canopy of tall ($>2\text{m}$) shrubs with $>67\%$ coverage. Juniper coverage $<5\%$, usually composed of young to mid aged individuals.

Bromus tectorum (Brte)

Closed annual herbland: Herbaceous coverage $>67\%$ dominated by cheatgrass forming thick dense mats.

Taeniatherum caput-medusae (Taas)

Closed annual herbland: Herbaceous coverage $>67\%$ dominated by medusahead forming thick dense mats.

Active Agriculture

Mines

Water

Appendix B. Procedures for the supervised classification.

I. Required Software

II. Preprocessing of the Image

- a.) Conversion to at satellite reflectance
- b.) Reprojection of the image
- c.) Subsetting the image
- d.) Creating additional ancillary layers (NDVI, MSI, Tassel Cap)
- e.) Layer stack

III. DOQQ's

- a.) Instructions for DOQQ application

IV. Training Sites

- a.) Training site instructions
- b.) Shape file creation

V. Supervised Classification

- a.) Classification setup
- b.) Signature editor
- c.) AOI merge
- d.) SAS test to create error matrix
- e.) Study area division
- f.) Final SAS classification
- g.) Grid creation
- h.) Decision rules

VI. Additional Resources (Located on CD)

- Training site data sheet
- Training site excel template
- Error matrix template

I. REQUIRED SOFTWARE

Software that was utilized in this process can be seen in Appendix E.

IIA. CONVERSION TO AT SATELLITE REFLECTANCE

Conversion from digital numbers (DN) to at satellite reflectance was done in ERDAS IMAGINE using the **Modeler, Model Maker** function. Because each Landsat image will have different values that must be entered into the Modeler only a figure of the models will be provided, see Appendix F. A website by Irish (2000) will also be provided in the reference section, which will provides additional insight in to the thought process along with chapter descriptions on conversion to radiance (11.3.1) and conversion from radiance to reflectance (11.3.2). See Appendix G for an example of a sample Landsat header file that provides the location of parameters such as: LMIN, LMAX, and ESUN values required in the model.

IIB. REPROJECTION OF THE IMAGE

Reprojection on the raw Landsat image can be done by a variety of programs. This example shows how this process can be done in ERDAS IMAGINE. To reproject an image click on **Data Prep** followed by **Reproject Image**. From this window the input file needs to be entered along with an output file name. Under categories (or desired map projection) select UTM Clarke 1886 NAD 27 north, and under Projection select UTM Zone 11. See Appendix H. Select Units to be meters. Select Ignore Zero in Stats. Select the Re-sampling Method that is appropriate to the desired application. Nearest neighbor was used for this project. Select Rigorous Transformation or Polynomial Approximation depending on appropriate method for the application. More detailed information about Resample Methods, Rigorous Transformation, and Polynomial Approximation can be found by clicking on the Help button at the bottom of the window. Once all the settings have been selected click Okay.

IIC. SUBSETTING THE IMAGE

ERDAS IMAGINE was used to subset the image that has been converted to reflectance to the actual study area. The study area was defined by the Idaho boundary along the west side. The Owyhee River on the southern extent and elevation boundary along the east and northern extent. The elevational boundary was created by using a DEM or digital elevational model. The DEM was reclassified to have a contour interval of 1250-m. In IMAGINE the Landsat image was opened in one viewer along with the Idaho boundary shape file to define the western boundary. In another viewer the DEM was added along with the Idaho boundary shape file. Using the AOI Tool by clicking on the **AOI** title then **Tools** the polygon box below the pointer was used to create the study area. By looking at the DEM fairly rough study boundaries were created on the Landsat image. By double clicking when the boundary has been defined an AOI was created. After a few attempts the project boundary was created and the AOI was saved. To save an AOI go to **File, Save, AOI Layer As**.

Next a subset of the entire Landsat image can be created based on the saved AOI. To do this select **Interpreter** on the main IMAGINE window, then **Utilities**, followed by **Subset**. The input image is the entire Landsat file and the output file can be any new name. Click on the four corners circle, check the Ignore zeros box and click on the AOI button at the bottom. Select the AOI file circle and locate the AOI created above. When all the regions have been defined the Okay button can be selected.

IID. CREATING ADDITIONAL ANCILLARY LAYERS (NDVI, MSI, TASSEL CAP)

After the image has been subset to the project boundary additional layers can be created that can help in the classification. Any number or combination of these layers can be created based on past research or the research question. We used the NDVI, MSI, and Tassel Cap layers.

In IMAGINE click on the **Interpreter** button on the top tool bar. Next click on the **Spectral Enhancement** button. Next click on the **Indices** button. From here the image converted to reflectance can be entered in to the input file and a new output file name needs to be added such as NDVI or something else. The sensor will be Landsat TM and the output file will be floating single. Either the NDVI function, or MSI, which in IMAGINE is called the ferrous minerals, can be selected from the function list. Click on Okay to complete. Do this for any indices of interest that can be created from the list.

To create the tassell cap layers the defaults selection under spectral enhancement was not used because it was designed for the Landsat TM5 sensor. A custom model was used to create the layers based on Landsat 7 ETM + coefficients. Click on the **Modeler** button on the top of the tool bar just like when the raw image was converted to reflectance. Next click on **Model Maker**. Refer to Appendix I for a graphical representation of the model. The coefficients for the Landsat 7 ETM+ image were taken from a paper by Huang et al. (2002) who used 5-paired images to create the coefficients. Make sure that the number of bands in the image corresponds to the number of bands of coefficients. Make sure that it is also a floating single file. Click on Okay to complete. The coefficients for all six layers were used and acquired from the paper by Huang et al. (2002).

III. LAYER STACK

Once all the layers have been created they need to be stacked together to form one image with multiple layers. For example 11 layers were used for this classification with the following order, which can be seen in Appendix J.

To create the layer stack click on the **Interpreter** button. Then click on the **Utilities** button followed by the **Layer Stack** button. Add the reflectance image first and add the six layers required. Next add the Tassel cap image to the input file and add the first three layers. Next input the NDVI layer followed by the MSI layer. Give the new image a name in the output

file and make sure that the output data type is floating single. Click Okay. This will be the image used in the classification process.

III. INSTRUCTIONS FOR DOQQ APPLICATION

DOQQ's can be downloaded free of charge for the entire Owyhee study area from the following web site. (<http://www.insideidaho.org/>).

Once at the website click on **Geodata** title bar on the left and click on find data. Next under grouping double click on scale. The very first entry in the set of boxes should have the name **Digital Orthophoto Quarter-Quads**. Double click on the download button and the areas across the state that have DOQQ's will come up. From here to located individual DOQQ's by name select the Quarter-Quad Info button and select a square. The zoom in and out buttons can also be used to help locate a DOQQ within a given area. Once the DOQQ of interest has been located click the download button and click on the correct DOQQ. Save to a folder or on a CD.

Once all the DOQQ's have been downloaded they must be unzipped. Open the file from my computer and double click on each. Using WinZip extract each of the DOQQ files into another folder just for DOQQ's such as doq's_2003. One all of the DOQQ's have been extracted the must be converted to correct file format.

Open the folder designated for DOQQ's. Open a word pad file to create an AML header file, which will be used to format the DOQQ's. It should include the following info.

```
/** w c:/aroth/doq_2003 (location where DOQQ's area and will be reformatted to)
/** &r runaml (&r is the command used to run the process followed by the file name)
```

```
&r makhead hurrupcr_24kqq_usgs_doqq062198ne.nes bil new nad27 0 0
&r makhead hurrupcr_24kqq_usgs_doqq062198nw.nws bil new nad27 0 0
&r makhead hurrupcr_24kqq_usgs_doqq062198se.ses bil new nad27 0 0
```

Next copy and paste the new DOQQ names into the new file where the bold print is located above. Once this is complete resave the file. Once the file has been saved make sure the file has the file extension .aml not (.txt) and is saved in the same location as the DOQQ's.

Next open Arc workstation in ArcGIS. Locate the working directory were the DOQQ's files are located. Next type in the correct drive and file name where the DOQQ's are located also making sure a copy of the AML is in the same folder.

```
Arc: w c:\aroth\doq_2003 (working directory)
```

Hit enter. It will state WARNING: New location is not a workspace.

```
Arc:
```

Next type in

Arc: &r runaml (the command and file name). Then hit enter. The program should then convert the DOQQ's to the correct file type which will have the DOQQ name followed by .bil

indimead_24kqq_usgs_doqq071898se.bil

Next to view the DOQQ's in IMAGINE so that more than one can be opened at the same time the correct projection and units must be specified. To do this open IMAGINE. Open each DOQQ individual in the view by finding the appropriate file type called Arc/Info & Space Imaging BIL. Click on the **Id** button, which is the third from the left in the view window. Or click on utility and then Layer info.

Next click on **Edit, Change Map Model**. And set Units to Meters and Projection to UTM. Click Okay and then yes. Next click on **Edit, Add/Change Projection**. Projection Type should be UTM. Spheroid Name should be Clarke 1866. Datum Name NAD 27. UTM zone 11 and North. Click Okay and yes. This must be done for all of the DOQQ's if more than one DOQQ's is to be viewed in the same view or used to create a view file or to be linked to the Landsat image. To create a view file open each DOQQ one at a time making sure to uncheck Clear Display under **Raster Options** when opening the .bil files. Then once all the DOQQ's are in the view go to **File, Save, View** and save the file with a .vue file extension. Then by opening the view file the next time all the DOQQ's will come up together.

IVA. TRAINING SITE INSTRUCTIONS

Depending on the objective or vegetation type of interest the size of the ideal training site will vary. For example the smallest training site that was taken in Pixley Basin was an aspen patch, which was about 10x10-m. These smaller aspen patches will be used to determine the probability of locating much smaller aspen patches with higher resolution images. For all other PVT and aspen stands involved in the main project the ideal training site would be 100x100-m with continuous homogeneous vegetation. Depending on the PVT and SS many or very few may fit this size requirement. In some cases the training site were placed in areas smaller than the 100x100-m standard.

The first step is to determine what PVT and SS the possible site would fall within based on ocular estimates of the dominant shrub and tree species based on the PVT and SS guide. Next located the central area of the training site. Record the date. Determine a plot numbering system. Create and record a unique value for each GPS Unit used in creating training sites. With the GPS unit, obtain a good averaged reading for that location and record it in UTM coordinates. Also record the elevation on the data sheet. If the GPS coordinate can be saved on the unit it is often a good idea to have saved values in multiple places. Using a compass record the aspect based on degrees from true north. Using a clinometer record the slope of the training site. Generally the direction in which water would travel down the slope where the observer is standing is used as the aspect of the entire training site if the terrain is complex. If pictures are taken the photo number can also be recorded.

The **life form composition** is used to create an ocular estimate of canopy cover based on important species and groups of species. For the training site to qualify for a particular PVT and SS the percentages must fall within the ranges given on the guide. See PVT and SS guide in Appendix A. All species falling into a particular category will be added together to get an overall estimate.

The **Tree structure** section of the data sheet will only be used on PVT's that include Aspen, Douglas-fir, and anywhere aspen is mixed with Douglas-fir or western juniper. This is important in tracking canopy structural trends, and can also indicate the size distribution of encroaching conifers into aspen stands. Upper canopy surface is any canopy of a particular species above 2-m and is also measured ocularly. The lower canopy surface is estimated by the amount of tree canopy below 2-m.

The **Comments section** is used to write down important comments about the plot.

IVB. SHAPE FILE CREATION

After returning from the field all of the information from the training sites needs to be entered into Excel. A worksheet with the appropriate headings is included in the attached files. Only the information needed for the classification was used in the shape file data table. A separated Excel file was created with the following columns; **TSN, NUMBER, PVT, SS, X COORD, Y COORD, YEAR, CODE, RANDOM, TRAINING, and VALIDATION**. **TSN** stands for training site number and was used to keep track of how many sites each class represented. **NUMBER** was the actually number recorded on the paper-training site. **PVT** is the Potential Vegetation Type for that particular site. **SS** is the Structural Stage of each site. **X COORD** is the x coordinate or easting taken from the GPS unit. **Y COORD** is the y coordinate or northing taken from the GPS unit. **YEAR** was used to keep track of the year in which the training sites were collected. **CODE** was used to keep track of the data sets collected by different people or at a different time so that it would be easy to go back to the appropriate data set if needed. **RANDOM** represent the set of randomly generated numbers to be used to determine which training sites were going to be used as training sites or validation. The rand function in Excel was used to create the numbers first in a row and then the entire row was copied and pasted using paste special, value command so that the random number remained the same and did not change. **TRAINING** represents all the sites within each PVT and SS that were used to train the computer. **VALIDATION** represents the sites that were set aside and not used to create the classification but were used to create and accuracy assessment for the classification. **For each PVT and SS class 20% of the total number of training sites were set aside for validation.** The lowest numbers created by the random numbers were used to create the validation set. For example Wet Meadow class has 10 training sites in which 8 were used as training sites and 2 were used as validation data. The next class, Mountain Shrub, had 14 total training sites in which 11 were used as training sites and 3 were designated validation. This was repeated for each class making sure that at least 20% of each sampled class were reserved for validation. Once this is complete save the file as a DBF 4 (dbase IV) (*.dbf), or (.txt) file.

Next open Arc View 3.3 Click on **Table**, then on the **Add** button. Open the dbf file just created in Excel. A similar table should open with all of the same values as the Excel spreadsheet.

Open a view set to the correct properties. Highlight the view box, which will bring the view box over the top of the table. Next go to **View** and then down to **Add Event Theme**. Make sure the correct table title is in the Table box. For the x box make sure that the X COORD is inserted and for the Y box the Y COORD. Click Okay and all of the points should now be in the view. Next convert the dbf file to a permanent shape file. Make the theme active then go to **Theme, Convert to shape file** and save the file.

The next step is to take the shape file containing all of the points and break it down into shape files based on training sites and validation sites. Creating folders to save shape files for both training sites and validation points is a good idea. Next highlight the shape file with all the points and open the table. Highlight each of the training sites for a particular class by clicking on each site and holding down the shift key. When all the points have been highlighted activate the view window again and save as a shape file as described above. Next do the same steps for the validation set. This must be done for each and every class based on PVT and SS attributes. Once this is complete the shape files are ready to be used in ERDAS IMAGINE.

VA. CLASSIFICATION SETUP

Open IMAGINE. Open the stacked image in one viewer and open a second viewer, which will be used for viewing the DOQQ's. The DOQQ were divided into the three mountain ranges do to the size of the study area and the size of the DOQQ files. The process can be started with any of the classes, but following the alphabetical order may make things the easiest. In the view with the image the shape files need to be laid on top of the image so that they can readily be seen. To open a shape file click on the folder and navigate to where the shape files are located. In **Files of Type:** select Shape file (*.shp) and click Okay. This will put the points on the image. To better view the shape files by PVT, SS, or any of the other column titles Click on **VECTOR** then **View properties**. Click on the Attributes box and then select any of the column names from the drop down box. Next click on the box next to the small circle. This will open the **Symbol Chooser**. The size of the circle can be changed as well as the color. Click apply, and then Okay. Click Apply again and then close. Opening the same shape file on the viewer with the DOQQ's should result in the points being the same color and size as the view with the image.

Once both views have the shape file present they can be linked. This is done by right clicking on either of the viewers and selecting **geo. link/unlink**. This will allow the movement in one viewer to be followed in the other viewer automatically. The seeding tool or tools to capture the area that will be used to define a particular class can be opened by clicking on **AOI** in the view with the Landsat image, and then **Tools**.

The region-growing tool was used to locate the boundaries on the Landsat image. The region-growing tool is the magnifying glass with the x in the center. Region growing properties can be altered by changing the spectral Euclidean Distance or the number of pixels depending on how the boundary looks after the first attempt. This tool has the magnifying glass within a box. Increasing the spectral Euclidean Distance will make a larger boundary. The boundaries can also be manipulated by the mouse to fit the boundary defined by the user. Once the boundary is properly defined the values from those pixels must be entered into the signature editor. The total number of pixels can also be restricted or enhanced with this tool. Most AOI's created were restricted to 40 pixels or less.

To open a signature editor click on the **Classifier** button on the top tool bar and then on the **Signature Editor**. After a training site area has been defined click on the button in the signature editor that has + sign with a down to the right arrow, which will add the signature for that site. For each site enter the unique signature into two signature editors. The first one should be saved to include all signatures for all classes. The second will be used to remove and combine any classes that are spectrally similar or very different. Also for each individual area defined on the image or AOI, each file must be saved. To do this click on **File, Save, AOI Layer as**.

This must be done for each individual location and saved as a unique name for each class. Therefore, if there are 10 training sites for the ABLA class 10 signatures should be entered into the first signature editor and 10 individually AOI should be saved to mark the location of the boundaries of each area. Make sure only the active AOI is saved as an individual file. A separate signature editor should be created for the training site data set and the validation site data set.

VB. SIGNATURE EDITOR

Once all the training site AOI's and unique signature values have been entered for both the training sites and validations set, statistical analysis to create a unique signature for each class as a whole can begin. The required tools can be found on the Signature Editor tool bar. The two most useful are mean plots and histograms. Buttons for each of these tools are located on the signature editor tool bar and can also be accessed by clicking on **View** and then selecting the wanted tool. The mean plot button looks like a bent string or lightning bolt and the histogram button looks like a graph. The mean plot function is useful in looking at the signature for a single training site or group of training sites over each band layer. This can be useful in separating out outlier training sites. The histogram option is useful in looking at the statistical distribution of a single or group of training sites based on each band or data layer. To view all bands select All Selected signatures and All Bands. Select multiple training sites by right clicking and holding the mouse button down. To skip a selection hold down the shift key and click on the training sites that you want to include. Remove outlier classes by right clicking on the training site number and selecting delete.

VC. AOI MERGE

Once the outlier training sites have been removed the single AOI for each class must be saved as a single file. To do this, open the AOI for a particular class one at a time. When all AOI's for the class have been opened they can be saved as a single file in the view by going to **File, Save, AOI Layer as**. Save each class as the same unique name. Make sure to clear away all the AOI's for the last class before beginning a new class. Do this first for all the training sites and then again for all of the validation sites.

PIXEL CONVERSION

Once this has been completed for each class the pixel values for each band must be converted to an ASCII file to be used by SAS for classification purposes. To do this select **Utilities** on the main ERDAS IMAGINE tool bar. Next select **Convert pixels to ASCII**. Then enter the image file in the input file box and click on Okay. Then click on the AOI circle. Enter the AOI file for a particular class. Next enter the same name as the AOI file and save the ASCII file in a new folder.

DATA ORGANIZATION

Next open up Excel and open the newly created file using the space-delimited format. Remove the top three rows and label each row with the appropriate class name. Name the top row Cover which will be next to the X column. Save the file in Excel format and keep the same name. When all classes are completed create a single file with all the classes combined. See Appendix K below for an example of what the final file should look like noting only five bands are shown. Once this is completed for all the training sites repeat the process creating a separate file for the validation set.

VD. SAS TEST AND ERROR MATRIX CREATION

The error matrix can be created before the entire image has to be classified. To do this import both the training site Excel spreadsheet and the validation site spreadsheet into SAS. Enter the script below into the command box and run. Export the output table, which in this case is called cvout, into an Excel compatible format. Important statistical values in the error matrix include the maps overall accuracy, the producer's accuracy, the user's accuracy, and the kappa statistic. The PROC step disc determines which layers add significance to the classification or which layers are non-significant and are then excluded and not used in the classification

Nonparametric discriminant analysis SAS code

```
PROC DISCRIM DATA=train method=npair k=7 CROSSVALIDATE
testdata=validate testout=nonP;
ods select ClassifiedCrossVal ;
ods output ClassifiedCrossVal = cvout ;
CLASSES cover;
```

```

VAR B1 -- B11;
RUN;
PROC stepdisc DATA=train method=backward;
CLASSES cover;
VAR b1 -- b11;
RUN;

```

Quadratic Parametric discriminant analysis SAS code

```

PROC DISCRIM DATA=train method=normal POOL=no CROSSVALIDATE
testdata=validate testout=parvalidation;
ods select ClassifiedCrossVal ;
ods output ClassifiedCrossVal = cvout ;
CLASSES cover;
VAR B1 -- B11;
RUN;
PROC stepdisc DATA=train method=backward;
CLASSES cover;
VAR b1 -- b11;
RUN;

```

Data – train = training site file

Testdata- validate = validation file

Cvout = cross validation file to export into Excel

VAR b1—b11 represents bands used in the classification

Once the cvout file has been exported out of SAS and into Excel the error matrix can be created. Either use the Excel template provided, or create a new matrix based on the following definitions or the example in Appendix L. The overall accuracy is computed by dividing the total correct (sum of the major diagonals) by the total number of pixels in the error matrix (Jensen 1996). The producer's accuracy is a measure important to the analyst in determining how well a certain area can be classified. The error of omission is calculated by taking correct pixels in a column and dividing it by the total number of pixels for the column. The statistics indicates the probability of a reference pixel being correctly classified (Jensen 1996). The user's accuracy measures the probability that a pixel classified on the map actually represents the category on the ground. The total number of correct pixels in a row is divided by the total number of pixels that were actually classified in the row, which results in the commission error (Jensen 1996).

The kappa statistic incorporated off-diagonal elements to produce a measure that determines if the results presented in the error matrix are significantly better than a random test, or to compare two similar matrices to determine if they are significantly different (Jensen 1996). The formula for the kappa statistic can be found below, and a template for calculating the kappa statistics can be found in the attached Excel template.

Kappa Statistic

$$K \text{ hat} = \frac{N \sum_{i=1}^r x_{ii} - \sum_{i=1}^r (x_{i+} \cdot x_{+i})}{N^2 - \sum_{i=1}^r (x_{i+} \cdot x_{+i})}$$

Where r is the number of rows in the matrix, x_{ii} is the number of observations in row i and column i , and x_{i+} and x_{+i} are the marginal totals for row i and column i , respectively, and N is the total number of observations (Jensen 1996). Once the final number of classes and satisfaction of the error matrix has been reached the study area next needs to be classified.

VE. STUDY AREA DIVISION

Depending on the size of the study area the image will need to be cut into smaller pieces to be able to be imported into SAS. For the study area the image was divided into 9 horizontal boxes with approximately the same amount of study area in each. Overlapping is required and will not affect the end result. In Arc View the image was opened as an image file. Boxes were then created and placed over the image until the entire image was covered. All the boxes were saved as a shape file that could be used in IMAGINE. In IMAGINE open the shape file with the boxes covering the image. Highlight one box at a time, which will make the box turn yellow. Click on the **AOI** title and then click on **Copy section to AOI**. The selected box should now have dotted lines. Click on the box again so that an AOI box is displayed around the boundary of the box. Next go **File – Save- AOI layer as ...** and save the AOI in a file with a separate name. Do this for each of the boxes making sure to keep track of the box and corresponding AOI file.

Next we need to clip the image to the size of the AOI. To do this click on **DATA PREP** from the main title bar of IMAGINE. Then click on **Subset Image**. The input file name is the name of the whole Landsat image that you have been using. The output image name should correspond to the name of the AOI file that you will use to clip out the image. For example, Box1. Clip on the **AOI** button at the bottom of the window. Then click on **AOI file**, and open the appropriate file for example Box 1. Everything else in the window should stay as the defaults except check Ignore zeros in the stats and make sure that the number of layer corresponds to the number of layers in the original image. Click Okay and repeat for each of the AOI created in the previous steps.

Next we need to convert the box sections of the image into a grid. This is a required step to convert the image pixel values to a table format that can be read and analyzed in SAS. This can be done by clicking on the **Import** button on the IMAGINE main key. Click on **Export**. The type is a **GRID**. Media is **file**. The input file is the file created in the previous step. The output file name can be the same name or a different one. Click on Okay. Another window will open and click on Okay again. This completes the work needed in IMAGINE.

Now open Arc. Type in w space and then the drive and folder where the grids can be found. For example.

Arc: w c:\aroth

Then type in lg

It then should define a workspace based on the folders used above. It will also give the available grid names. Multiple grids will be present for each band or layer that you had in the image. In this case 11 grids were created for each section or box of the study area. Type in grid and hit enter.

Now type in the name of the file plus a period and txt. Then space = space sample parenthesis followed by the name of each grid with a comma and space in between each and ending with a parenthesis. See example below. A txt file will be created combining each of the eleven layers in a tab-delimited file that can then be exported into SAS for analysis. Do this for each section of the study area.

Grid: Fun.txt = sample (box1_11, box1_11, box1_12, box1_3, box1_14, box1_15, box1_16, box1_17, box1_18, box1_19, box1_110, box1_111)

VF. SAS CLASSIFICATION

Next each box of the study area needs to be classified. Open SAS. File to Import. Selected the file format (.txt), the very last option at the bottom, and select next. Open the file just created in ArcGIS with the appropriate txt ending. Click Next. Within the workspace name the file the same as the name in the SAS code. Click on Next then Finish.

Next make sure that the headings are the same for the file just imported and the training site file used to classify the image. To do this open the imported file in SAS by clicking on Library then Work and then on the file with the name just imported. Often the band layers in the Excel file will have to be changed to match the other file. Do this to the training site data sheet in Excel before importing the file into SAS.

When the titles match import the Excel file in the same way as the (.txt) file making sure to select the Excel option on the first page. When both files have been imported the command statement can then be added to the editor. The script should look similar to the one used to create the error matrix with a few exceptions. The main difference is instead of using the validation data set, the area or section to be classified is used in the testdata line, and instead of creating an error matrix, the actual classified area is created in the testout command.

After the program has run which may take some time, the file needs to be exported so that it can be imported into Arc View. Click on the Explorer tab on the right side of the left column at the bottom. Locate the file name used in the testout line, for example class 1. Right click on the file and export. Click next. Then select the txt format again. Save to a folder on a computer with ample hard drive space.

Nonparametric discriminant analysis SAS code

```
PROC DISCRIM DATA=train method=npair k=7 CROSSVALIDATE
testdata=box1 testout=class1;
CLASSES cover;
VAR B1 -- B11;
RUN;
```

Quadratic parametric discriminant analysis SAS code

```
PROC DISCRIM DATA=train method=normal POOL=no CROSSVALIDATE
testdata=box5 testout=class5;
CLASSES cover;
VAR B1 -- B11;
RUN;
```

VG. GRID CREATION

Once a section or the entire image has been classified the export output data need to be imported into Arc View. Open Arc View, click on the table icon and then click on add. Find the file just created and click Okay. With a view open click on View and then on Add new Event theme. For the table selected to file that you just opened. For the x field select the x and for the y field select y. Click Okay. When the shape file comes up go to select theme convert to grid. Save all grids in the same place. Output grid extent should be the same as the shape file. Output grid size should be 30-m and the cell size will depend on the size of the box. Select Okay. Then selected the title at the very bottom, which corresponds to the class name. Repeat for each of the others.

Next the grids need to be merged together in ARC Grid. First create a zero grid by reclassifying a grid of the entire study area so that all values are equal to zero. Next make sure to set the Analysis properties so that all the required fields have the zero grid as the main theme. This will remove the noise that is outside the study area. To do this we must first remove everything outside the study area that is not need as well and create the proper code so that each section of the study area has the same class value. To do this open one of the grids with all 32 classes represented. Export this table as a dbf to be viewed in Excel. In Excel open the file and remove the count column. Change the column name value to code. Save the new file and open it in Arc view. This will serve as the master look up table for cover classes. Open the tables in each of the classified grids one at a time. Join the S-value so that the new code column is located in the classified grid table. Once this is complete highlight the view box click on **Analysis and Map Calculator**. Click on the title with the corresponding grid followed by the word code. Click on evaluate and save the new grid with a unique name. Once all of the grids have been evaluated the next step is to combine them all into one grid. To do this open up Arc. Define the working directory and locate the grids. Type in Grid and hit enter. Next type in setwindow zero grid hit enter. Then type in setmask zero grid hit enter. Then type in setcell 30 and enter. Next define the output grid name followed by a space equals sign then another space. Then type in merge followed by the

name of each grid followed by a comma and a space. Make sure there are parentheses around the first grid name and the last grid name.

```
setwindow zerogrid
setmask zerogrid
setcell 30
```

```
grandgrid = merge(class1, class2, class3, class4, class5)
```

VH. DECISION RULES

Different decision rules were applied to the three mountain ranges of the study area. The study area was divided into three sections, one for Silver City Range, one for South mountain, and one for Juniper mountain. Using ArcView 3.3, watershed boundaries based on a watershed boundary layer were selected for each of the mountain ranges and resulted in the creation of unique shape files for each area. Within each shape file table a new string field was added and called zone. Then click on **Field calculator** and selected the mountain range that corresponds to that shape file. When this was completed for each of the three shape files the **Geoprocessing Wizard** was used to merge the three mountain ranges into one shape file. Next set the Analysis Properties to the zero grid so that only the actual area of the study site would be used. Then convert the shape file into a grid based on the zone name. Hit enter.

In word pad an AML file was create to be used in ARC. A sample of both elevational boundaries and aspect boundaries can be found below, and a list of each aspect rule can be seen in Appendix C and elevation rules in Appendix D.

```
setcell 30
setwindow zerogrid
setmask zerogrid
```

This is required at the top of each AML file.

Elevational Boundary Sample

```
/*If Brte is greater than 1850 m classify as Artr R1*
```

```
DOCELL
if (final_32 == 10 & dem_04 > 1850) temp = 3
else temp = 0
```

```
END
```

```
brte2_no = setnull(temp == 0, 3)
kill temp
```

All of Class 10, which is BRTE above 1850 meters, was reclassified to represent Artr R1 or Class 3. brte2_no is the new grid file created that will then be merged into the final grid.

Aspect Boundary Sample

/*IF PsmeF4 250- 60 remain Psme F4, if Psme F4 59-249 classify as Artr W4

```
DOCELL
if (final_32 == 31 & aspect > 60 & aspect < 250) temp = 2
else temp = 0
END
```

```
artrw4_no = setnull(temp == 0, 2)
kill temp
```

All of Class 31 which is Psme F4 with and aspect greater than 60 and less than 250 was converted into class 2 or Artr W4.

In ARC locate the workspace where all the grids are located. Then enter &r and the file name to be run such as &r veg_fix_asp. After all of the grids are created for each decision rule they can be merged into the original grid one at a time using the same process described in creating the study area layer stack

RIPARIAN BUFFER

Riparian buffers were created by first creating a 30 meter buffer around the stream shape file in ArcView 3.3 using the Spatial Analysis extension for the entire Owyhee area. This was done by selecting **Analysis, Find Distance**. After this was created the classes that were determined to closely represent riparian areas were masked out to be converted into the Riparian/ Broadleaf class. The classes that were selected include Wet Meadow and Mountain Shrub. Using the **Analysis Map Query** function these classes were removed from the entire map by creating a mask. The mask was then evaluated using the riparian buffer layer created above, again using the **Map Query** function. After the evaluation process the map query can then be reclassified to represent a new class number. Go to **Analysis, Reclassify** and reclassify the new classes into a new class not represented by the 32-class classification. Next use either **ARC Grid** or the **Transform Grid Merge** function, which can be found on the Transform Grids extension in ArcView 3.3 to combine the newly created layers.

Step 1: (Asp_elev_test = 9.AsGrid) or (Asp_elev_test = 11.AsGrid)

Asp_elev_test = map grid, 9 = class 9 = Mountain Shrub, 11 = class 11= Wet meadow

Step 2: Distance_steam ≤ 40 and map Query = 1

Distance_stream = stream buffer layer, ≤ 40 = extent size used to create riparian buffer boundaries

An active agriculture class was also created for a portion of the Reynolds's Creek area. A shape file was created around the know areas and pixels classified as wet meadow or mountain shrub were reclassified to be come active agriculture. The same process of creating a mask was used as described above. Once the query is reclassified to represent a new value another merge can be used to create a final map with the addition of Riparian broadleaf class and an active agriculture class. In the classification Riparian became class 33 and active agriculture became class 34.

VI. Additional Resources (Located on CD)

- 1). Training site data sheet
- 2). Training site excel template
- 3). Error matrix template

Appendix C. Aspect boundary decision rules.

If Abl_a is found between 61 - 269 classify as Psme F4
 If Psme F4 is found between 59 - 249 classify as Artr W4
 If Psme F3 is found between 59 - 249 classify as Artr W2
 If Psme F2 is found between 59 - 249 classify as Artr W1
 If Brte is found between 251 - 139 classify as Artr R1
 If Taas is found between 241 - 139 classify as Artr R1

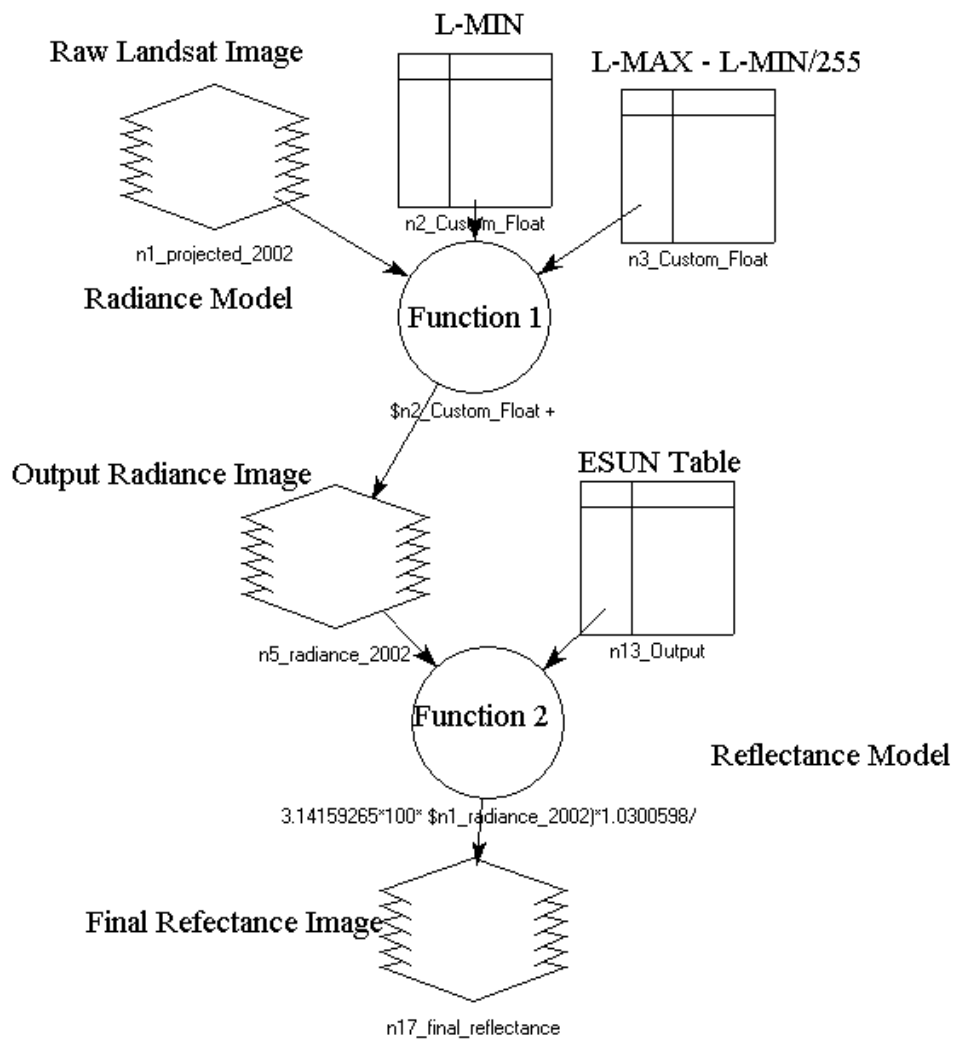
Appendix D. Elevation boundary decision rules.

If Taas is greater than 1500 meters classify as Brte
 If Brte is greater than 1850 m classify as Artr R1
 If Abl_a is less than 1900 m then classify as Psme F4 (Silver City only)
 If Abl_a is found on South Mountain Classify as Psme F4
 If Abl_a is found on Juniper Mountain classify as Artr W4
 If Psme F4 is found on Juniper Mountain classify as Artr W4
 If Psme F3 is found on Juniper Mountain classify as Artr W2
 If Psme F2 is found on Juniper Mountain classify as Artr W1
 If Psme F3 is less than 1900 m classify as Artr W2 on South Mountain and Silver City
 If Psme F2 is less than 1900 m classify as Artr W1 on South Mountain and Silver City

Appendix E. List of software used to create the supervised classification.

ERDAS IMAGINE 8.6
 ArcView 3.3
 ArcGIS 8.3
 SAS 8.02
 Microsoft Excel

Appendix F. Radiance and reflectance model used to convert the raw Landsat image to exo-atmospheric reflectance.



Appendix G. Example header file from a Landsat image where gains, biases, sun elevation angle, and sun azimuth angle can be found.

REQ ID =080001128003800002 LOC =042/0270000 ACQUISITION DATE =20002707
 SATELLITE =LANDSAT7 SENSOR =ETM+ SENSOR MODE =NORMAL LOOK ANGLE = 0.00
 LOCATION = ACQUISITION DATE =
 SATELLITE = SENSOR = SENSOR MODE = LOOK ANGLE =
 LOCATION = ACQUISITION DATE =
 SATELLITE = SENSOR = SENSOR MODE = LOOK ANGLE =
 LOCATION = ACQUISITION DATE =
 SATELLITE = SENSOR = SENSOR MODE = LOOK ANGLE =
 PRODUCT TYPE =MAP ORIENTED PRODUCT SIZE =FULL SCENE
 TYPE OF PROCESSING =SYSTEMATIC RESAMPLING =NN

VOLUME ## IN SET =01/01 PIXELS PER LINE = 7944 LINES PER BAND = 7548/ 7548
 START LINE # = 1 BLOCKING FACTOR = 1 REC SIZE = 7944 PIXEL SIZE = 28.50
 OUTPUT BITS PER PIXEL = 8 ACQUIRED BITS PER PIXEL = 8
 BANDS PRESENT =123457

FILENAME =L71042027_02720000727_B10.FSTFILENAME =L71042027_02720000727_B20.FST
 FILENAME =L71042027_02720000727_B30.FSTFILENAME =L71042027_02720000727_B40.FST
 FILENAME =L71042027_02720000727_B50.FSTFILENAME =L72042027_02720000727_B70.FST

REV L7A

GAINS AND BIASES IN ASCENDING BAND NUMBER ORDER

-6.199996948242188	0.775686264038086
-6.399993896484375	0.795686244964600
-5.000000000000000	0.619215667247772
-5.100006103515625	0.965490221977234
-0.999998092651367	0.125725477933884
-0.350000381469727	0.043725494295359
0.000000000000000	0.000000000000000
0.000000000000000	0.000000000000000

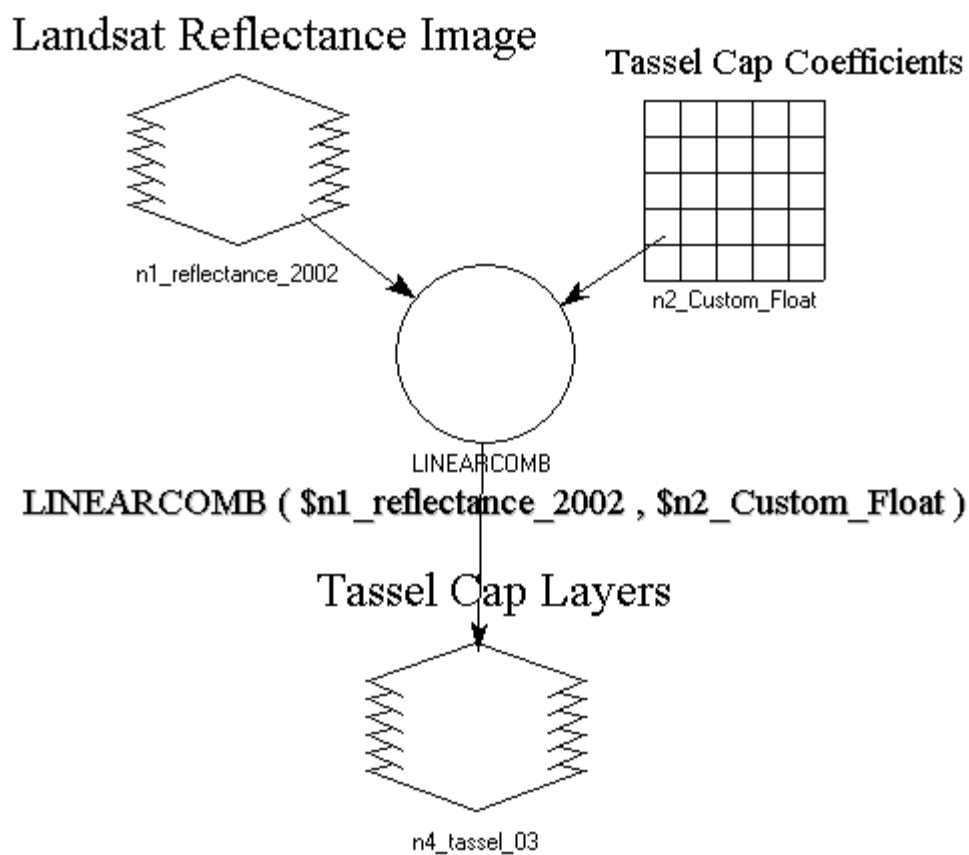
GEOMETRIC DATA MAP PROJECTION =UTM ELLIPSOID =WGS84 DATUM =WGS84
 USGS PROJECTION PARAMETERS = 6378137.000000000000000 6356752.314140000400000

0.000000000000000	0.000000000000000	0.000000000000000
0.000000000000000	0.000000000000000	0.000000000000000
0.000000000000000	0.000000000000000	0.000000000000000
0.000000000000000	0.000000000000000	0.000000000000000

0.000000000000000 USGS MAP ZONE = 11
 UL = 1171144.2282W 482505.0796N 485526.000 5362788.000
 UR = 1140816.6566W 482257.4822N 711901.500 5362788.000
 LR = 1141427.2905W 462658.4359N 711901.500 5147698.500
 LL = 1171118.8558W 462857.7258N 485526.000 5147698.500
 CENTER = 1154059.4768W 472731.1163N 599250.745 5256973.937 3991 3714
 OFFSET = 0 ORIENTATION ANGLE = 0.00
SUN ELEVATION ANGLE =57.2 SUN AZIMUTH ANGLE =141.7

Appendix H. Geo-reference information needed to project the Landsat image.

Projection:	UTM
Units:	Meters
Zone:	11
Spheroid:	Clark 1866
Datum:	Nad 27

Appendix I. Tassel Cap model used to create the greenness, wetness, and brightness layers used in the final classification image.

Appendix J. Landsat band layers and vegetation indices used to create the final stacked image.

Layer	Band and Indices Used
Layer 1	TM Band1
Layer 2	TM Band2
Layer 3	TM Band3
Layer 4	TM Band4
Layer 5	TM Band5
Layer 6	TM Band7
Layer 7	Tassel Cap 1
Layer 8	Tassel Cap 2
Layer 9	Tassel Cap 3
Layer 10	NDVI
Layer 11	MSI

Appendix K. Sample training site or validation site Excel spreadsheet used in SAS 8.02

COVER	X	Y	B1	B2	B3	B4	B5-11
ABLA	514200	4769220	9.6536	7.4428	6.1023	17.248	8.3270
ARARR1	524640	4761840	9.5027	7.2772	5.3381	18.664	7.4740
ARARR3A	524640	4761810	9.5027	7.2772	5.6438	18.310	8.7535
ARARR3A	524670	4761810	9.3519	7.1117	5.9495	17.602	7.4740

Appendix L. Sample error matrix with user's and producer's accuracies

	ABLA	ARARR1	ARARR3A	Total	Commission error	Error (%)	User's accuracy
Example ABLA	33	0	0	33	0	0.0	100.0
ARARR1	0	202	3	205	3	1.5	98.5
ARARR3A	0	1	151	152	1	0.7	99.3
Total	33	203	154	390			
Omission error	0	1	3		Total	=33+202	
Error (%)	0.0	0.5	1.9		Correct	+151 = 386	
Producer's accuracy	100.0	99.5	98.1				
Overall accuracy	98.97						
kappa statistic	98.19						